Journal of the National Academy of Forensic Engineers®

http://www.nafe.org

ISSN: 2379-3252

DOI: 10.51501/jotnafe.v40i2

Vol. 40 No. 2 December 2023

National Academy of Forensic Engineers®

Journal Staff

Technical Review Process

The Technical Review Committee Chair chooses the reviewers for each Journal manuscript from amongst the members and affiliates of the NAFE according to their competence and the subject of the paper, and then arbitrates (as necessary) during the review process. External reviewers may also be utilized when necessary. This confidential process concludes with the acceptance of the finished paper for publication or its rejection/withdrawal. The name(s) of authors are included with their published works. However, unpublished drafts together with the names and comments of reviewers are entirely confidential during the review process and are excised upon publication of the finished paper.

National Academy of Forensic Engineers®

Board of Directors

President
Joseph Leane, PE, DFE
Fellow

President-Elect
Steven Pietropaolo, PE, DFE
Senior Member

Senior Vice President
Michael Aitken, PE, DFE
Senior Member

Vice President
Tonja Koob Marking, PhD, PE, DFE
Senior Member

Treasurer
Bruce Wiers, PE, DFE
Senior Member

Secretary
James Drebelbis, AIA, PE, DFE
Fellow

Past Presidents
Samuel Sudler, PE, DFE
Senior Member

Liberty Janson, PE, DFE
Senior Member

James Petersen, PE, DFE
Fellow

Directors at Large
Daniel Couture, PEng, DFE
Senior Member

Robert Peruzzi, PhD, PE, DFE
Member

Executive Director
Amanda Hendley

Journal of the National Academy of Forensic Engineers®

Editorial Board

Submitting Proposed Papers to NAFE for Consideration

Please visit the Journal's author page at
http://journal.nafe.org/ojs/index.php/nafe/information/authors for submission details.

We are looking for NAFE members who are interested in giving presentations on technical topics that will further the advancement and understanding of forensic engineering at one of the academy's biannual meetings and then developing those presentations into written manuscripts/papers, which will go through a single-blind peer review process before publication. Only papers presented at a NAFE regular technical seminar and that have received oral critique at the seminar will be accepted for review and publication. We recommend that you review the About the Journal page for the journal's section policies as well as the Author Guidelines listed on the Submissions page. Authors need to register with the Journal prior to submitting, or (if already registered) they can simply log in and begin the process. The first step is for potential authors to submit a 150-word maximum abstract for consideration at an upcoming conference into the online journal management system.

Copies of the Journal

The Journal of the National Academy of Forensic Engineers® contains papers that have been accepted by NAFE. Members and Affiliates receive a PDF download of the Journal as part of their annual dues. All Journal papers may be individually downloaded from the NAFE website. There is no charge to NAFE Members & Affiliates. A limited supply of Volume 33 and earlier hard copy Journals (black & white) are available. The costs are as follows: $15.00 for NAFE Members and Affiliates; $30.00 for members of the NSPE not included in NAFE membership; $45.00 for all others. Requests should be sent to NAFE Headquarters, 1420 King St., Alexandria, VA 22314-2794.

Comments by Readers

Comments by readers are invited, and, if deemed appropriate, will be published. Send to: Ellen Parson, Journal Managing Editor, 3780 SW Boulder Dr, Lee's Summit, MO 64082. Comments can also be sent via email to journal@nafe.org.

Table of Contents

§ Paper presented at the NAFE seminar held in July 2022 in Toronto.
ϕ Paper presented at the NAFE seminar held in January 2022 in Tucson.
ʊ Paper presented at the NAFE seminar held in July 2023 in Kansas City.
‡ Paper presented at the NAFE seminar held in January 2023 in San Antonio.

Methodology for Reconciliation of Different Forms of Electronic Data in Vehicle Collision Reconstruction

By Shawn Ray, PE, DFE (NAFE 970S), John Swanson, PE, and Derek Starr, PE

Abstract

Collision analysis utilizing electronic data recorders, videos, traffic signal timing data, and other electronic records adds valuable input but can be a challenge to tie together due to the lack of a finite time stamp or common recording rate. However, overlapping data streams that have a common point-in-time identifier can be resolved. A strategic approach was developed by the author for unifying and validating the vehicle positions and time-distance reconstruction. The method outlines the steps for establishing known data points, forming a common time line, identifying overlapping information, and linking together independent records. A case study demonstrates a crash at a traffic signal-controlled intersection in which each vehicle entered on their respective green lights without conflict; however, the collision still occurred. The crash reconstruction will highlight driver options and demonstrate the value of combining multiple data streams into one time line.

Keywords

Collision, accident reconstruction, electronic data, crash event data, event data recorder, EDR, CDR, airbag, black box, traffic signal timing, video, surveillance, camera match, time distance, vehicle, tractor/trailer, motion capture

Background

A collision occurred at a traffic signal-controlled intersection in the western suburbs of the greater Miami, Florida metro area. Both vehicles reported having a green light upon entry, and no malfunction of the signal occurred.

An SUV (Vehicle A), traveling northbound across the main boulevard, entered the intersection on a green traffic signal, but was delayed by a left-turning vehicle coming from the opposite side of the intersection. After proceeding across the intersection to the north, a collision occurred. A sedan (Vehicle B), traveling westbound, entered the intersection on a green traffic signal, and struck the front right side of the SUV. The collision fatally injured an occupant in the sedan. A surveillance video was recovered showing a portion of the incident; however, the traffic control signals were not visible. The road surface was dry, it was daylight but overcast, and the posted speed limit for through traffic was 45 mph.

Motivation

A dispute regarding right of way and failure to yield ensued due to a lack of clarity regarding the collision timing and the specific sequence of the traffic light at the time of the collision, since each vehicle reported having a green light upon entry — and no malfunction of the traffic signal occurred.

The initial task was to collect evidence, orient the vehicles at impact and final rest, and determine how the collision occurred. Airbag control module (ACM) data was collected and evaluated for the crash. Crash reconstruction analysis confirmed the ACM recorded speeds. Diagrams stepping back in time several seconds just prior to the collision were created to establish the positions of the vehicle on scaled diagrams. Since this incident was partially captured on surveillance video, synchronizing the video to the ACM data — and matching the vehicle motion to the traffic signal timing — became one of the more significant tasks.

A generalized protocol for reconciliation of these different types of electronic data will be presented in this paper as a result of the efforts in this reconstruction. The order of evaluating or anchoring the known data points may be incident specific. However, the author will demonstrate a logical progression, establishing known positions, and working backward in time to determine unanswered questions.

Shawn Ray, PE, SEA, Fort Lauderdale, FL 33301, (888) 771-0591, sray@sealimited.com

The methodology follows a similar pattern to the typical accident reconstruction teaching. Due to the desire of blocks of time and distance data from different sources needing to be synchronized together, the author hopes that this document can be used to simplify the process and reduce the number of iterations required.

It is important to keep in mind that a forensic investigation/analysis of any incident is likely to be a complex and scientific endeavor. Therefore, the methodology of such an endeavor must include the comprehensive, objective, and accurate compilation/analysis of the available data. Both the quality and quantity of data will vary depending on the situation and should be considered accordingly.

Accident Site

The accident site was a six-lane, boulevard-style street with three through lanes of traffic in each direction. The opposing lanes were separated by a raised median covered with grass and trees. At the intersection, east- and westbound traffic utilized dedicated left turn lanes to allow traffic to cross when permitted. Westbound traffic also had a dedicated right turn lane servicing a gated community to the north. **Figure 1** shows an aerial photograph of the accident site. For orientation purposes, north is at the top.

Intersection design was typical for south Florida suburban areas[1]. The primary boulevard continued across the developed residential area. The speed limit was posted as 45 mph, and it was clear, dry, and daylight with no environmental factors contributing to the accident. The cross-street services private gated residential communities to the north and south.

A guard shack to the south of the intersection, shown in **Figure 2**, was equipped with a security camera that recorded the SUV leaving the property and a partial view of the crash. The surveillance camera video was recorded at 30 frames per second (fps); however, the orientation and field of view limited the useful images — as the crash occurred at the top edge of the frames, and Vehicle B only entered into view just before the collision.

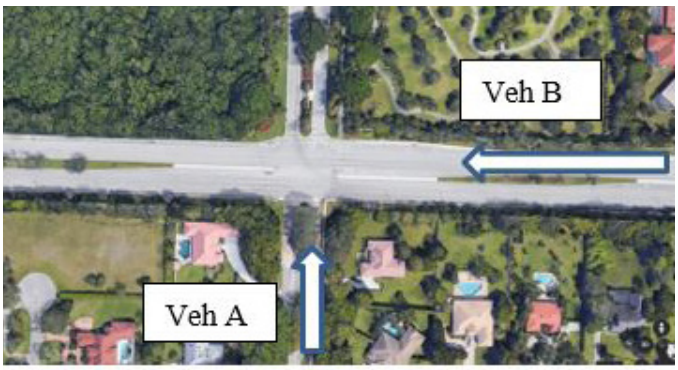

Figure 1
Google Earth image of the intersection.

Vehicle A (SUV)

Vehicle A was a 2010 four-door SUV (**Figure 3**). The curb weight was 5,983 lb. The SUV was powered by a 5.7-liter V8 gasoline engine. It was equipped with an ACM that stores crash data during an impact. Data was downloaded and analyzed showing that the speed at impact was 20 mph — and that the car was accelerating at the time of collision.

Event data recorder (EDR) data imaged from Vehicle A shown in **Figure 4** helped establish the pre-impact position, speed, and driver inputs.

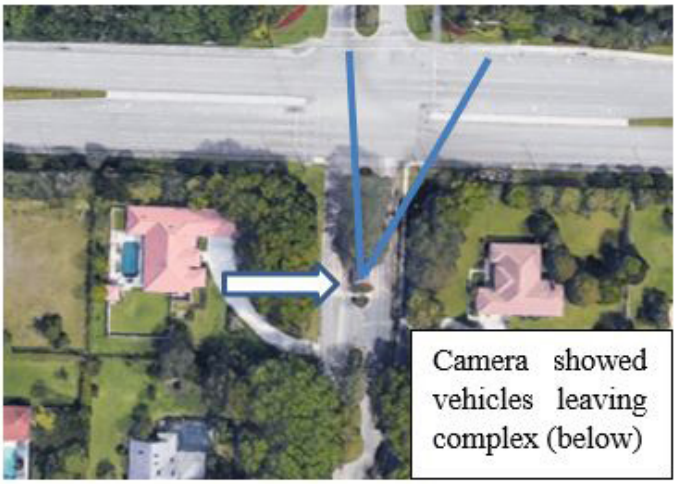

Figure 2
Google Earth image of locating the guard house and security camera.

Figure 3
Damage to right side front of Vehicle A was consistent with the EDR data.

Pre-Crash Data -5 to 0 seconds (Most Recent Frontal/Rear Event, TRG 2)						
Time (sec)	-4.3	-3.3	-2.3	-1.3	-0.3	0 (TRG)
Vehicle speed (mph [km/h])	1.2[2]	1.2[2]	6.2[10]	12.4[20]	19.9[32]	19.9[32]
Brake switch	ON	OFF	OFF	OFF	OFF	OFF
Accelerator rate (V)	0.78	1.29	1.33	1.48	0.78	0.78
Engine rpm (RPM)	400	400	1.200	2,400	3,200	3,200
Pre-crash data status*	Valid	Valid	Valid	Valid	Valid	Valid

* Invalid may be set for M/T vehicle

Figure 4
Vehicle A EDR pre-crash data.

Vehicle B (sedan) was a 2016 passenger car (**Figure 5**). The curb weight was 2,555 lb. The sedan was powered by a 1.6-liter four-cylinder gasoline engine. It was equipped with an ACM that stores crash data during an impact. Data was downloaded and analyzed showing that the speed at impact was 37 mph — and that the car had been accelerating prior to the collision.

EDR data imaged from Vehicle B shown in **Figure 6** helped establish the pre-impact position, speed, and driver inputs.

Figure 5
Damage to left front of Vehicle B was consistent with the EDR data.

The first step in evaluating the traffic signal sequencing was determining whether the intersection in question participated in the Federal Highway Administration's Automated Traffic Signal Performance Measures (ATSPM) program. Intersections for which high-resolution ATSPM data is recorded allow for analysis of time-stamped status data for every moment of their operation[2].

It should be noted that analysis of ATSPM data would still require the reconciliation of the signal status time-stamps to the recovered vehicle ACM and ECM data in addition to any reconstructed vehicle positional data.

Unfortunately, it was determined that no high-resolution data had been recorded for the subject intersection. Therefore, the traffic signal sequencing and timing was analyzed via a review of the traffic signal programming. Of particular utility was analysis of the time-based programming for the intersection[3]. This analysis resulted in a data set indicating minimum and maximum timings for signals in each direction based on vehicle demand, in addition to the sequencing of the various signals.

A review of the programmed time and sequency for the traffic in each direction enabled a determination of how long the green-red signal condition existed relative to the determined vehicle positions. By reviewing other

Time (sec)	Vehicle Speed (kph)	Engine RPM (RPM)	Engine Throttle (%)	Acceleration Pedal (%)	Service Brake (on/off)	ABS Activity (on/off)	Stability Control (on/off/engaged)	Steering Input (degree)
-5.0	66 (41 mph)	1300	5	0	ON	OFF	ON	0
-4.5	64 (39.8 mph)	1200	4	0	ON	OFF	ON	0
-4.0	62 (38.5 mph)	900	4	0	ON	OFF	ON	0
-3.5	60 (37.3 mph)	1000	5	0	ON	OFF	ON	0
-3.0	58 (36.0 mph)	1100	5	0	OFF	OFF	ON	-5
-2.5	57 (35.4 mph)	1900	29	25	OFF	OFF	ON	-5
-2.0	57 (35.4 mph)	2200	57	27	OFF	OFF	ON	0
-1.5	58 (36.0 mph)	2200	59	27	OFF	OFF	ON	0
-1.0	59 (36.7 mph)	2200	59	30	OFF	OFF	ON	0
-0.5	60 (37.3 mph)	2400	62	33	OFF	OFF	ON	0
0.0	59 (36.7 mph)	2100	8	0	ON	OFF	ON	-40

Figure 6
Vehicle B EDR pre-crash data.

non-related traffic also visible in the surveillance video and coordinating the analyses helped refine the change in signal timing.

Reconstruction Outline

The next phase was the collision reconstruction. The first step was to establish known facts, and then to evaluate the working theory regarding signal timing to determine the traffic control conditions — and if the working theory was consistent with the evidence.

The reconstruction included establishing known data points based on the data collected during the accident investigation, which included a detailed analysis of the physical evidence, roadway geometry, and specific vehicle dimensions and geometry, using high-definition three-dimensional (3D) laser scanning and unmanned aerial vehicle (UAV) aerial imagery. The physical evidence and area of impact were identified and highlighted on an aerial image of the intersection (**Figure 7**).

Each vehicle recorded crash data in the airbag control modules. However, few vehicles time and date stamp EDR data; in this case, neither did. Five seconds of pre-crash data is recorded but must be reconciled with the other information. In addition, the consistency of the recorded data — and the speeds, in particular — only need to be verified by traditional accident reconstruction techniques.

The authors believe it can be potentially troublesome to accept and use EDR data without confirmation and/or verification of consistency with the given collision evidence.

Figure 7
UAV aerial image of the intersection showing physical evidence.

Conservation of linear momentum[4,5,6] crash simulation programs[7,8] would confirm speeds based on the documented area of impact and final rest position for each vehicle. Another option, which could be employed if the impact and final rest positions were unknown, would be a camera-matching technique using the security camera video.

Camera-matching is a close-range photogrammetry analysis of 2D imagery. This process utilizes 3D data of the scene to match the perspective of 2D imagery in 3D space, and it allows for spatial analysis of objects, features, or people in videos and photographs[7]. Computer software imports the 2D imagery and 3D data into one digital environment where common points between the two data sets are identified. The software calculates the relative location of the points in 3D space compared to their corresponding location in the 2D imagery and determines the necessary camera location/settings to create a replica of the camera in 3D space. The result is a virtual camera in the 3D space of the laser scan data that matches the real-world camera that captured the imagery. When viewed through this virtual camera, the 3D data is aligned to the imagery, allowing for accurate placement of additional 3D objects.

In vehicle accident reconstruction, camera-matching can be used to track the position of vehicles over time. With the 3D scan data aligned to video of an accident, 3D vehicle models are constrained to the ground plane established with the laser scan data and then moved in 3D space to match the position within the frame of the 2D imagery. Physical evidence, EDR data, and other information can be incorporated into positioning of the 3D vehicle models to improve accuracy. Positioning vehicles periodically over time results in a 3D animation of the accident that can be analyzed as part of an accident reconstruction as well as providing demonstratives for visualizing the motion of the objects.

The accuracy of a camera-match is a function of the quality of the site 3D data as well as the quality and characteristics of the 2D imagery. The lens distortion was corrected, and camera orientation was accounted for using commercially available software and commonly accepted techniques. The orientation and field of view limitations of the security video in this matter made an accurate determination of the speeds solely through camera-matching challenging and less useful in this particular case. The specifics of the speed determination are not the focus of

this manuscript; therefore, the author proposes that the EDR data was determined to be accurate, and those recorded speeds will be used.

Multiple graphics and 3D digital images were used to demonstrate the findings of the accident reconstruction and illustrate the vehicle location at specific timing, visibility, driver's view, including the ability to see the other vehicle and other factors that led to this event. Production of these graphics provides an opportunity to double check the analysis. Some will be used throughout this paper to assist with explanation. **Figures 3** through **10** are one example in 2-D form of the graphics used to illustrate and confirm the specific vehicle locations, orientations, and line-of-sight for the drivers.

Traffic signal timing plans were provided by the local Department of Transportation and evaluated. Analysis of the time-based programming for the intersection provided minimum and maximum signal timings in each direction and the sequencing of the various signals. Of interest in this incident was the introduction and time of the northbound and southbound green ball with permissive (but not protected) left turn as well as the transition to and conclusion of the red signal.

A permissive left turn is a left turn that occurs during a solid green indication (no turn arrow) and requires the driver to determine a safe turning window between opposing thru-traffic. The evaluation of traffic light timing accidents (and who had the red light) are always difficult to evaluate absent independent information or specific timing, which can be related to the light condition. Techniques for determining speeds and matching the video recorded motion with the traffic signal phase was outlined by Couture[8]. He established a guideline of steps to be followed for a video analysis as shown below.

Step 1	Create a spreadsheet with signal color by road, validity, time, observations by road with position in frame.
Step 2	Set one interval per row, matching seconds (or ticks).
Step 3	Observe the video, and note the number of vehicles, actions, and positions for each interval.
Step 4	Code the range of interest; then add the signal phase timing to the spreadsheet.
Step 5	Compare the activities and observations to the phase, and rank according to rules.
Step 6	Iterate the placement of phases until a validity acceptance criteria is met.
Step 7	Verify the timing assumptions by validating the actions with an external source (SAE papers, data from third parties).
Step 8	Set the signal phase sequence, and tie it to the observations.

Couture also addressed "analysis of indirect video," some of which can be employed in this case example — the premise being that vehicles proceed through the intersection on a green light, and there is a high probability of vehicles stopping for a red light.

Forensic Engineering Analysis and Collision Evaluation

The collision evaluation included a review of the following material:

1. Police traffic crash report and police investigation material.
2. Scene photographs.
3. Witness statements and depositions.
4. Surveillance video from a security entrance near the intersection.

The investigation tasks included:

1. Documented the site with photographs and video at ground level and from the air.
2. Documented the path and typical speed of traffic on this road under similar condition with aerial video.
3. Documented the roadway with HD 3D laser scans.
4. Examined, photographed, and measured the SUV and the sedan.
5. Documented the SUV and the sedan with HD 3D laser scans.
6. Imaged the crash data from the SUV and the sedan's ACM.
7. Reviewed and evaluated the traffic signal timing plans for the intersection.

Analytical Method

The forensic engineering evaluation of the pre-collision events utilized event data from ACM, computer -aided drawing and design (CADD), video analysis, and traffic signal timing evaluation. The graphical, geometric,

and analytical methods that were applied in the analysis included the following:

1. Created 2D and 3D CADD models based on the photographs, measurements, and laser scans of the vehicles to evaluate crash and pre-crash time and distance positions.

2. Created digital model of the site based on measurements, laser scans, and mapping with aerial photos.

3. Determined positions of vehicles on the road along the travel path leading up to impact. For this case, the team used ACM data and physical evidence at the site.

4. Exemplar vehicle was used to measure the roadway drag factor at the site, under similar conditions, utilizing techniques described in SAE J2505.[9]

5. Synchronized the vehicle movements with one another, based on the surveillance video and EDR data.

6. Based on the traffic signal timings and coordination programming, determined the traffic signal sequence and range of potential timings.

7. Synchronized the traffic signal timing to the vehicle movements. For the example presented, additional video footage was acquired, and the motion of traffic through the intersection on multiple traffic signal cycles was utilized. Increasing the number of samples can reduce the variability associated with the driver reaction time[10,11]. However, when less video timing is available, initiation of a green light precedes stopped vehicle motion. Some perception-response time needs to be accounted for prior to the observed vehicle acceleration[12]. For this incident, a 1.5-second PRT was used for evaluating possible avoidance scenarios. The EDR data established when driver input changed and was incorporated into the overall reconstruction analysis. Caution should be used when determining perception-response and stopping due to a yellow or red signal, as decision and braking time vary more widely than the acceleration light from a stopped position when given a green light.

8. Additional traffic and additional video can allow more refinement of the sequence for the traffic signal timing, which improves the synchronization with other data sources.

Note: Some traffic signal plans allow for extensions or triggered changes during specific times or days. Careful evaluation of the signal timing plan should be used so as not to incorrectly synchronize a non-standard sequence.

Results

The resulting time and distance position, visibility and key position are best described showing graphical recreation of the scenario. **Figures 8** through **15** demonstrate the approach of each vehicle. Vehicle A approach is from the bottom of the image, and Vehicle B enters from the right — but not until the fourth image. The last image shows the impact.

Summary of the Methodology

A summary of the key elements is provided to assist the reader when synchronizing data in an similar incident.

Figure 8
Aerial image showing time and distance position and traffic signal state.

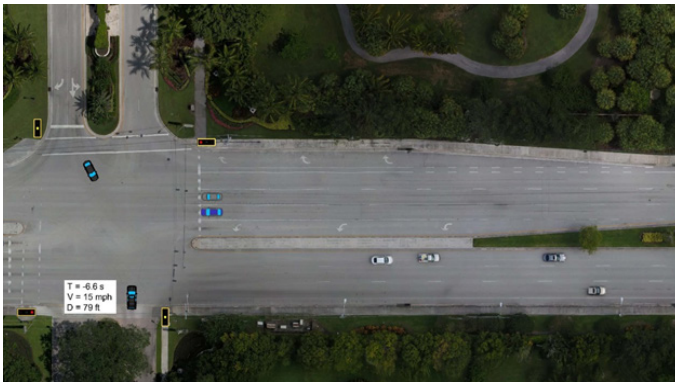

Figure 9
Aerial image showing time and distance position and traffic signal state.

- Determine vehicle speeds and impact positions using generally accepted accident reconstruction methods.

- Identify known time and distance relationships in order to establish relative vehicle positions. Note: This will likely not include the timing aspect of yet-to-be-determined blocks such as traffic signal sequence.

- Fix known position with physical evidence, such as point of impact. If the area of impact is not

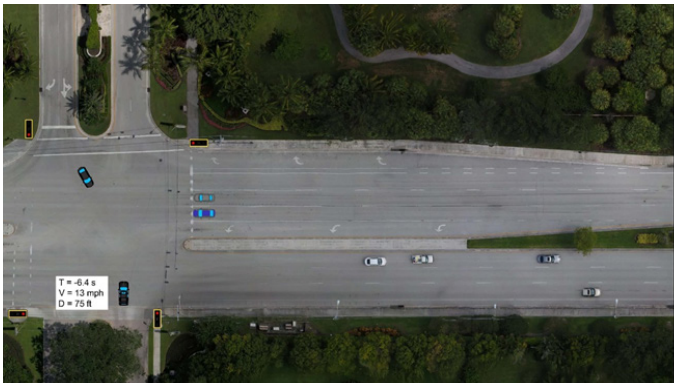

Figure 10
Aerial image showing time and distance position and traffic signal state.

Figure 11
Aerial image showing time and distance position and traffic signal state.

Figure 12
Aerial image showing time and distance position and traffic signal state.

Figure 13
Aerial image showing time and distance position and traffic signal state.

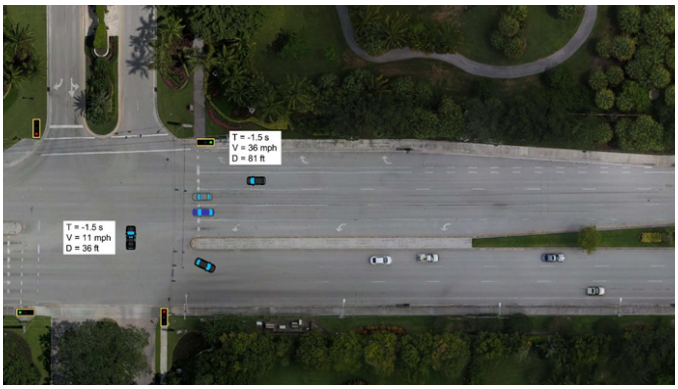

Figure 14
Aerial image showing time and distance position and traffic signal state.

Figure 15
Aerial image showing time and distance position and traffic signal state.

known, the area of rest can be used. Reconstruction of the post impact motion to determine an area of impact will introduce error, which should be quantified. Bracketing[4,5,6] accident simulations[13,14] Monte Carlo method or uncertainty analysis[15,16] can be used to evaluate the accuracy of the reconstruction analysis. Camera matching can also be used to verify vehicle position or to augment the determined position, speed, or motion of objects captured on video[16].

- Don't try to "fit" positions based on other evidence, such as witness statements or narratives in reports until all known physical evidence or established data has been exhausted. Later, if a "fit" must be used, disclose the extrapolation and uncertainty associated with placement.

- Determine which "known positions" can be tied to electronic data. Anchor time and distance data to the scene data with the best known or established point geometrically and in time. In this incident, area of impact was established by physical evidence and allowed a convenient anchor for both geometry and time.

- Determine or establish any additional vehicle positions that are consistent with the other data. This may include other objects, actions, or non-involved vehicles.

- When a precise anchor between vehicle data blocks is unknown, develop time and distance chart for ACM/EDR independent of other input. The data is a record of the vehicle's sensors and should be evaluated or verified independent of scene and other inputs until a known site data point, physical evidence, or additional information is established.

- Asynchronism of ACM/EDR data and data being reported at different frequencies is common and should be evaluated carefully. Additional caution is warranted when combining EDR data due to this factor.

- Look for overlapping electronic data, such as a known time or known position, which can be used to confirm the theory regarding using physical evidence or reconstructed positions.

- Identify and combine common/overlapping positions in the time domain.

- Synchronization of video may require extra video records of traffic not related to the incident. Note: It may be helpful to observe additional video during the time preceding this event. Viewing non-related traffic movements through the intersection, stopping and starting at the signal can be used to evaluate the signal sequence without viewing the lights. It is necessary to account for a potential lack of precision, but this technique may be helpful to gain an understanding of the traffic signal timing related to the surveillance video.

- Reconstruct any remaining positions, and fill in time and distance as needed while recognizing these are not known data points, but rather reconstructed positions.

- Check for consistency.

Summary

The detailed forensic engineering evaluation and reconstruction of this collision event created the situation prompting the methodology for reconciliation of different forms of electronic data to be established. Utilizing the methodology, the following conclusions were determined for this incident:

- Vehicle A entered the intersection on a green/yellow light, approximately 90 feet from the collision.

- Vehicle B entered the intersection on a green light, approximately 50 feet from the collision.

- Due to a delay, Vehicle A had not cleared the intersection prior to the arrival of Vehicle B, and a collision occurred in the right westbound lane.

- Traffic signal sequence was determined using traffic flow and video analysis, combined with an analysis of programmed time-of-day programming for the intersection.

- Synchronization of traffic signal timing and ACM data as well as surveillance video was accomplished by a sequential systematic matching of known data points.

Conclusion

Arising from this unfortunate traffic accident was the development of a methodology for synchronizing electronic data from multiple sources internal and external to the involved vehicles. A strategic approach was developed by the author for unifying and validating the vehicle positions and time-distance reconstruction. The method provides systematic steps for establishing known data points, forming a common time line, identifying overlapping information, and linking together independent records. The case study demonstrates the value of combining multiple data streams into one time line, thus enabling a clear understanding of how the event occurred.

References

1. D. P. Couture, "Forensic Engineering Analysis of Traffic Signal Timing and Speeds Prior to Collision by Rule-Based Triage of Indirect Video," J. Natl. Acad. Forensic Eng., vol. 34, no. 1, 2017.

2. "Automated Traffic Signal Performance Measures (ATSPM)." https://ops.fhwa.dot.gov/arterial_%0Amgmt/performance_measures.htm (accessed Apr. 26, 2022).

3. J. R. Effinger, "Automated Traffic Signal Performance Measures."

4. P. Koonce and L. Rodegerdts, "Traffic signal timing manual.," United States. Federal Highway Administration, 2008.

5. J. Daily, N. S. Shigemura, and J. Daily, Fundamentals of traffic crash reconstruction, vol. 2. Institute of Police Technology & Management, 2006.

6. R. M. Brach and P. F. Dunn, Uncertainty analysis for forensic science. Lawyers & Judges Publishing Company, 2004.

7. R. Limpert, Motor Vehicle Accident Reconstruction and Cause Analysis 7th Edition. LexisNexis, 2023.

8. M. A. Callahan, B. LeBlanc, R. Vreeland, and G. Bretting, "Close-Range Photogrammetry with Laser Scan Point Clouds," SAE Technical Paper, 2012.

9. Society of Automotive Engineers, "Measurement of Vehicle-Roadway Frictional Drag," 2010.

10. P. L. Olson and E. Farber, Forensic aspects of driver perception and response, 2003.

11. Institute of Police Technology and Management, "Human Factors in Traffic Crash Reconstruction," 2019.

12. T. F. Fugger, J. L. Wobrock, B. C. Randles, A. C. Stein, and W. C. Whiting, "Driver characteristics at signal-controlled intersections," SAE Technical Paper, 2001.

13. E. Dynamics and Company, "HVE Software Version SP1".

14. MEA Forensic, "PC-Crash Version 13.0".

15. D. P. Wood and S. O'Riordain, "Monte Carlo simulation methods applied to accident reconstruction and avoidance analysis," SAE Trans., pp. 893–901, 1994.

16. M. Brach, J. Mason, and R. M. Brach, Vehicle accident analysis and reconstruction methods. SAE International, 2022.

Factors to Consider in Developing Conceptual Scopes of Repair for Common Low-Slope Roofing Assemblies

By Chad T. Williams, PE, DFE (NAFE 937M) and Drew Jamison

Abstract

Forensic engineers are commonly asked to develop conceptual scopes of repair as part of their work. Many factors impact these recommendations, including building codes, construction feasibility, manufacturer assessment, and installation requirements. In addition, the conditions present on and within the existing roof surfaces can limit the repairability of a commercial roof assembly such that removal and replacement of the entire roof section is the appropriate or only feasible repair option. This paper will focus on common limitations to be considered when developing a conceptual scope of repair for common commercial roof systems, including single-ply membranes, built-up roofing, metal panel roofing, spray polyurethane foam roofing, and the application/maintenance of roof coatings. It will also discuss an assessment methodology that can assist in developing a broader understanding of the condition of the roof surfaces.

Keywords

Forensic engineering, roofs, roofing, repairability, commercial roofing, conceptual scope of repair, repairs, roof sections, built-up roofing, modified-bitumen built-up roofing, ethics, feasible, feasibility, life safety, low slope, single-ply

Introduction

Forensic engineers are commonly engaged to determine the cause and extent of damage to various roofing systems, and then asked to develop conceptual scopes of repair for identified damage. Developing a conceptual scope of repair requires significant knowledge about and experience with the construction of roof assemblies and how any proposed repair would interact with other building components and perform over an extended period. These determinations require careful consideration and the ability to properly assess not only the entire roofing system, but also its geographic location, exposure to chemicals or oils, and other factors that dictate the types of roof assemblies used. Many proposed conceptual scopes of repair do not fully consider the existing conditions that would limit or prohibit the completion of repairs. This understanding is imperative for developing effective repair recommendations because minute details can impact the entire layout and structure of the roofing system.

This paper offers observations and recommendations commonly associated with low-slope roof assemblies, including built-up roofing, modified-bitumen cap sheets, various types of single-ply roof membranes, and others. These roofing systems collectively are referred to as "commercial roofing." The discussion of materials compatibility and manufacturer or industry practices related to repairs would also apply to metal panel roofing assemblies, asphalt-composition shingles, and others.

Finally, damage can occur to roof surfaces from numerous causes. It is not the intent of this paper to discuss the assessment of the specific causes of damage or the establishment of the extent of the damage but rather to focus on determining what factors can limit the overall repairability of a roof assembly upon which damage was identified.

Conceptual Scopes of Repair Objective

Conceptual scopes of repair for roof assemblies are commonly developed to provide broad guidance for the work necessary to repair or replace the assembly. This guidance must comply with applicable building codes, industry and manufacturer's standards or recommendations, and (as necessary) to protect the health, welfare, and safety of the general public. They are typically used to assist with the development of cost estimates and are not intended to represent complete construction

Chad Williams, PE, 1926 East 133 Place South, Bixby, OK 74008 (918) 970-4722, chad.williams@valorforensics.com

documents. Since conceptual scopes of repair are not final, signed, and sealed construction documents, they should not be used by contractors or owners to obtain a building permit or complete necessary repairs.

Code References and Definitions

The 2018 edition of the "International Building Code" (2018 IBC) and the 2018 edition of the "International Existing Building Code" (2018 IEBC) are referenced herein. A review of the specific language of the applicable building code for a specific building is recommended, as the specific references indicated may not apply to all buildings.

A. General Code Provisions

When considering repair options, it is necessary to consider general code provisions.

2018 IBC Section 101.2: General: Scope states:

> *"The provisions of this code shall apply to the construction, alteration, relocation, enlargement, replacement, repair, equipment, use and occupancy, location, maintenance, removal and demolition of every building or structure or any appurtenances connected or attached to such buildings or structures."*[1]

2018 IBC Section 114.1: Unlawful Acts states:

> *"It shall be unlawful for any person, firm or corporation to erect, construct, alter, extend, repair, move, remove, demolish or occupy any building, structure or equipment regulated by this code, or cause same to be done, in conflict with or in violation of any of the provisions of this code."*[2]

2018 IBC Section 1503.1: Weather Protection: General states:

> *"Roof decks shall be covered with approved roof coverings secured to the building or structure in accordance with the provisions of this chapter. Roof coverings shall be designed in accordance with this code, and installed in accordance with this code and the manufacturer's approved instructions."*[3]

B. Health, Welfare, and Safety of the Public

As discussed previously, when developing a conceptual scope of repair, it is essential to keep the health, welfare, and safety of the public at the forefront when considering repair options. Not only is this in keeping with the morally accepted duties and obligations of being an engineer, but it is also codified in engineering canons.

The 2018 IBC Section 101.3: General: Intent states:

> *"The purpose of this code is to establish the minimum requirements to provide a reasonable level of safety, public health, and general welfare through structural strength, means of egress facilities, stability, sanitation, adequate light and ventilation, energy conservation, and safety to life and property from fire, explosion, and other hazards, and to provide a reasonable level of safety to fire fighters and emergency responders during emergency operations."*[4]

2018 IEBC, Section 101.3: General: Intent states:

> *"The intent of this code is to provide flexibility to permit the use of alternative approaches to achieve compliance with the minimum requirements to safeguard the public health, safety, and welfare insofar as they are affected by the repair, alteration, change of occupancy, and relocation of existing buildings."*[5]

The National Society of Professional Engineers (NSPE) Code of Ethics for Engineers Section I Fundamental Canons states (in part):

> *"Engineers, in the fulfillment of their professional duties, shall: 1. Hold paramount the safety, health, and welfare of the public…"*[6]

While obviously inherent to all engineering practices, it bears repeating and emphasis: Inadequate repairs can lead to health and safety issues associated with failure, microbial growth, water incursion, hazardous or toxic exposures, and the like. The recommendations resulting from a conceptual scope of repair — like all other aspects of engineering — require deliberate care and consideration to ensure safe spaces for human occupancy.

C. Roofing Cover and Assembly

It is common for the top weathering surface of a building to be referred to as the "roof." As defined in the 2018 IBC, the visible roof covering is but one component of the broader roof assembly.

1) Roof covering as:

IBC 2018 defines "Roof Covering"

"The covering applied to the roof deck for weather resistance, fire classification, or appearance."[7]

2) Roof assembly

IBC 2018 defines "Roof Assembly" as:

"A system designed to provide weather protection and resistance to design loads. The system consists of a roof covering and roof deck or a single component serving as both the roof covering and roof deck. A roof assembly can include an underlayment, a thermal barrier, insulation, or a vapor retarder."[8]

Similarly, the National Roofing Contractors Association (NRCA) has a definition for a roof assembly that resembles that of the IBC:

"An assembly of interacting roof components including the roof deck, air or vapor retarder (if present), insulation and membrane or primary roof covering designed to weatherproof a structure."[9]

When evaluating roofing damage and developing a conceptual scope of repair, the full construction of the roof assembly should be considered — not just the condition of the roof covering.

D. Roof Repair and Replacement

The terms "roof repair" and "roof replacement" are frequently used interchangeably when discussing or evaluating repair methods. However, it is important to keep the distinction clear as the scale of work associated with each definition is vastly different. The following definitions emphasize the differences between the two.

1) Roof repair

IBC 2018 defines a "roof repair" as:

"Reconstruction or renewal of any part of an existing roof for the purpose of its maintenance."[10]

2018 IEBC defines a "roof repair" as:

"Reconstruction or renewal of any part of an existing roof for the purposes of correcting damage or restoring the predamaged condition."[11]

2) Roof replacement

Both IBC 2018 and IEBC 2018 share the same definition for the term "roof replacement":

"The process of removing the existing roof covering, repairing any damaged substrate, and installing a new roof covering."[12,13]

It is important to note that neither the IBC nor the IEBC includes a definition for the term "damage"; however, distinguishing when damage is a result of an unexpected action versus when it is the result of natural aging or environmental conditions may be requested. The presence of natural and ongoing weathering is often a factor that can limit the overall repairability of a roofing assembly.

E. Roof Section

When developing a conceptual scope of repair, it can be beneficial to demarcate the roof area by mapping it into discrete roofing sections. While there is no specific definition of a "roof section" included within the 2018 IBC, 2018 IEBC, or from the NRCA, the 2020 edition of the Florida Building Code defines a roof section as:

"A separating or division of a roof area by existing expansion joints, parapet walls, flashing (excluding valley), difference of elevation (excluding hips and ridges), roof type or legal description, not including the roof area required for a proper tie-off with an existing roof system."[14]

If the damage can be contained to individual roof sections, developing a conceptual scope of repair for unaffected portions may not be necessary. In some cases, however, this may not always be possible. Smaller buildings may not have physical characteristics that allow for the division or designation of individual roof sections.

Primary Repairability Limitations

The following discussions include common issues that are encountered with commercial roof assemblies. The conditions addressed are not intended to represent every possible issue or situation that may be present. In addition, multiple conditions may exist. In some situations, these conditions may occur simultaneously. As such, the forensic engineer should seek any additional information regarding the site-specific conditions that may affect or

limit the overall repairability of the roof.

A. Roof Assembly Configuration/Construction

When damage is identified to a commercial roofing system and a forensic engineer is requested to develop a conceptual scope of repair, it may be necessary for the engineer to open the roof section to identify the layers and overall construction of the roof assembly. This process is commonly referred to as "coring."

Coring a roof typically consists of drilling a small (2-inch) cylindrical core through the roof assembly to the roof deck or opening a rectangular section to view larger portions of the roof assembly. The roof core can provide an understanding of the type and number of layers present within the roof assembly, the presence of moisture as well as the condition of roof assembly components. Roof core material composition, dimensions, condition, and the presence of moisture should be documented.

When examining the core or section of a roof assembly, it is important to consider any code constraints. For example:

IBC 2018 Section 1511.3.1.1: Reroofing: Exceptions states (in part):

> *"A roof recover shall not be permitted where any of the following conditions occur:*
>
> *3. Where the existing roof has two or more applications of any type of roof covering."*[15]

In these cases, a roof replacement would need to be advised, and, in accordance with the IBC, the replacement would require the full removal of all existing layers.

IBC 2018 Section 1511.3: Reroofing: Roof replacement states (in part):

> *"Roof replacement shall include the removal of all existing layers of roof covering down to the deck."*[16]

Therefore, the presence of two or more roof coverings on an existing roof system represents a repairability limitation.

While the building code would prohibit the recommendation of a third layer of roof covering in these situations, some jurisdictions have adopted local amendments to the building code and permit the construction of a third layer. However, in these situations, a professional engineer must verify the building framing to ensure it can continue to carry the necessary loads. In circumstances where it is permissible to construct a third roof, not only is it recommended to consider the overall structural capacity of the roof framing, but it is also important to consider and assess the interaction of the new roof relative to existing roof drains and other appurtenances.

B. Moisture within the Roof Assembly:

Moisture within the roofing assembly is another common issue that should be assessed. The presence of moisture is a multifaceted concern. Not only does water present issues resulting in the degradation of roof assembly materials, but it can also impact the underlying structure. In addition, entrapped water can increase the weight of the roof assembly. Finally, there are issues associated with bacterial or fungal growth, thereby potentially compromising the air quality within the building.

All of these issues can have a cascading effect over the life of the system, potentially resulting in further water intrusions or failure of the roofing assembly.

IBC 2018 Section 1511.3.1.1: Reroofing: Exceptions states (in part):

> *"A roof recover shall not be permitted where any of the following conditions occur: ...*
>
> *1. Where the existing roof is water soaked or has deteriorated to the point that the existing roof or roof covering is not adequate as a base for additional roofing."*[17]

The 2018 IBC and previous editions do not provide a specific definition for "water soaked." Nevertheless, the analysis of the existing roof system should attempt to identify areas where free water may be present or where the localized moisture contents exceed representative "dry" baselines for the subject roof. Determining the presence of moisture within the roof assembly may include non-destructive assessment methods, including electrical impedance moisture meters or infrared evaluations. However, it is also recommended that direct readings be taken through surface or pin moisture meters from core sampling when possible and in accordance with the manufacturer's instructions. Additional considerations related to obtaining moisture readings are discussed in ASTM International standard D7954, "Standard Practice for Moisture

Surveying of Roofing and Waterproofing Systems Using Non-Destructive Electrical Impedance Scanners."

It is important to note that the building code limitations, as referenced in IBC Section 1511.3.1.1, do not address the causes or potential sources of moisture within the roof assembly. Consequently, the presence of moisture from any cause within a given roof assembly represents a repairability limitation that must be considered.

C. Surface Drainage

Failures related to ineffective surface drainage to modified roof assemblies have been observed. Section 705.1 of the IEBC regarding reroofing states that the re-covering or replacing of an existing roof covering shall comply with the requirements of Chapter 15 of the IBC with the following exception:

> *"Roof replacement or roof recover of existing low-slope roof coverings shall not be required to meet the minimum design slope of one-quarter unit vertical in 12 unit horizontal (2 percent slope) in Section 1507 of the International Building Code for roofs that provide positive roof drainage…"*[18]

This code provision does not indicate that roof drainage during repairs or reconstruction of commercial roofing can be ignored. While the term "positive roof drainage" is not defined in the 2018 IEBC, it is in the definitions section of the IBC.

> *"The drainage condition in which consideration has been made for all loading deflections of the roof deck, and additional slope has been provided to ensure surface drainage of the roof within 48 hours of precipitation."*[19]

Thus, applying the exception from IEBC's Section 705.1 should be viewed relative to IBC's definition of "positive roof drainage." While the IEBC provides flexibility in completing building repairs and alterations, it also emphasizes the need to safeguard public health, safety, and welfare. IEBC Sections 101.3 and 701.2, respectively, underscore these points:

> *"The intent of this code is to provide flexibility to permit the use of alternative approaches to achieve compliance with minimum requirements to safeguard the public health, safety, and welfare insofar as they are affected by the repair, alteration, change of occupancy, addition, and relocation of existing buildings."*[20]

> *"An existing building or portion thereof shall not be altered such that the building becomes less safe than its existing condition."*[21]

To safeguard public health, safety, and welfare, forensic engineers should consider if drainage issues are present in the given roof assemblies and ensure that the conceptual scope of repair resolves such issues. This includes the prolonged presence of water following rain events, the resulting degradation of the roof surface in areas of accumulated water, and issues related to inadequate or ineffective drainage at inlets, scuppers, and roof perimeters.

The paper "Foreseeable Failure: Roof Collapses and Roof Drainage Deficiencies" by Stewart M. Verhulst, P.E., and Travis G. Ebisch, P.E., presents case studies where modifications to buildings resulted in drainage failures, which ultimately contributed to the partial collapse of roof framing and assemblies. In the final part of their paper, Verhulst and Ebisch concluded:

> *"The authors have worked on numerous other collapses caused or contributed to by inadequate roof drainage. Based on these experiences and on conditions that we have observed throughout the built environment, it is clear that roof drainage and the water loads on roof framing resulting from deficient drainage are not properly considered in the design, construction, maintenance, and repair of buildings…"*

> *"Based on the prevalence of dangerous drainage deficiencies and the repeated occurrences of resultant roof collapses, it is the authors' opinion that roof drainage should be treated as a critical life safety issue."*[22]

D. Material Availability or Obsolescence

Decades may pass between the construction of a building and its ultimate demise. However, removing and replacing roof sections for these decades-old buildings is common. In fact, manufacturers often make such changes every few years, including the types of materials produced, the manufacturing processes, and the dimensions in which materials are manufactured. This is especially common with metal roofing panels and decking but has also been noted in other building products. These changes can affect the chemistry of the materials, the colors available, shapes, etc.

When developing a conceptual scope of repair, it is

necessary to confirm if the existing roof's materials are still manufactured or compatible with the current inventory. The lack of material compatibility, such as that occurring from the change in the shape of metal roof panels, may represent a repairability limitation that would need to be considered and resolved as part of the development of a conceptual scope of repair.

E. General Condition of the Roof Assembly

Ongoing degradation is inherent to roofing assemblies; therefore, it is necessary to consider the general condition of the roof assembly and its ability to sustain a durable repair.

General surface degradation of built-up roof systems, including blistering or surface flaking and wearing of the exposed asphalts, is of concern as these conditions allow moisture to enter the roof assembly. Therefore, when surface flaking, wear, or degradation of the seams is noted on the surface of a built-up roof, these conditions represent a repairability limitation.

The side and end laps for commercial roofing systems are susceptible to wear from long-term exposure to the elements and issues potentially related to the original construction. When separations in the form of seam welds or adhesion failures are apparent, this can allow for accelerated degradation of the roofing assembly. Such conditions reduce the ability to conduct a localized repair successfully due to the inability to tie into the system. Furthermore, when a roofing assembly has a history of previous repairs or age-related deterioration, the general condition of the roof assembly may be a repairability limitation.

The condition of roof appurtenances, including wall and cap flashing, HVAC or plumbing boots, and other roofing components, will also degrade over time. Therefore, it is necessary to consider the condition of the roof appurtenances and their tie-ins to the roof assembly as part of determining the overall repairability of the roof assembly.

Finally, the safety of accessing the roof to complete the necessary repairs should also be considered. For example, in cases where metal roof decking is corroded with section loss or water-logged poured gypsum roof decking is present, accessing the roof surfaces to complete repairs may place roof repair personnel at risk of injury or death. As such, it is necessary to consider whether or not the existing roof assemblies have conditions present that would represent a safety risk to those accessing the roof.

F. Construction Defects

Construction defects relative to this section are those defects or deviations from manufacturer requirements that can contribute to water or air intrusions into the roof assembly. Such defects can reduce the capacity of the roof assembly to resist wind and other design loads, and can accelerate weathering of the roof covering.

These types of defects can be present in numerous ways, including incomplete seam bonds/welds, wrinkling of the roof membrane during construction, and many others. However, when such construction defects are present, the consequences of these defects should be assessed to determine if they will contribute to (or result in) the failure of an intended repair. Construction defects contributing to the roofing assembly's failure or subsequent repairs should be resolved before or as part of the conceptual scope of repair.

G. Material Defects

Material defects for commercial roofing will vary depending on the type of roof assembly. For example, modified-bitumen cap sheet material defects may include areas of focused granule loss in reoccurring patterns or locations or linear strips. For single-ply membranes, material defects include, but are not limited to, areas of failure of the membrane surface. The presence of material defects within roof assemblies can allow water to seep through the roof surfaces over time and contribute to accelerated degradation of the roof assembly, which can also contribute to failure of the attempted repairs.

If material defects are present within roofing assemblies, the implications of such conditions should be considered to determine if the noted defects represent a repairability limitation that should be resolved prior to developing repair recommendations.

H. Surface Contamination and Degradation

External contamination can degrade the surface conditions of roof membranes. General Aniline & Film (GAF), a commercial roofing manufacturer, discusses the chemical resistance of thermoplastic polyolefin (TPO), polyvinyl chloride (PVC), and polyvinyl chloride ketone ethylene ester (PVC KEE) membranes in the article, "Chemical Resistance: an 'Engineered' Approach."

> *"In general, roofs should be protected from exposure to chemicals that can damage the roofing system. However, GAF recognizes that leaks from*

grease traps, occasional releases of chemical mists, and other chemical attacks on the roofing system may occur. Strong acids of any type, oxidizers, and most strong bases are known to cause issues with most roofing membranes regardless of type."[23]

(Note: PVC KEE membranes are a chemically resistant PVC blend.)

GAF further addresses chemical degradation to TPO, PVC, and PVC KEE membranes from de-icing salts, dilute acids, strong acids, grease, oils, vegetable fats, animal fats, diesel and jet fuel, and solvents.

In addition, a discussion of surface contaminates appears in a 2017 NRCA article, "Chemical Considerations" (Fester, 2017), in which similar cautions and concerns are echoed:

"A roof membrane, whether it is built-up, polymer-modified bitumen or single-ply, can prematurely age when there is not chemical compatibility with its surroundings. Sources of chemicals that may be incompatible with roof membranes can be found in all sorts of places from exhausts to cleaning supplies to other roofing materials."[24]

Modified-bitumen cap sheets are also susceptible to degradation from exposure to surface contaminants. The Asphalt Roofing Manufacturers Association (ARMA) addresses this in the article "Potential Effects of Contaminants on Modified Bitumen Sheet Materials":

"Modified bitumen roof membranes may be adversely affected by exposure to cooking oils (animal or vegetable) and greases. Unprotected membrane may experience degradation around exhaust vents, where the roof membrane has repeated contact with these contaminants. The organic substances contained within oils and greases may weaken and eventually break down the polymer-bitumen network, causing premature failure of the roof."[25]

The ARMA also addresses other forms of surface contamination, including petroleum-derived products, bacteria, and fungi, and their ability to contribute to the degradation (e.g., swelling, softening, and slumping) of the bitumen compounds.

These conditions, therefore, necessitate the need to identify and consider the presence of surface contamination in a conceptional scope of repair — as they can either limit the ability to complete repairs or reduce the anticipated service life of these repairs.

Primary Repairability Limitations Checklist

The following checklist provides an itemized synopsis of the topics discussed above. It is a general guide of considerations when assessing roof assemblies and developing a conceptual scope of repair. While the concerns listed here are often applied to individual roof sections, there may be situations where they apply universally to a roof assembly, depending on its construction. As in all engineering aspects, there may be additional concerns or considerations beyond what has been addressed here, so it is incumbent upon the forensic engineer to apply due diligence when using this checklist.

The presence of any of the items listed below indicates a repairability limitation that needs to be considered and addressed when developing a conceptual scope of repair.

Primary Repairability Limitations:

- The presence of two or more layers of roof assemblies.
- Elevated moisture or free water is present throughout the roof assembly.
- Elevated moisture or free water present in isolated portions of the roof assembly.
- Indications of poor surface drainage resulting in the accumulation of water, sediments, or debris.
- Suitable and/or compatible building materials are not available to complete repairs.
- Existing roof assemblies exhibit age-related deterioration and/or degradation.
- Construction defects that detrimentally impact the condition or drainage of the roof systems.
- Indications of previous repairs to the existing roof assemblies.

- Indications of previous repairs that have subsequently failed.
- Indications of corroded, waterlogged, or otherwise compromised roof decking.
- Indications of oils, chemicals, or other surface contaminants or related degradation present on the roof surfaces.
- The presence of damage to underlying insulation or other roof assembly components.

If one or more of the factors listed are present and cannot be resolved to meet life safety, building code, and/or manufacturer requirements, then the conceptual scope of repair should include the recommendation for replacing the given roof or roof section.

Additional Repairability Considerations

A. Energy Conservation Codes

Energy conservation codes and the insulation required within roofing assemblies have changed over time. In some locations, jurisdictions will require repairs to comply with current energy conservation codes. When replacing only one area of a roof or roof section and bringing that area up to code, the resulting insulation thickness can result in uneven roof surfaces that will detrimentally affect roof drainage. When it is necessary to construct a roof repair in compliance with current energy codes that are incompatible or do not align with the surrounding roof sections, the removal and replacement of the given roof section is recommended.

B. Roof Coatings

Roof coatings are commonly proposed as an alternative to roof replacement. However, using these coatings introduces additional factors that need to be addressed before recommending the application of such a coating within a conceptual scope of repair.

The IBC does allow for the application of a protective coating over an existing roof covering:

> *"The application of a new protective coating over an existing roof coating, metal roof panel, built-up-roof, spray polyurethane foam roofing system, metal roof shingles, mineral surfaced rolled roofing, modified bitumen roofing, or thermoset and thermoplastic single-ply roofing shall be permitted without tear off of the existing roof coverings."*[26]

However, the code does not waive the specific installation requirements of respective coating manufacturers — nor does it waive the necessity of the proposed repair coating to meet appropriate fire code or other building code requirements[27]. Therefore, it is incumbent on the engineer to ensure all applicable conditions and repair criteria are met.

The primary concern when considering the use of coatings as part of a repair is bonding of the proposed coating to the existing roof coverings or any existing roof coatings. The composition of the numerous types of roof coatings will vary significantly among manufacturers and can change over time. In addition, it is important to follow manufacturer recommendations, as some coating manufacturers will limit the use of their respective products when surface corrosion, standing water, or contamination is present. Additional factors, such as the conditions of the existing roof surface and the potential for surface moisture, should also be considered. In these situations, some coatings will not perform well over an extended period when chronically exposed to standing water.

It is necessary to determine not only the type of existing coatings present on a roofing surface but also to evaluate their condition to ensure they can be safely and effectively used with the proposed repair coating. It is also recommended that any testing necessary to establish proper bonding (e.g., a pull test) be completed per the manufacturer's requirements before including a coating recommendation. Given the numerous coating variations, it is recommended that the forensic engineer discuss proposed repairs with the respective technical or manufacturing representatives.

C. Cost Considerations

While cost considerations can be a weighty influence on any repair or replacement recommendation, professional engineers are obligated to consider this aspect of their recommendation only after ensuring the proposed repairs meet life safety considerations, applicable building codes/industry standards, environmental considerations, and manufacturer's recommendations and guidance.

Conclusion

Forensic engineers are commonly requested to develop conceptual scopes of repair as part of their work. Identifying the potential damage associated with commercial roofing systems is a complex process. It is not simply a matter of specifying existing roofing materials or methods but requires careful analysis of the present conditions. Therefore,

it is important for the forensic engineer to consider the factors listed herein and other provisions specific to their given situation. Failure to wholly assess the conditions impacting the roof assembly and subsequent supporting structure can not only compromise the recommended repair, the roofing assembly, and the structure, but it can also unnecessarily place the health, welfare, and safety of the public at risk.

It is understood that conceptual scopes of repair are at times developed by individuals other than forensic engineers. The repairability limitations indicated herein should be considered by anyone considering a scope of repair or developing a conceptual scope of repair.

References

1. INTERNATIONAL BUILDING CODE (IBC) | ICC DIGITAL CODES, Section 101.2 Scope, 2018. [Online.] Available: https://codes.iccsafe.org/content/IBC2018/chapter-1-scope-and-administration.

2. INTERNATIONAL BUILDING CODE (IBC) | ICC DIGITAL CODES, Section 114.1 Unlawful Acts, 2018. [Online.] Available: https://codes.iccsafe.org/content/IBC2018/chapter-1-scope-and-administration.

3. INTERNATIONAL BUILDING CODE (IBC) | ICC DIGITAL CODES, Section 1503.1 Weather Protection – General, 2018. [Online.] Available: https://codes.iccsafe.org/content/IBC2018/chapter-15-roof-assemblies-and-rooftop-structures.

4. INTERNATIONAL BUILDING CODE (IBC) | ICC DIGITAL CODES, Section 101.3 General - Intent, 2018. [Online.] Available: https://codes.iccsafe.org/content/IBC2018P6/chapter-1-scope-and-administration.

5. INTERNATIONAL EXISTING BUILDING CODE (IEBC) | ICC DIGITAL CODES, Section 101.3 General - Intent, 2018. [Online.] Available: https://codes.iccsafe.org/content/IEBC2018P4/chapter-1-scope-and-administration.

6. National Society of Professional Engineers | Code of Ethics, Section I - Fundamental Canons, July 2019. [Online.] Available: https://www.nspe.org/resources/ethics/code-ethics.

7. INTERNATIONAL BUILDING CODE (IBC) | ICC DIGITAL CODES, Section 202 Definitions – Roof Coverings, 2018. [Online.] Available: https://codes.iccsafe.org/content/IBC2018P6/chapter-2-definitions.

8. INTERNATIONAL BUILDING CODE (IBC) | ICC DIGITAL CODES, Section 202 Definitions – Roof Assembly, 2018. [Online.] Available: https://codes.iccsafe.org/content/IBC2018P6/chapter-2-definitions.

9. National Roofing Contractors Association. "Glossary – 'Roof Assembly'." NRCA.net. Accessed: Feb. 16, 2023. [Online.] Available: https://nrca.net/technical/glossary.

10. INTERNATIONAL BUILDING CODE (IBC) | ICC DIGITAL CODES, Section 202 Definitions – Roof Repair, 2018. [Online.] Available: https://codes.iccsafe.org/content/IBC2018P6/chapter-2-definitions.

11. INTERNATIONAL EXISTING BUILDING CODE (IEBC) | ICC DIGITAL CODES, Section 202 Definitions – Roof Repair, 2018. [Online.] Available: https://codes.iccsafe.org/content/IEBC2018P4/chapter-2-definitions.

12. INTERNATIONAL BUILDING CODE (IBC) | ICC DIGITAL CODES, Section 202 Definitions – Roof Replacement, 2018. [Online.] Available: https://codes.iccsafe.org/content/IBC2018P6/chapter-2-definitions.

13. INTERNATIONAL EXISTING BUILDING CODE (IEBC) | ICC DIGITAL CODES, Section 202 Definitions – Roof Replacement, 2018. [Online.] Available: https://codes.iccsafe.org/content/IEBC2018P4/chapter-2-definitions.

14. FLORIDA BUILDING CODE, EXISTING BUILDING, 7TH EDITION | ICC DIGITAL CODES, Section 202 General Definitions – Roof Section, 2020. [Online.] Available: https://codes.iccsafe.org/content/FLEBC2020P1/chapter-2-definitions.

15. INTERNATIONAL BUILDING CODE (IBC) | ICC DIGITAL CODES, Section 1511.3.1.1 Exceptions, 2018. [Online.] Available: https://codes.iccsafe.org/content/IBC2018P6/chapter-15-roof-assemblies-and-rooftop-structures.

16. INTERNATIONAL BUILDING CODE (IBC) | ICC DIGITAL CODES, Section 1511.3 Roof replacement, 2018. [Online.] Available: https://codes.iccsafe.org/content/IBC2018P6/chapter-15-roof-assemblies-and-rooftop-structures.

17. INTERNATIONAL BUILDING CODE (IBC) | ICC DIGITAL CODES, Section 1511.3.1.1 Exceptions, 2018. [Online.] Available: https://codes.iccsafe.org/content/IBC2018P6/chapter-15-roof-assemblies-and-rooftop-structures.

18. INTERNATIONAL EXISTING BUILDING CODE (IEBC) | ICC DIGITAL CODES, Section 705.1 – General, 2018. [Online.] Available: https://codes.iccsafe.org/content/IEBC2018P4/chapter-7-alterations-level-1.

19. INTERNATIONAL BUILDING CODE (IBC) | ICC DIGITAL CODES, Section 202 Definitions – Positive Roof Drainage, 2018. [Online.] Available: https://codes.iccsafe.org/content/IBC2018P6/chapter-2-definitions.

20. INTERNATIONAL EXISTING BUILDING CODE (IEBC) | ICC DIGITAL CODES, Section 101.3 Intent, 2018. [Online.] Available: https://codes.iccsafe.org/content/IEBC2018P4/chapter-1-scope-and-administration.

21. INTERNATIONAL EXISTING BUILDING CODE (IEBC) | ICC DIGITAL CODES, Section 701.2 Conformance, 2018. [Online.] Available: https://codes.iccsafe.org/content/IEBC2018P4/chapter-7-alterations-level-1.

22. S. M. Verhulst, and T. G. Ebisch, "Foreseeable Failure: Roof Collapses and Roof Drainage Deficiencies," ASCE Forensic Engineering 2022. [Online.] Available: https://doi.org/10.1061/9780784484548.007.

23. GAF. "Chemical Resistance An "Engineered" Approach." https://www.gaf.com/. Accessed: Mar. 4, 2023. [Online.] Available: https://www.gaf.com/en-us/document-library/documents/productdocuments/commercialroofingsystemsdocuments/pvcdocuments/pvcmembranesdocuments/pvcfleecebackdocuments/everguardpvc50fleecebackmembranedocuments/Guide__Chemical_Resistance_Guide_for_TPOPVC.pdf.

24. K. B. Fester, "Chemical consideration," Professional Roofing Magazine., vol. 47, issue 11, Nov. 1, 2017. [Online.] Available:https://www.professionalroofing.net/Articles/Chemical-considerations--11-01-2017/4127.

25. Asphalt Roofing Manufactures Association, "Technical Bulletin - Potential Effects of Contaminants on Modified Bitumen Sheet Materials." www.asphaltroofing.org Apr. 20, 2020. Retrieved March 4, 2023, [Online.] Available: https://www.asphaltroofing.org/the-effects-of-greases-oils-and-chemicals-on-modified-bitumen-sheet-materials/.

26. INTERNATIONAL BUILDING CODE (IBC) | ICC DIGITAL CODES, Section 1511.3.1 Roof recover Paragraph 4. , 2018. [Online.] Available: https://codes.iccsafe.org/content/IBC2018P6/chapter-15-roof-assemblies-and-rooftop-structures.

27. M. S. Graham, "Coating concerns - Building Code Compliance for Roof Coatings is Limited." Professional Roofing, p, 24–25, Mar. 2019. [Online.] Available: https://www.nrca.net/Technical/PDF?id=175908&k=25444.

Utilizing ASCE/SEI 7 to Estimate Wind Speeds for Forensic Investigations

By Lucas Pachal, PE (NAFE #1232A) and Paul Warner, PE (NAFE #1234A)

Abstract

The American Society of Civil Engineers/Structural Engineering Institute (ASCE/SEI) 7 standard is utilized to determine design wind loading on buildings and other structures. However, it can also be utilized in a forensic capacity to approximate a wind speed that would cause specific conditions to occur, such as the overturning of a structure. This paper provides a brief overview of the ASCE/SEI 7 method for wind loading and discusses the use of various adjustment factors used to determine the wind on structures, including wind directionality factor, velocity pressure coefficient, topographic factor, and the ground elevation factor. A clear understanding of these factors — and how to apply them — is crucial to estimating a wind speed and resulting force to cause a particular event or condition to occur.

Keywords

ASCE 7, ASCE/SEI 7, wind, overturning, sliding, yielding, forensic investigation, forensic engineering

Introduction

Much work has been published through industry organizations related to wind and resulting damage to buildings and structures. Damage surveys following natural disasters such as hurricanes have correlated measured wind speeds to expected building performance based on current code provisions[1]. Dynamic finite element analysis has evaluated the effects of wind shedding on tall slender structures following collapses[2].

Investigations have been completed related to the design and construction practices for temporary structure installations after failures to identify shortcomings in the employed processes[3]. Many more publications documenting testing, research, or investigations may be cited to understand how known wind or other environmental conditions have affected structures. But what about when environmental conditions are unknown, and an event has occurred? Many times in forensic engineering, what is needed to assist the trier of fact understand a sequence of events is a straight-forward determination of complex engineering principles to demonstrate if a minimum standard of care was or was not met. One such example is determining minimum wind speeds necessary to cause a specific structural response.

The ASCE/SEI 7 standard[4] is frequently used to determine design loading, including wind on buildings and other structures. Determining the force required for a specific condition to occur, such as overturning a structure, moving an item, or yielding a component, is a simple calculation if you have basic information regarding the geometry, weight of the structure and any supported cladding or components, and, if necessary, material strength characteristics.

This paper is focused on estimating a wind speed required to cause an event or action to occur — not in evaluating weather station data to determine an applied load on a structure at a particular time. The design wind pressure (loading) for a given structure is based on various adjustment factors considering the structure type and geometry, height, site location, statistics, probabilities, and topography of the site. Appropriately estimating a wind speed resulting in specific forces acting on a structure requires an understanding of these factors and their appropriate application.

The ASCE/SEI 7 standard, which is intended for design of structures, is organized in a manner considering design engineers will be using the document. However, the application of all factors used in design may not be relevant. For this paper, ASCE/SEI 7-16[4] is referenced, which considers some differing factors (such as the ground elevation coefficient), and utilizes an importance factor of 1.0 for all wind. These factors differ from earlier versions of

Lucas Pachal, PE, 217 Grandville Ave SW #302, Grand Rapids, MI 49503, (800) 222-1868, lpachal@nederveld.com

the standard; however, the same procedure may be modified and applied to those earlier code editions. Additionally, this method may be used directly with the provisions of ASCE/SEI 7-22, the most recent published edition of the standard, if adopted by the local building department. Utilization of an earlier version of the ASCE/SEI 7 standard is not recommended by the authors though, as additional testing and research has resulted in the refinement of wind force determination in ASCE/SEI 7.

Background

Estimating the wind speed required to induce forces large enough for a particular structural reaction to occur is most likely to be used in the jurisprudence process resulting from a claim of property loss, injury, and/or harm. Therefore, use of accepted standards and methods is crucial to the work being admissible in a legal setting.

The ASCE/SEI 7 standard was developed as a progression of the ANSI A58 standard following extensive testing, modeling, and statistical analysis. ASCE/SEI 7 is widely referenced by current and historical model building codes and actively utilized in industry as a method for calculating wind loading (and other environmental forces) for buildings and structures. Larger, global structural failures (or investigations of structures outside the scope of Chapters 27, 28, or 29 of ASCE/SEI 7) require additional consideration and would likely warrant a structure-specific evaluation such as a wind tunnel analysis.

The ASCE/SEI 7 equation 26.10-1 is used to determine the velocity pressure at some height "z" above the ground. The velocity pressure coefficient is then used to calculate a pressure on the structure based on the structure type[3].

$$q_z = .00256\, K_z K_{zt} K_d K_e V^2 \quad \text{(EQ 26.10-1)}$$

Review of each of these factors is crucial to applying them appropriately to determine the wind speed to overturn a structure.

The 0.00256 factor accounts for the stagnation pressure at mean sea level and standard atmospheric pressure. This is a constant value, but is based on variables, which are accounted for in the latter coefficients.

K_z is the velocity pressure exposure coefficient evaluated at height "z" above the ground surface. The ASCE/SEI 7 standard is based on a normalized three-second gust at 33 feet (10 meters) above the ground for exposure category C. The standard measurement elevation and exposure is noted in the wind speed maps and is apparent with review of Table 26.10-1 of the standard. This factor is used to adjust the wind pressure on a structure based on exposure category and height of the structure (or part of that structure). Heights below 15 feet have a constant value[4].

To account for different wind slowdown or drag effects, three exposure categories are utilized in ASCE/SEI 7 based on obstructions in the area of consideration. The exposure categories are based on Surface Roughness Categories B, C, and D. The exact definitions are within the standard, but generally roughness B is an urban or suburban area with many close obstructions, roughness C is an open area with scattered obstructions, and roughness D is an unobstructed area like water[4].

K_{zt} is the topographic factor used to account for wind speed-up effects at terrain features such as hills or escarpments[4]. This factor requires specific placement of a structure on or adjacent to a terrain feature as well as specific geometry of the feature itself. The resulting increase in velocity pressure is the result of a speed-up effect that has been demonstrated in wind-tunnel testing.

K_d is the wind directionality factor. Commentary section C26.6 of ASCE/SEI 7 states that this factor accounts for two effects: "(1) The reduced probability of maximum winds coming from any given direction and (2) the reduced probability of the maximum pressure coefficient occurring for any given wind direction."[4]

K_e is the ground elevation factor to adjust the calculated pressure for altitude (air density)[4]. As the air density decreases with altitude, so does the resulting velocity pressure caused by wind.

V is the wind speed used to calculate the pressure based on the wind speed maps[4]. In the authors' procedure, they are solving for this velocity; therefore, the wind speed maps are not required for use.

Application

The purpose of this procedure is to estimate the wind speed required to cause an event or action to occur — not estimating the forces acting upon the structure from weather data at local weather stations. This is an important distinction to make when the information is provided and/or explained to others (clients, attorneys, jurors, etc.). Three key points result from this distinction that affect the

calculation of the wind pressure on a structure using the ASCE/SEI 7 methodology:

1. The exposure category of the surrounding area (used in determination of the velocity pressure exposure coefficient, K_z) is only considered to modify the wind pressure as it varies with height. Following the design load development provisions of ASCE/SEI 7 and altering pressures due to variances between exposure C (at a standardized measurement location) and the exposure of the subject structure is not applicable. This is because the methodology being considered is not comparing weather station data (reported within exposure category C) to the structure location. Instead, it is considering the effects of wind at different elevations. This change in pressure profile with height is affected by the wind interacting with the terrain and is most evident when the values for each exposure category are normalized about 15 feet in height (**Figure 1**).

Figure 1
Force required to overturn a short structure in the desert.

Figure 2
Force required to overturn a short structure in the city.

While this may seem counter intuitive to the ASCE/SEI 7 methodology, consider the following: A structure less than 15 feet in height located in an urban setting (exposure B) would be subjected to the same force for a given wind speed as an identical one at an airport (exposure C). This is because the pressure/force on a structure for a given wind speed is calculated based on the geometry/type of the structure. Any structures 15 feet or less in height have a constant velocity pressure coefficient, and they would develop the same pressure/force for a given wind speed (**Figure 1** and **Figure 2**). Therefore, the velocity pressure coefficient should be normalized about 15 feet in height to account for the above-described conditions as well as account for pressure changes with height (**Figure 3**).

2. Topographic features such as hills are relevant as they change the assumed wind speed/pressure profile with respect to the height of a structure. Reviewing the calculations for the topographic factor (K_{zt}), it can be noted that the coefficient varies by exposure category. Therefore, for the same reason as noted above, this value needs to be normalized. The height about which the values

Height	Exposure B	Exposure C	Exposure D
15	1.00	1.00	1.00
20	1.09	1.06	1.05
25	1.16	1.11	1.09
30	1.23	1.15	1.13
33	1.26	1.18	1.15
40	1.33	1.22	1.18
50	1.42	1.28	1.23
60	1.49	1.33	1.27
70	1.56	1.38	1.30
80	1.63	1.42	1.34
90	1.68	1.46	1.36
100	1.74	1.48	1.39
120	1.82	1.54	1.44
140	1.91	1.60	1.48
160	1.98	1.64	1.50
180	2.05	1.68	1.53
200	2.11	1.72	1.56
250	2.25	1.80	1.63
300	2.37	1.87	1.68
350	2.47	1.93	1.73
400	2.58	1.99	1.77
450	2.67	2.04	1.81
500	2.74	2.08	1.83

Figure 3
Velocity pressure coefficients (K_z) normalized about 15 feet for each exposure category.

are normalized should be the same height as the velocity pressure coefficient.

3. The wind directionality factor (K_d) is not applicable. This factor is used in a design application to account for the reduced probability that a maximum design wind speed and resulting pressure coefficient occur in a direction that is critical to the structure. Review of ASCE/SEI 7-16 Table 26.6-1 has values ranging from 0.85 to 1.0 for various structure types. It also notes that the factor should only be applied when wind tunnel testing is not being used to determine wind forces acting upon a structure. This is not the condition being considered when estimating a wind speed to cause a specific condition to occur like overturning. This process considers the wind pressure being applied to the structure in the critical direction to produce the most conservative results.

The ground elevation factor (K_e) is appropriate to apply, as the density of air changes with elevation. This air density is assumed to be that which is present at sea level — so at elevated sites, the decrease in air density will revise the 0.00256 stagnation pressure factor noted previously.

Additional factors, such as the gust effect (G), external pressure coefficients (C_p), and solidity ratio (ε), require consideration for application in each specific investigation. The applicability of each factor is beyond the depth of this paper. Further, the application of the Envelope Procedure, provided in Chapter 28 of ASCE/SEI 7, may be considered if the structure being considered is a low-rise structure (less than 60 foot mean roof height). The Envelope Method was developed for use with low-rise buildings only; therefore, it is not appropriate for taller or non-building structures.

Case Study

Consider a portal frame-type structure (**Figure 4**) that is constructed of aluminum pre-engineered box truss sections (commonly used for stages and supporting equipment) at an entrance to a public event with a sign attached to the horizontal beam member as well as decorative faux foliage attached to the truss members. People would pass under the structure to enter the event. The structure is 11 feet tall by 11 feet wide and weighs 350 pounds (with a calculable weight distribution with respect to height). In this specific case study, it is a temporary structure, and is not anchored to the ground, relying solely on structure weight to resist overturning.

Structures such as this can be subject to various codes and/or standards, depending on what has been adopted by the local authority having jurisdiction (AHJ). In the case of the subject structure, the local jurisdiction had adopted the International Building Code (IBC) and made it applicable to temporary structures of this construction type that references the ASCE/SEI 7 standard. However, in lieu of local requirements, standards (such as ANSI E1.21-2013 *Entertainment Technology - Temporary Structures Used for Technical Production of Outdoor Entertainment Events*) could be utilized to provide guidance that will ultimately reference the ASCE/SEI 7 and ASCE/SEI 37-02 (*Design Loads on Structures During Construction*) standards. Had the AHJ not adopted IBC for this structure, a minimum design wind speed of 40 mph with a factor of safety of 1.5 would be considered using the above ANSI standard[5,6].

Due to the actual mechanism of failure being overturning of the structure, sliding or uplift of a light structure such as this may also be appropriate to consider. However, for the purpose of this paper, these failure mechanisms were not evaluated.

The structure is less than 15 feet tall; therefore, the velocity pressure is constant for the full height of the structure. Since the structure was considered a trussed tower, the solidity ratio (solid area divided by gross area of the face) of the framework is used to calculate the force coefficient for the truss sections. A different force coefficient

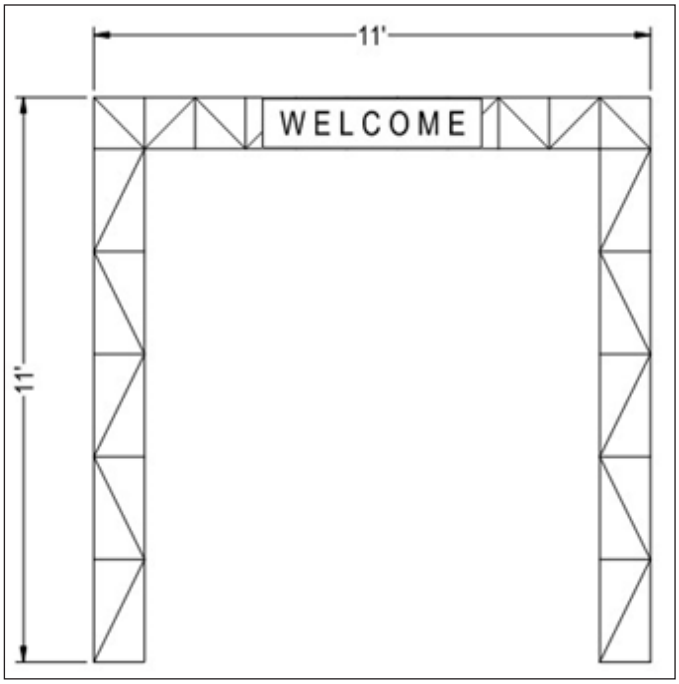

Figure 4
Diagram of structure for case study.

must be utilized for the sign versus the framework, as it is a solid surface.

Utilizing the appropriate force coefficients for the structure and the attached sign, one can calculate the resulting loading on each component for a given wind speed. Since the sign and truss sections use different force coefficients, it is necessary to set up equations for each component referencing the same wind speed variable. Using systems of equations for overturning forces for the various components, a resulting wind speed involved in overturning of the structure can be determined.

The decorative faux foliage added to the frame would increase the solidity ratio but is difficult to accurately quantify. As such, the authors determined that by considering the faux foliage to increase the solidity ratio of the structure, it resulted in a lower calculated wind speed required to cause overturning. This decrease in calculated windspeed is because there is more considered surface area for the wind to interact with, resulting in more force applied to the structure for a given wind speed.

In practice, this can be accounted for by varying the considered area and providing a range for the overturning wind speed. For the purposes of this paper, the area of faux foliage was held constant to make the comparison easier to understand.

The calculation to determine the overturning wind speed was performed in the three exposure categories with the unmodified factors and compared to the modified factors previously identified herein (indicated as the "NA" column of **Figure 5**). For this case study, the estimated overturning windspeed varied from 7% to 44% higher than the modified factor calculation, when (inappropriately) considering all the ASCE/SEI 7 prescribed design factors.

Exposure	B	C	D	NA
K_{zt}	1	1	1	1
K_z	0.57	0.85	1.03	1
K_d	0.85	0.85	0.85	1
K_e	1	1	1	1
$V_{overturning}$ (mph)	35.8	29.3	26.6	24.9
% Difference	44%	18%	7%	—

Figure 5
Comparison of overturning wind speeds for the case study in the three exposure categories with no modification to the factors (B-D) compared to modified factors.

Potential Next Steps

Though the purpose of this paper is to present the method to utilize ASCE/SEI 7 to estimate wind speeds that would cause a particular event or condition to occur, this may be taken further in a forensic application. There are a number of engineering and design codes, such as the International Building Code (IBC)[7], the International Residential Code (IRC)[8], and AASHTO Signs, Luminaires, and Traffic Signs[9] that refer to ASCE/SEI 7 for wind loads and calculations methods. Other codes could be reviewed for applicability for the methods shown here. In addition, engagement with a forensic meteorologist may be warranted if local weather stations are not within reasonable proximity to the site in question. Through the involvement of forensic meteorology, in conjunction with these calculations, it is possible to substantiate causation of a particular event or condition on a specific date.

Conclusion

The ASCE/SEI 7 method for calculating wind loading on structures can be utilized in a forensic capacity; however, it is critical that engineers performing the calculations understand what information they are presenting. This paper considered the ASCE/SEI 7 method for estimating the wind speed required to cause a particular event to occur, such as to overturn a structure. This is likely to be applicable to engineering standards and codes that reference ASCE/SEI 7 for wind-related design criteria.

Modification of the velocity pressure coefficient (K_z) and wind directionality factor (K_d) are necessary to accurately perform the calculation. If no modification of the factors is performed, it can lead to an inaccurate estimation. As illustrated in the case study, overestimation of the wind speed required to overturn the structure ranged from 7% to 44%, considering the simple structure presented. This will vary based on the size and type of structure being considered.

References

1. Jean-Paul Pinelli, Ph.D., PE, M.ASCE, et al; Overview of Damage Observed in Regional Construction During the Passage of Hurricane Irma over the State of Florida; Proceedings of Forensic Engineering 8th Congress; National Science Foundation; 2018.

2. E. S. Lim, et al; Forensic Investigation of a Slender High-Rise Structure Subject to Dynamic Wind Conditions; 2019 IOP Conference Series: Earth and Environmental Science 244; 2020.

3. Dan Eschenasy, PE, M. ASCE; Wind Related Failures of Temporary Construction Installations; Forensic Engineering 2009: Pathology of the Built Environment; American Society of Civil Engineers; 2010.

4. American Society of Civil Engineers, ASCE/SEI 7-16 Minimum Design Loads and Associated Criteria for Buildings and Other Structures, Reston, Virginia: American Society of Civil Engineers, 2017.

5. American National Standards Institute, ANSI E1.21-2013 Entertainment Technology - Temporary Structures Used for Technical Production of Outdoor Entertainment Events, Washington, DC: American National Standards Institute, 2013.

6. American Society of Civil Engineers, ASCE/SEI 37 - Design Loads on Structures during Construction, Reston, Virginia: American Society of Civil Engineers, 2010.

7. International Building Code; International Code Council, Inc.; 4051 Flossmoor Road, Country Club Hills, IL 60478; 2020

8. International Residential Code; International Code Council, Inc.; 4051 Flossmoor Road, Country Club Hills, IL 60478; 2020

9. AASHTO LTS, 6th Edition; Standard Specifications for Structural Supports for Highway Signs, Luminaires, and Traffic Signals; American Association of State Highway and Transportation Organizations; 555 12th Street NW, Suite 1000, Washington, DC 20004; 2022.

Forensic Engineering Investigation of a Machine Guarding-Related Injury

By Jason McPherson, PE, DFE (NAFE 852M)

Abstract

OSHA regulations and industry-accepted standards are intended to be used in conjunction to help prevent worker injury. Despite the aforementioned intention, a point of operation injury occurred to an employee while he was operating a hydraulic rotary bending machine. The machine had been retrofitted with a two-hand control device that was intended to act as a means of point of operation safeguarding. A forensic engineering analysis of both the electromechanical design and programmable logic code — combined with a performance and prescriptive requirement analysis — ultimately revealed flaws in the design of the electromechanical system and software design. It also demonstrated a lack of adherence to the applicable industry-accepted standards related to machine guarding. These factors led to the point of operation injury.

Keywords

Forensic engineering, standards, machine guarding, safeguard, ANSI B11, OSHA, point of operation, normative reference, NFPA 79

Automated Machinery Hazards

Automated machinery is being used in growing numbers. While the automated machine may be used to alleviate one set of problems (e.g., repetitive motions), machinery may present a different set of hazards. There are several types of hazards related to machinery, such as electrical, noise, and burns. The largest number of injuries to operators occurs at the point of operation in the area where the machine tooling interfaces with the in-process part. As of 2021, machine guarding-related amputations and injuries remain on OSHA's top 10 list of most frequently cited issues[1]. Mechanical hazards are those that can generally be addressed by using machine guarding.

Examples of machine mechanical hazards are[2]:

- Power transmission
- Point of operation
- In-running nip points
- Rotating or reciprocating machine parts
- Flying chips, sparks, or parts

Machine Guarding Requirements

To address the issue of operator injury, OSHA requires that one or more methods of machine guarding be used to protect workers. As it relates to machine guarding, OSHA requirements are performance based — not prescriptive based. Therefore, for point of operation guarding, OSHA requires the guarding be in conformity to any appropriate standards[3], which provide the designer with prescriptive measures used to meet the performance requirements set forth by OSHA.

Voluntary Standards

The American National Standards Institute does not generate standards. Instead, it provides a framework for standards development. There are currently approximately 230 ANSI-accredited standards organizations. Examples of ANSI-accredited standards organizations are B11 Standards, Inc., National Fire Protection Association, ASTM International, and the American Society of Safety Professionals.

Machine Guarding Standards

Machine guarding standards employed within the United States include the American National Standards Institute B11 standards for machine guarding, which are generated by B11 Standards, Inc. These prescriptive-based

Jason McPherson, PE, PO Box 888682, Grand Rapids, MI 49588-8682; (616) 566-5669; jasonmcpherson05@gmail.com

standards specify methods for both the manufacturers of machines (suppliers) and the end-users (users) of machines to utilize in order to minimize the risks involving machine hazards.

The ANSI B11 *Machine Guarding Standards and Technical Reports* consist of documents pertaining to machine guarding. Essentially, these are standards that a person exercising reasonable skill and care would utilize during the design of machine guarding. They are also used by both federal and state OSHA. Additionally, they are used by the legal community in cases related to the safety of machinery[4].

In order to utilize the ANSI B11 standards, the person(s) utilizing the standards must understand their basic structure. The ANSI B11 standards are structured in the ISO type A, B, C structure (**Figure 1**). Type A standards are considered basis standards; they provide basic concepts and principles for design. Type B standards are considered generic safety standards, covering one or more safety topics for safeguards that can be applied to a variety of machinery. Type C standards contain safety requirements for specific machinery[5].

The ANSI B11 standards, like many other types of standards, contain normative references, which are additional documents (or portions of documents) that are incorporated into a standard by reference — meaning they become part of the referencing standard.

Case Study

The following case study details an investigation related to a partial amputation workplace injury involving an automated hydraulic rotary bending machine that was utilized to bend metal tubing. **Figure 2** shows the automated hydraulic rotary bending machine that was involved in the accident.

Figure 2
Automated hydraulic rotary tubing bender.

Machine Tooling

The main tooling components are the mandrel, pressure die, clamp die, bend die, wiper die, and bend arm (**Figure 3**). The components are defined as follows:

- Mandrel — provides internal support for the tubing walls during the bend operation.
- Clamp die — holds the tube against the bend die.
- Bend die — the tube is rotated around the bend die during the bend operation.

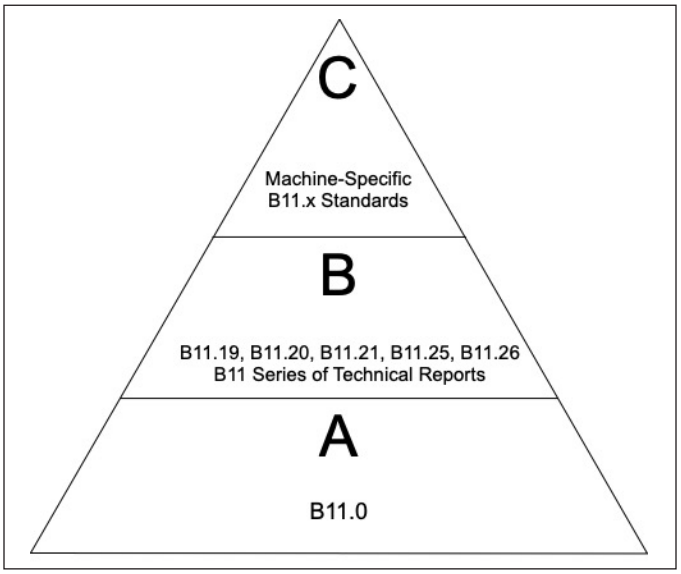

Figure 1
ISO type A, B, C structure, ANSI B11.0 Safety of Machinery[5].

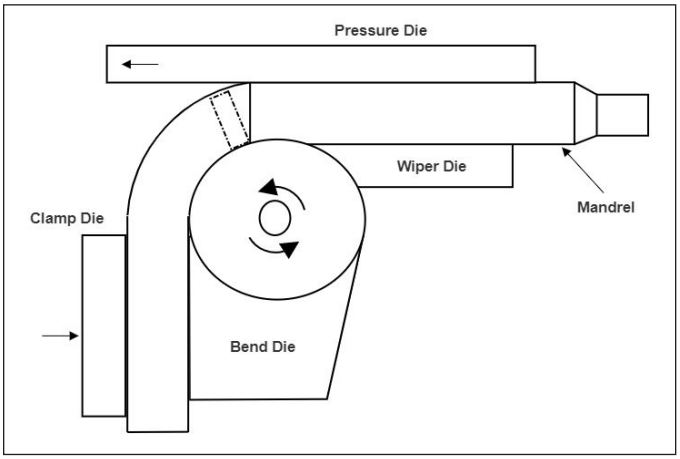

Figure 3
Tooling, ANSI B11.15[6].

- Pressure die — reduces drag and damage to the tube during bending.
- Wiper die — option tooling for use during tight bends to prevent wrinkles.
- Bend arm — rotates the bending die.

In an effort to comply with safety regulations regarding point of operation guarding set forth by OSHA[3], the manufacturing facility purchased a dual palm remote stand (**Figure 4**) from the hydraulic rotary bending machine manufacturer. Per the manufacturer's proposal, the device was intended for enhanced operator safety, and was installed/integrated into the hydraulic rotary bending machine's control system by the machine manufacturer.

Bend Cycle

The machine home position consists of the bend arm in the home position, the clamp die and pressure die open, and the mandrel in the advanced position. In the home position, the machine is ready to have a tube loaded into the point of operation. The operator slides the tube over the mandrel. The operator initiates a bend (forward) cycle by concurrently depressing and maintaining the two forward pushbuttons located on the dual palm remote stand. The clamp die would clamp the tubing, and the bend arm would rotate the bending die. During a forward cycle, the programmable logic controller would monitor the status of the field-mounted bend arm home limit switch in **Figure 5**. The limit switch actuator would be depressed by a bar that would move in concert with the bend arm.

If the limit switch contacts were closed, the programmable logic controller would consider the bend arm to be in the home position. If the limit switch contacts were open, the programmable logic controller would consider the bend arm to be away from the home position. At this point, the operator could remove their hands from the two forward pushbuttons. Once the forward cycle was complete, the bend arm would return to the home position, the mandrel would retract, clamp dies would open, and then the mandrel would advance to await the next cycle. The machine would then wait for the operator to initiate a forward cycle.

The Accident

The intent of the dual palm remote stand was to initiate a machine forward cycle only when each of its forward cycle pushbuttons were depressed concurrently and maintained throughout the time the point of operation hazardous conditions existed. However, the machine operator sustained a partial amputation injury to one of his hands, when the machine performed an unexpected start[5] while he was trying to correct a part placement. He was not depressing both forward cycle pushbuttons when the machine performed the unexpected start.

The Investigation

The operator was not available for interview, but it was learned by interviewing plant personnel that the operator initiated a forward bend cycle and inadvertently depressed the emergency stop pushbutton located on the dual palm remote stand while the bend arm was at a low bend angle position. The operator attempted to resolve the situation by using the reverse cycle to return the tooling to

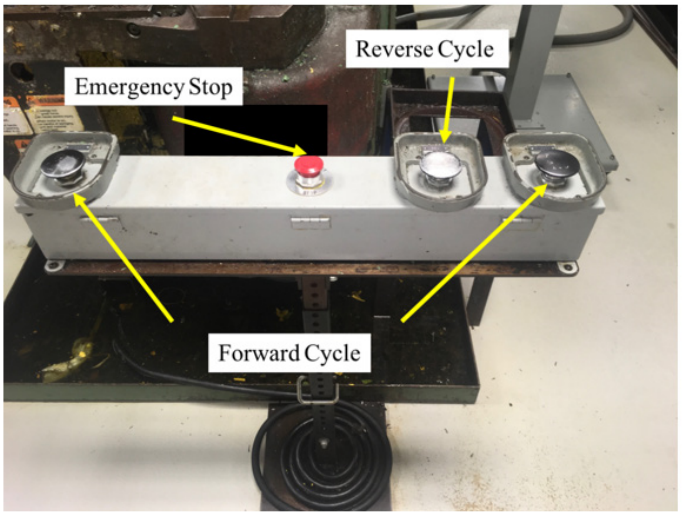

Figure 4
Dual palm remote stand.

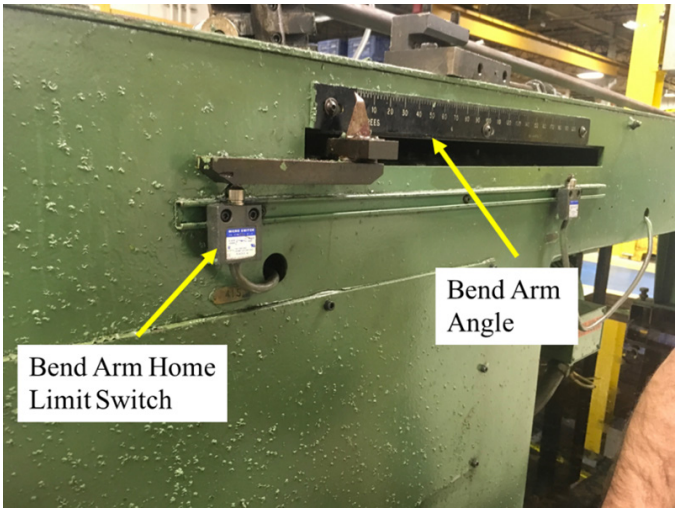

Figure 5
Limit switch.

their home positions. The tubing became dislodged when the mandrel advanced forward to its home position. The operator attempted to grab the tubing and feed it over the mandrel, when the part clamp dies closed unexpectedly — ultimately causing the injury.

Manufacturer's Evaluation

A field service technician from the machine manufacturer performed a separate investigation of the incident. Subsequently, a service report was written. The report indicated that there were three scenarios that would result in an unexpected start. The report indicated that the personal injury was simply the result of a mis-adjustment of the bend arm home limit switch in **Figure 6**. Subsequent to the injury, an updated version of the programmable logic controller software was implemented that was intended to address this issue.

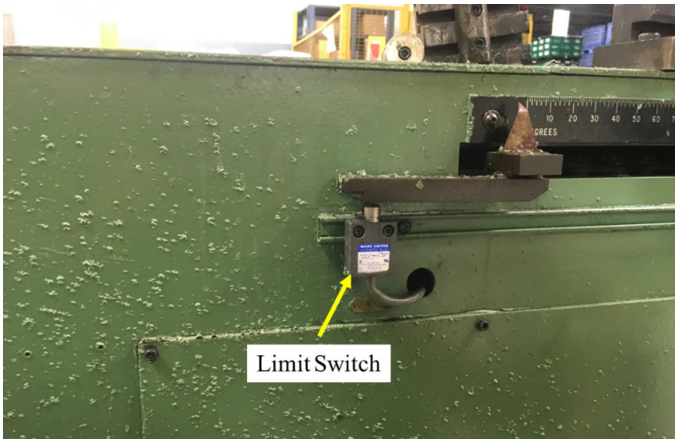

Figure 6
Limit switch alleged to be misadjusted.

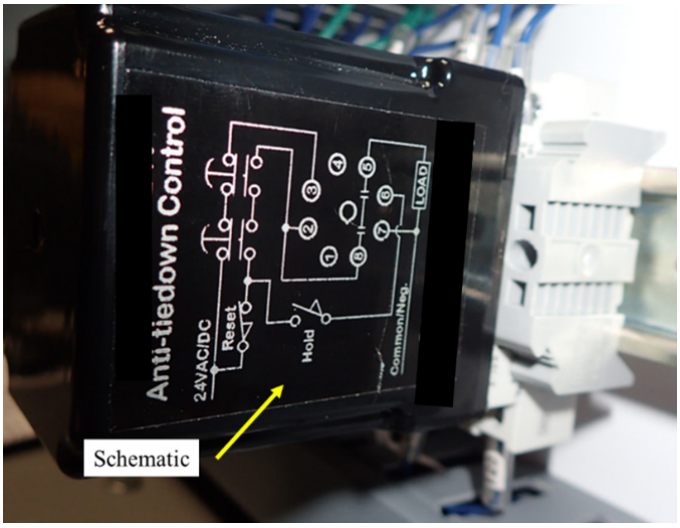

Figure 7
Anti tie-down module.

Forensic Engineer's Evaluation

As a part of the analysis of the failure, the wiring of the system and suitability of the PLC device/PLC code were evaluated. Through analysis of the PLC code, it was determined that the PLC code contained an error where — under certain conditions — an unexpected start could occur.

Figure 7 shows the anti-tiedown safety interface module (SIM) that was used to interface the two forward cycle pushbuttons with the control system. The two pushbuttons were wired into the SIM. According to the manufacturer's documentation (**Figure 8**), the output contacts of the SIM were supposed to be hard-wired to a load, which represents the hazardous machine motions. However, in this instance, the SIM contacts were wired directly to a PLC input.

In this instance, wiring the SIM contacts into the PLC was a design error because the machine was controlled via an off-the-shelf PLC that is not intended for safety-related functions. It should be noted that there are PLCs that are designed for safety-related functions[7,8].

When a machine guarding injury occurs, the goal of the forensic engineer is to determine how and why the injury happened by analyzing the system design. This can involve, in part, machine design, machine controls design, and machine guarding design. After the analysis is complete, the design choices are compared to the applicable standards for machine control and guarding to determine if the design met or exceeded requirements set forth in the applicable standards.

The Type C standard applicable to hydraulic rotary bending machines is ANSI B11.15.[6] ANSI B11.15 contains a flow chart that outlines the responsibilities for addressing machine-related risks. Main risk reduction responsibilities are shared between the supplier and user. The operator needs to comply with safety training and safety procedures. The flow chart contained in ANSI B11.15 further details

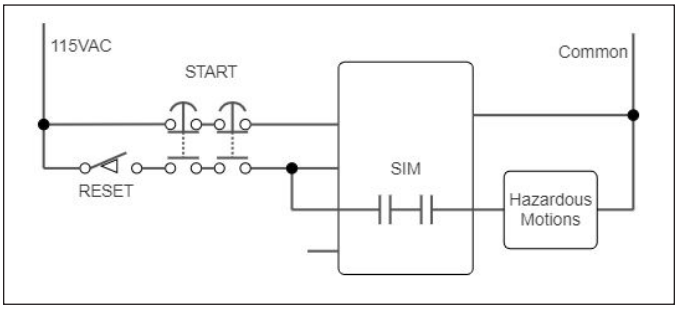

Figure 8
Anti tie-down module schematic.

the applicable ANSI B11 standard(s) for specific tasks.

Machine Safeguarding Device

As stated earlier, the dual palm remote stand (as shown in **Figure 4**) was intended as the safeguarding device, which is one of the methods of safeguarding listed in ANSI B11.15.

Under normal operations, to initiate a machine forward cycle, the operator would depress both forward cycle pushbuttons concurrently and maintain them throughout the time the hazardous conditions exist. As it relates to the hydraulic tubing bender, the hazardous motions ceased when the clamp die clamped the tubing. Once the clamp die clamped the tubing, operators could remove their hands from the pushbuttons because it was then considered safe. ANSI B11.TR6 contains description and information related to two-hand control[9].

Comparison to Applicable Standards

ANSI B11.15 was the Type C standard applicable to Pipe, Tube, and Shape Bending Machines[6]. According to ANSI B11.15, two hand controls are a prescribed method for safeguarding. While a SIM designed specifically for two hand controls was used, it was wired into a PLC input that was not consistent with the SIM instructions and applicable standards, which required the final switching device be a hardwired electromechanical device[8]. There is an exception for PLCs that are listed for safety-related functions; however, the PLC used was not listed for such functions[8].

Discussion

Operator safety must be considered when machinery is utilized. When involving point of operation guarding, the performance-based clauses contained within OSHA require that guarding be done to any appropriate standards. The ANSI B11 series is an example of applicable standards. However, when the safeguarding device is not integrated properly into the machine control system, there is still a risk of operator injury. During the course of a forensic investigation relating to machine guarding, it is important to analyze the machine operation and control and compare those decisions to the applicable standards.

As implemented, the dual palm remote stand and associated components did not meet the requirements set forth by the applicable B11 standards nor the SIM instructions. The intent of hardwiring the SIM contacts to the hazardous machine motion actuators is to prevent operation of the actuators until the SIM contacts are in the closed position. At the time of the incident, the operator was not depressing the forward cycle pushbuttons; therefore, the SIM contacts where in the open position. Had the SIM been wired correctly, the contacts being in the open position would have blocked the start signal from the PLC (due to the programming error) to the actuators. Ultimately, this would have prevented the unexpected start and injury to the operator.

Conclusion

Based on the forensic investigation, it was determined that although it was appropriate to use a safeguarding device in lieu of fixed guarding, the safeguarding device was not properly integrated into the machine's control system. This, combined with a PLC programming error, resulted in an unexpected start and subsequent machine operator injury. Had the machine safeguarding device been properly integrated into the machine control system, the PLC programming error would not have been allowed to initiate the unexpected start, and the machine operator would not have sustained the injury.

References

1. OSHA. (2021). Top 10 Most Frequently Cited Standards for Fiscal Year 2021 (Oct. 1, 2020, to Sept. 30, 2021). Available: https://www.osha.gov/top10citedstandards.

2. C. R. Asfahl and D. W. Rieske, Industrial Safety and Health Management (no. 7th). 330 Hudson Street, NY 10013: Pearson, 2019, p. 515.

3. General requirements for all machines, OSHA.

4. Machinery Safety Standards. Available: https://www.b11standards.org/.

5. B11.0 Safety of Machinery – General Requirements and Risk Assessment, 2010.

6. B11.15 Safety Requirements for Pipe, Tube, and Shape Bending Machines, 2012.

7. B11.TR4 ANSI Technical Report for Machine Tools – Selection of Programmable Electronic Systems (PES/PLC) for Machine Tools, 2004.

8. NFPA 79 Electrical Standard for Industrial Machinery, 2012.

9. B11.TR6 ANSI Technical Report for Machines – Safety Control Systems for Machine Tools, 2010.

Investigation and Root Cause Analysis of Transformer Metering Destruction by Arc Flash

By John F. Wade, PhD, PE, DFE (NAFE #1174A) and David J. Icove, PhD, PE, DFE (NAFE #899F)

Abstract

An arc flash and fire in the secondary compartment of an industrial facility utility transformer resulted in destruction of newly installed electrical metering equipment. Inherent to this type of event are two loss-of-evidence challenges: extremely high heat burns or melts everything nearby, and urgency to restore normal operation may prevent comprehensive examination of the scene. The facility contractor's operations staff conducted an initial root cause analysis. The contractor's management called on an external forensic team to provide an independent assessment. Having an established investigation methodology allows the forensic examiner to better understand what was, and was not, evaluated by facility staff and prevents confirmation biases. This paper examines the facility's report, addresses shortcomings in its conclusions, and goes on to detail the methods and reasoning behind the forensic team's findings. The methodology presented in this paper is applicable to a wide range of industrial electrical fires.

Keywords

Arc flash, arc blast, electrical fire, work process, confirmation bias, methodology, root cause, fishbone diagram, forensic engineering

Introduction

Electrical system failures often exhibit sudden onset, short duration, and significant destruction. Such failures may arise from a variety of causes[1,2]. Among these are vandalism, age, installation or maintenance errors, or environmental conditions. These may result in an immediate event or produce a latent precursor.

When a failure in large, high-energy electrical gear produces a robust short circuit (e.g., introducing a highly conductive object, often metallic), then phenomena known as arc flash and arc blast are almost certain to result. Briefly, arc flash with blast is an event in an electrical system that releases megajoules of power in milliseconds in the form of an intense electrical arc and attendant heat-induced blast wave[3].

Since electrical failure events accompanied by arc flash and blast tend to be spectacular, it can be easy to focus on the event itself. However, such occurrences, whether immediate or delayed, are the end state of a cascade of contributors. Forensic analysis of both the event site and/or remains — as well as organizational dynamics and work processes — requires an integrated approach to fully reveal root causes. In an operating industrial facility, there can be significant pressure to quickly clean up equipment and restore electrical service. As with most fire sites, debris and photographs of the site may be all the physical evidence available to the investigator. However, analysis of work documents and unbiased interviews of associated personnel are essential to revealing what led to the event.

Background

The client operated an industrial plant that included large rotating machines. It is common[4,5] to power high-current equipment like this at 4,160 volts three-phase to keep feeder cable size manageable. The client had such equipment in one of its buildings and wished to add power usage monitoring.

The client's engineering group produced a design for added electrical metering in the 4,160-volt secondary side of the utility transformer supplying the building. The engineers also prepared the work packages that would facilitate installation of the new electrical meters and associated components.

The client's electrical workers assembled all specified parts and materials and performed the installation across a holiday outage. At the completion of the new installation,

John Wade, PhD, PE, 2325 Rocky Top Road, Lenoir City, TN 37771; (865) 456-1997; john.f.wade.pe@gmail.com

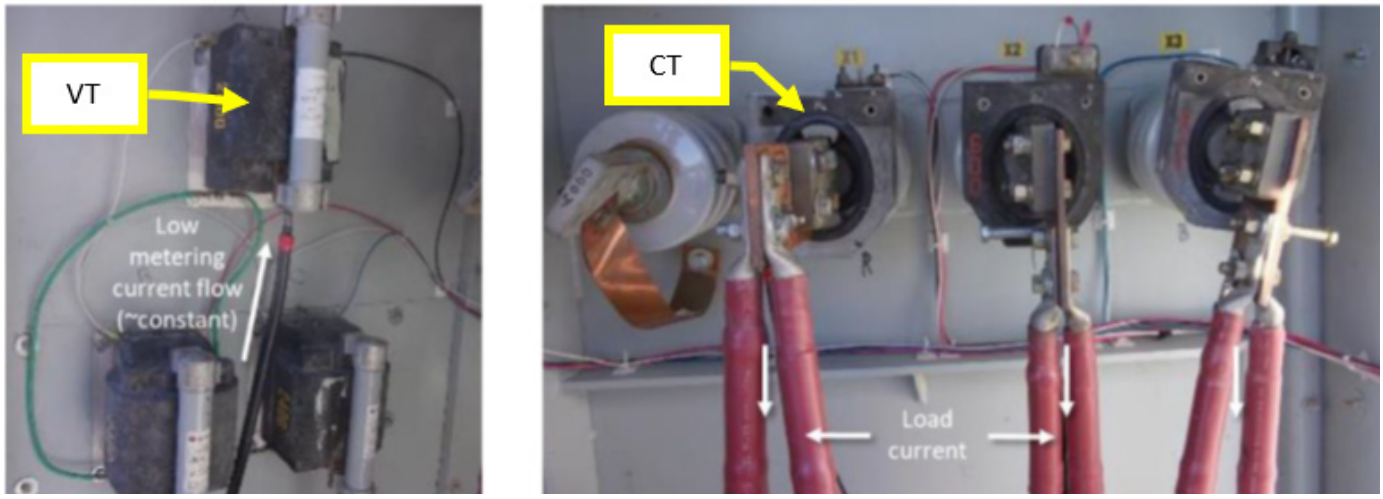

Figure 1
Newly installed VTs and CTs inside secondary compartment.

devices added to the interior of the transformer secondary compartment included three voltage transformers (VTs) on the left wall to step each of the three 4,160-volt phases down to 120 volts for connection to the power meter. Around each of three phase legs coming out of the transformer is a current transformer (CT) measuring amps and connected to the power meter. Photos of the completed installation were taken to submit with the work package completion, as shown in **Figure 1**. These images provided an important basis for comparison.

Approximately two days after installation was completed and the system was energized, a catastrophic failure occurred inside the utility transformer secondary compartment that burned wiring and damaged or destroyed components. The thermal overpressure was sufficient to blow open the locked transformer compartment doors.

Figure 2 shows the extensive heat damage to cables and equipment. The outer jackets on the large load cables were charred. Insulation on the medium-sized cables connected to the VTs was burned away in several places; one cable was missing a 12-inch section. The VTs were so damaged that all were scrapped.

Figure 3 shows the arc erosion of the large copper connector plates, erosion and melting of one cable end, and destruction of the VT "A" fuse clip. The loss of copper (erosion) at corners and edges is characteristic of arc endpoints: highly localized hot spots vaporized conductor material wherever arcs originated. Insulation in the nearby area melted due to the heat radiated from these arcs.

Figure 4 shows destruction of the "A" phase VT fuse due to textbook "arcing through char"[6,7] — a phenomenon

Figure 2
Post-event photos.

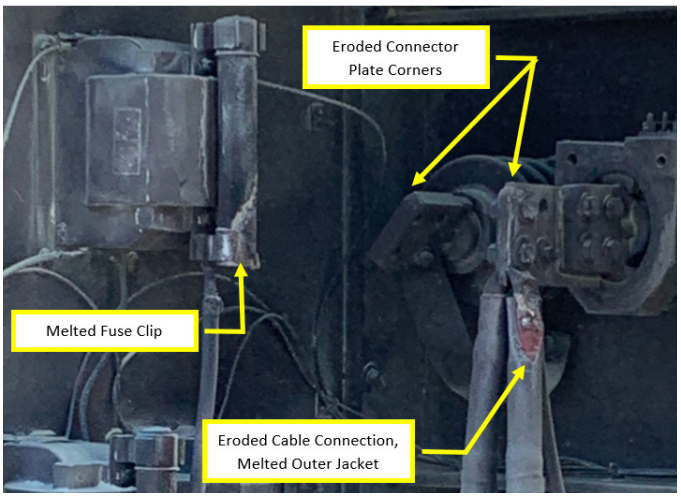

Figure 3
Arc erosion of connectors and cables.

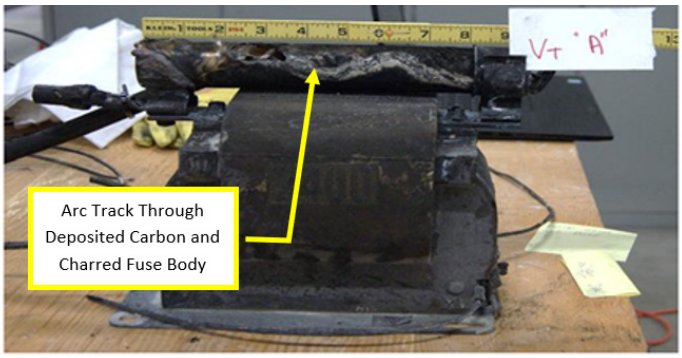

Figure 4
Post-event VT with arc tracking across destroyed fuse.

where carbonized material becomes an electrically conductive path. All these indications pointed at a powerful arc event — likely an arc flash.

Analytical Methodology

Informed by best practice (e.g., Liptai et al[8]), the independent forensic team divided the analysis of (and reporting on) the subject event into five main activities.

1. Prior to a site visit, collect and examine available documentation, client-performed analyses, and reports. Evaluate work packages and company directives. Develop a detailed timeline based on client-reported conditions supported by facts. Develop hypotheses and lines of questioning in preparation for the site visit.

2. Conduct a site visit to gather information through direct inspection of failed equipment and operating environment. Conduct interviews with managers, engineers, operators, and technicians.

3. Identify systemic contributors, such as those arising from the design, use of policies and procedures, and causes stemming from relationships between organizations. Evaluate barriers to failure that did not function as intended. Identify decision-making errors and causes arising from corporate culture. Examine how the various stakeholder organizations learn from accumulated knowledge.

4. Develop most probable cause as supported by documentation, verifiable conditions, and interviews. Conduct additional validation, including calculations, modeling, and simulations.

5. Assemble the report including recommendations.

Activity 1 — Initial Analysis

The client provided the team with all the prior root cause analysis and report materials. While this report correctly documented failures in configuration management, it fell short in lack of depth. Further, the client's investigators hypothesized a difficult-to-observe phenomenon called "circulating current" that can occur in a three-phase delta transformer secondary — the subject transformer was 34,500 volts primary and 4,160 volts secondary. This "circulating currents" condition arises from unbalanced transformer phase-to-phase loading for an extended period, resulting in winding overheating and insulation damage.

The forensic team found this conclusion flawed for two reasons: It did not explain the burned VT primary cables or the over-pressure that blew the doors open, and the transformer secondary was wye configured — not delta. Further, the client's report conclusion was not supported by reported or observed operating conditions.

Evaluation of the work packages required collecting both client's company procedures and policies as well as the work packages themselves. Organizational procedures for safety and work are the implementing documents for such standards as OSHA (29 CFR 1910 sub-parts I, R, and S)[9], NFPA 70 *National Electrical Code* (NEC)[10], and IEEE C2 *National Electrical Safety Code* (NESC)[11]. Understanding relevant standards is integral to correct evaluation of work planning based on them.

The client's electrical team kept accurate time records of activities and milestones during the installation evolution. The plant emergency responders also kept records of call-out and response times, and a report of "site secured." This aggregated information allowed the forensic team to assemble an initial timeline of activities, completion, and failure. Adding details gleaned from the utility company's supervisory control and data acquisition (SCADA) system history allowed precise determination of when the modified transformer was re-energized, the moment of failure onset, and duration of the failure event.

Activity 2 — Site Visit and Inspection

Research of work documentation and the timeline left the forensic team with questions that made a site visit necessary. After arriving at the client's plant and inspecting the restored transformer, the team divided into two task groups: evaluate debris and organize interviews.

The debris evaluation was possible because the

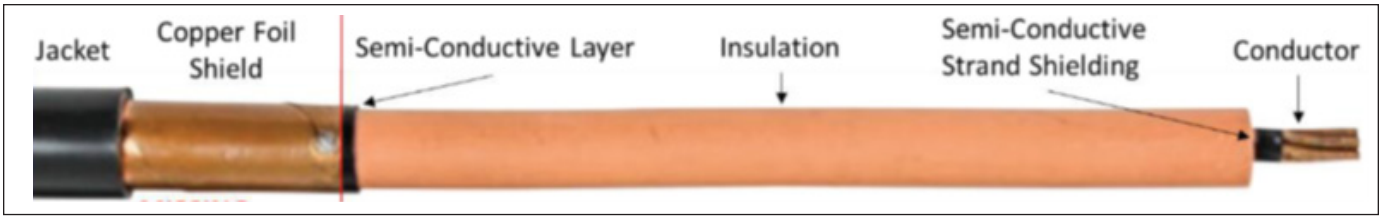

Figure 5
Medium-voltage electrical cable components.

client collected all remaining parts and pieces from the transformer secondary compartment. This included all mounting hardware and connection plates replaced as part of the restoration.

Examining Debris

The team arranged cable and component debris on a workbench. This addressed two analysis goals: understanding the relationships of failure indications (burn and melt points) and identifying the most likely point of initial failure. These, in turn, contributed to the sequence of events timeline, explaining why it took almost two days for the failure to occur.

A critical piece of information came from careful examination of the VT cables. Medium-voltage cable consists of six layers[12] (**Figure 5**): the central current-carrying conductor, a semi-conductive shield, insulation, another semi-conductive layer, a wound copper foil shield layer, and a protective outer jacket. When properly terminated and grounded, the copper foil shield equalizes the strong electric field (**Figure 6**) across the cable's insulation to prevent concentrated energy and burn-through.

Not all wiring in the compartment was burned. Some escaped damage, allowing direct examination of installed material. An example (**Figure 7**) shows the cables between utility transformer secondary and VT primaries were missing both the copper foil shield and the protective jacket.

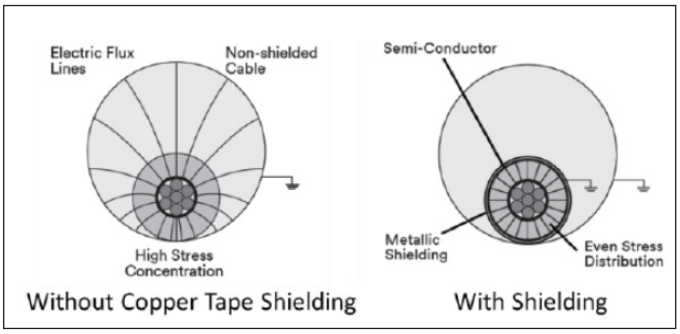

Figure 6
Electric field illustration from 3M power cable splicing and terminating guide[12].

This was evidenced by the absence of cable type identification print, the still visible "semi-conductive layer" print on this undamaged piece, and the spiral grooves showing where edges of the wound copper foil shield had been.

Using photographs of the open secondary compartment, the team used 3-point perspective[13] to create a geometric model of the compartment interior. This model revealed the cable from the transformer to the Phase "B" VT looped down and behind the others, laying against the edge of one of the transformer structural ribs or against another VT cable. Once energized, this would have allowed a concentration of electric field to produce a hot spot to form in the deficient cable, yielding burn-through and arcing. Chafing due to vibration of the unrestrained cable due to magnetic effects may have exacerbated friction erosion of the exposed semi-conductive insulation layer.

Accumulated contributors set the stage for a catastrophic arc flash involving all three transformer terminals

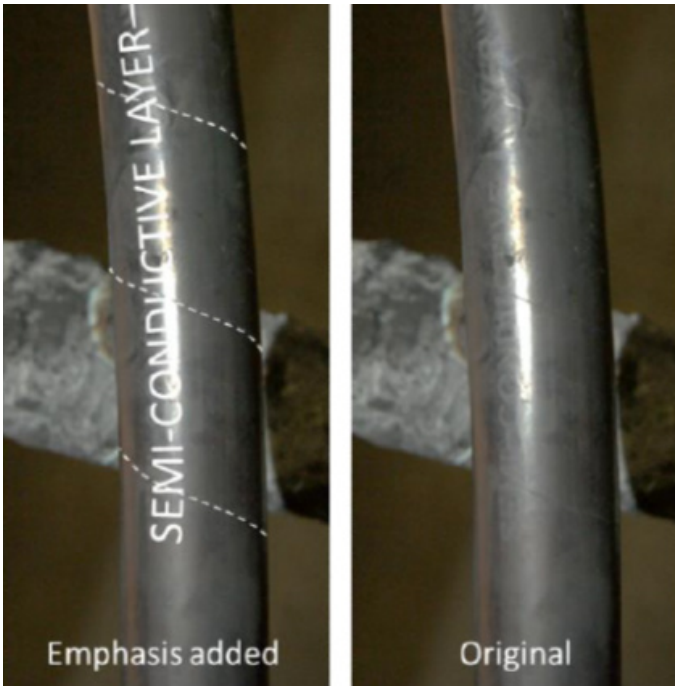

Figure 7
Faulty VT cable as installed.

and the exposed parts of the VTs. A conductive plume from the initial Phase "B" cable arc likely billowed up inside the secondary compartment. Such a plume was created around the initial arc flash (**Figure 8** event #1) when conductor material was vaporized yielding carbon from incinerated cable insulation and, more importantly, copper vapor[14,15]. The plume triggered additional arc events (**Figure 8** event #2) when convection carried metal vapor away from the initial arc flash location, dramatically increasing the conductivity of the air around the exposed transformer terminals and other equipment. But the question remained: What chain of technical and organizational precursors allowed this event to occur?

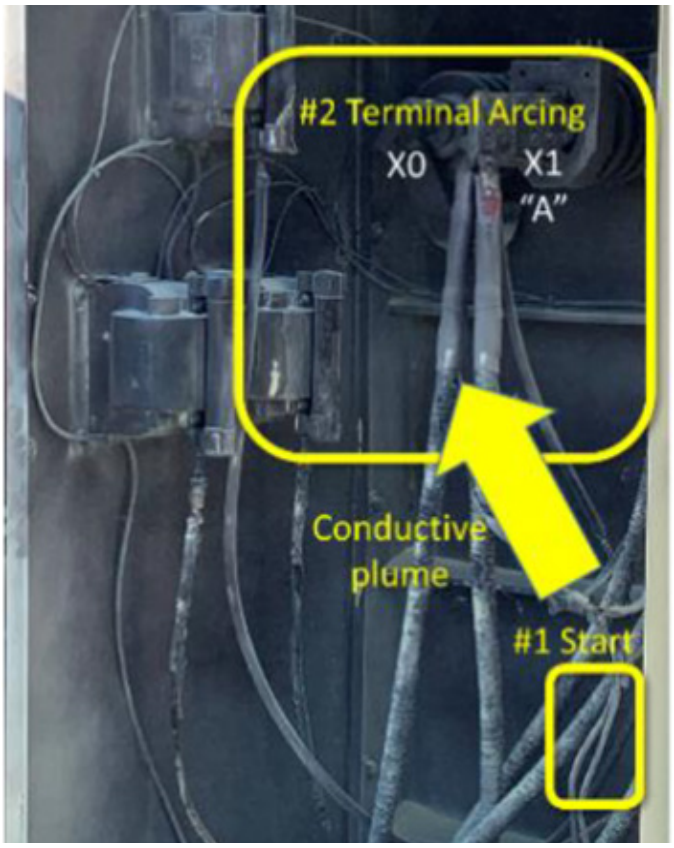

Figure 8
Arc flash propagation most-likely sequence.

Activity 3 — Evaluate Culture and Procedures; Conduct Interviews

While the physical reconstruction of the debris was key to understanding the physics of "what" happened, careful dissection of the client's organizational dynamics was central to identifying direct causal and contributory factors explaining "why" it happened. The forensic team found several ingrained institutional issues. These issues are included in an Ishikawa "fishbone" diagram[16,17], as shown in **Figure 9** and in the details following. Out of the full set of factors identified, the items and paths highlighted in red were those the team found to be most-likely

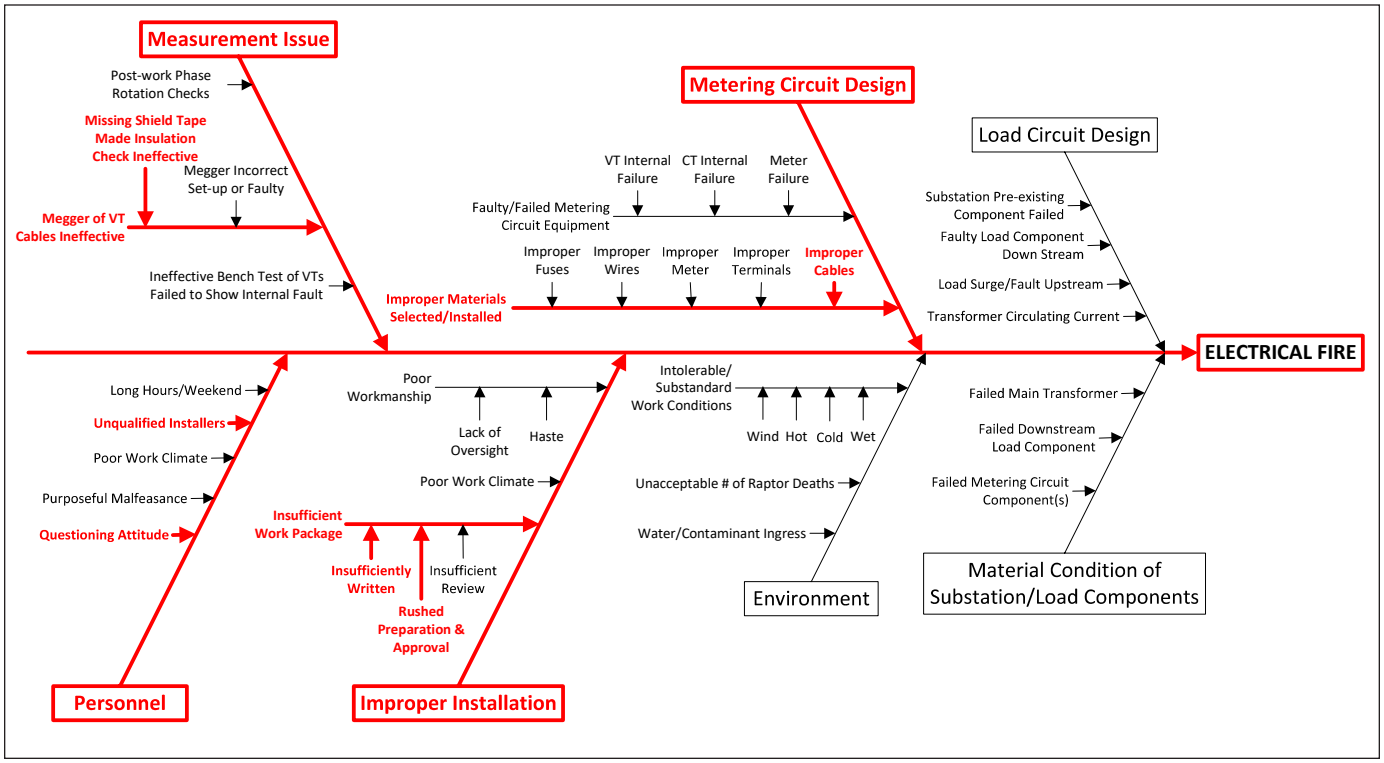

Figure 9
Ishikawa diagram.

primary contributors.

Documentation analysis and interviews revealed key missteps in the work package development and its processing.

1. The engineering team reused a previous design for a 480-volt installation, including stock details. The NEC and NESC treat systems below 1,000 volts differently from those above 1,000 volts. Design checking did not point out that the new work was for a 4,160-volt system with quite different requirements from the 480-volt example.

2. The work package itself reused the prior 480-volt material, including copying the "480V" system voltage designation. This led to the incorrect assignment of task team: In accordance with company policy and the labor agreement, industrial electricians were assigned. Had the system voltage been correctly identified, 4,160-volt qualified utility linemen would have been selected.

3. The work package was further designated "lowest level of risk" because utility workers would isolate the main service prior to work commencing. However, linemen were not on hand to confirm the transformer was de-energized. This violation of lockout/tagout protocol[18] could have resulted in the deaths of workers both because the utility crew could have incorrectly implemented the isolation, and the assigned team would not have carried appropriately rated test instruments to check the transformer's condition.

   In addition to the missing lockout/tagout documentation, the work packages also did not include the electrical hazard analysis required by NFPA 70E[18]. While the associated IEEE 1584[19] analysis results would not have informed the forensic investigation (1584 calculations do not apply to the interior of enclosed equipment), they would have been an important factor in proper safety preparations.

4. Planners scheduled the work as a sub-part of other plant utility changes during a holiday outage. Since planners believed there was adequate time, they identified the metering addition as "routine work." While the metering addition was itself believed to be minor, the overall effects of the outage were not. Planners perceived a rush to assemble work packages, and there was not adequate time allowed for travel to the job site. Even with a clear plan and careful staging of correct tools/parts, completing all installation tasks in the time allowed would have been difficult. The time pressure on the electricians led to missed or skipped inspections and verifications.

The interview team focused on three main sub-organizations: the engineers and work planners, the electrical workers, and the emergency responders. The team conducted interviews in group settings and took great care to establish a cooperative and non-confrontational atmosphere. The interview with the electricians showed this group to be professional, dedicated, and safety conscious. However, their responses brought to light several organizational weaknesses:

1. Questioning Attitude — Through the course of this investigation, it was apparent important questions went unanswered, and assumptions went unchallenged. The design relied heavily on examples and stock details — why wasn't there a tailored design drawing? The work package said "480V," but the task was on a 4,160-volt system — nobody pointed out the difference and stopped work. Had anyone checked the parts and materials provided? Why didn't the electricians insist on lockout/tagout paperwork?

2. Skills and Qualifications — The assigned electricians were not familiar with the properties of, or termination methods appropriate for, 4,160-volt cable. The electrical team foreman was responsible for kitting materials and parts. This is the person who selected the piece of sub-standard cable for connecting the VTs. How was someone clearly unfamiliar with the properties of 4,160-volt cable qualified to make this selection? The history of the deficient cable was completely unknown — how was scrap material allowed to remain in working stock, and how many months or years had it been in the outdoor storage yard?

3. Codes and Standards Compliance — The cable material used for the VT connections was altered from its manufactured form and did not meet installation requirements of NEC Article 311[10]. The altered and deficient nature, and unverifiable provenance, of the cable material also violated

several requirements of 29 CFR 1910.399[9].

The interview with the first response team served to narrow the field of possible causal contributors. The fire fighters had experience with previous electrical events and knew to capture information the forensic team would need, including:

- The transformer doors were open when they arrived, with the latch arms bent. This revealed a significant blast over-pressure inside the secondary compartment.
- There was no evidence of animal involvement. Animals crawling or landing on high-voltage equipment can cause an arc flash. That was not what happened in this case.
- There was minor flaming that they extinguished with dry chemical. The large load cables were just charred rather than consumed. This belied a short-duration event like arc flash rather than a prolonged fire.

Activity 5 — Report and Recommendations

The team prepared and presented a report that described all aspects of data collection, analysis, and conclusions. This report included recommendations for process and procedure improvements that would help the client avoid the cascade of avoidable errors that led to the investigated failure.

Summary

Electricity is not readily observable and often considered mysterious. Therefore, when a failure occurs, initial assessment may ascribe the event to equally mysterious or unobservable phenomena. To avoid succumbing to these biases, forensic analysis of an electrical system failure must be planned and systematic. It must include both a technical reconstruction of the physical events and a comprehensive examination of organizational and work-related climate, procedures, and processes.

In this investigation, the team organized work into five main tasks: initial research and analysis, site visit to perform reconstruction and interviews, thorough evaluation of interview results and correlation to research knowledge, aligning measured facts and data with knowledge of the physics and with organizational contributors to develop a most likely sequence of events, and preparation of the final report.

Conclusion

This investigation demonstrated the validity of the methodology for planning and conducting a forensic analysis of an electrical arc flash event even when the only available physical evidence from the site was debris and photographs. By staying focused on engineering principles supported by defensible facts that explained all the observed conditions, the team avoided the pitfalls of confirmation bias or rushing-to-judgement and agreeing with the results of an inadequate initial analysis.

This fundamental methodology can be applied to a variety of electrical failure and fire investigations. It is based on the understandings that “electricity is governed by physics, not magic” and “human behavior can be understood.” It allows a forensic investigator to approach electrical events with the confidence that underlying causes and contributors are discoverable. Sometimes these precursors may have occurred in the unknown past and have little initially apparent connection to the final failure.

Acknowledgements

The forensic team gratefully acknowledges the facilitating involvement of Oak Ridge Associated Universities (ORAU).

References

1. IEEE, 1402-2021 IEEE Guide for Physical Security of Electric Power Substations, 2021.
2. C. Cayanan, R. Nararro and E. Wagner, “A risk based approach for prioritizing electrical equipment replacement and repair,” in Industry Applications Society 60th Annual Petroleum and Chemical Industry Conference, Chicago, IL, 2013.
3. E. Hoagland, C. Maurice, A. Haines and A. Maurice, “Arc Flash Pressure Measurement by the Physical Method, Effect of Metal Vapor on Arc Blast,” IEEE Transactions on Industry Applications, vol. 53, no. 2, pp. 1576-1582, 2017.
4. IEEE, Std 141 Recommended Practice for Electric Power Distribution for Industrial Plants.
5. American National Standards Institute (ANSI), Std C84.1 - Power Systems and Equipment — Voltage Ratings (60 Hz).

6. NFPA 921 — Guide for Fire and Explosion Investigations, 2021.

7. V. Babrauskas, "How do electrical wiring faults lead to structure ignitions?" Fire and Arson Investigator, no. 52, pp. 39-45,49, 2002.

8. L. Liptai, A. Aleksander, S. Grainger, S. Hainsworth, R. Loomba and J. Unarski, "Global thinking and methodologies in evidence-based forensic engineering science," in Forensice Science - Current Issues, Future Directions, Wiley-Blackwell, 2013, pp. 292-309.

9. US Dept of Labor, "29 CFR 1910 - Sub-parts I, R, S," Occupational Safety and Health Administration, [Online]. Available: https://www.osha.gov/electrical/standards.

10. National Fire Protection Association, NFPA 70 - National Electrical Code, 2023.

11. IEEE, C2 - National Electrical Safety Code, 2023.

12. 3M, "Power Cable Splicing and Terminating Guide," 2018. [Online]. Available: https://www.anixter.com/content/dam/Suppliers/3M/Products and Application Guides/3M-Power-Cable-Splicing-Terminating.pdf. [Accessed 2023].

13. P. Dam, "A Guide to Using Vanishing Point in Photography," 30 January 2023. [Online]. Available: https://www.adorama.com/alc/the-vanishing-point/#:~:text=The easiest way to find,close to their starting point.

14 B. Cheminat and P. Andanson, "Conduction in an electric arc column contaminated by copper vapour," Journal of Physics D: Applied Physics, vol. 18, no. 11, pp. 2183-2192, 1985.

15. I. Babich, A. Veklich and V. Zhovtyanskii, "Physical features and diagnostics of the plasma of a free-burning copper-vapor electric arc," Journal of Engineering Physics and Thermophysics, vol. 71, no. 1, pp. 127-134, 1998.

16. American Society for Quality (ASQ), "Fishbone Diagram," [Online]. Available: https://asq.org/quality-resources/fishbone.

17. R. Kane, "How to Use the Fishbone Tool for Root Cause Analysis," University of Minnesota, 2014. [Online]. Available: https://www.cms.gov/medicare/provider-enrollment-and-certification/qapi/downloads/fishbonerevised.pdf.

18. National Fire Protection Association, NFPA 70E - Standard for Electrical Safety in the Workplace.

19. IEEE, 1584 - IEEE Guide for Performing Arc-Flash Hazard Calculations, 2018.

FE Investigation of Design and Quality Control-Related Issues Contributing to Metal-On-Metal Hip Implant Failures

By Olin Parker, Jahan Rasty, PhD, PE, DFE (NAFE 768S), and Matthew Mills, PE, DFE (NAFE 1199A)

Abstract

High levels of cobalt and chromium ions were detected in the bodies of multiple recipients of modular cobalt chrome molybdenum metal-on-metal hip implants, necessitating the revision of their implants. A forensic engineering investigation of provided discovery documents and existing literature regarding the design, manufacturing, and clinical testing of these modular hip implants was performed. The investigation revealed that the modular interfaces of the implant allowed for micromotion to induce mechanically assisted crevice corrosion at these surfaces. The debris from this corrosion resulted in the release of metal ions into the bodies of the users, forming pseudotumors and compromising the user's health and wellbeing. The effect of this corrosion was enhanced by the galvanic couple that existed between the modular components of the implant. In addition, scanning electron microscopy (SEM) and electron dispersive spectroscopy (EDS) analysis identified silicon carbide (SiC) and aluminum oxide (AL_2O_3) particles left behind from polishing, which were embedded in the ball and liners. These particles accelerated the wear of the hip implant and further exacerbated the release of metal ions. The designers of future hip implants should take care in preventing the occurrence of the above-stated factors.

Keywords

Hip implant, tribocorrosion, taper wear, metallosis, forensic engineering, design, quality control

Introduction

Three types of operations are currently performed to replace the hip of a patient: 1) total hip arthroplasty (THA), which replaces both the natural acetabulum and femoral head; 2) hemiarthroplasty, which only replaces the femoral side of the hip; and 3) hip resurfacing, which replaces the acetabulum, but only shaves down (or resurfaces) the femoral head. A comparison of these operations and their utilized components is shown in **Figure 1**.

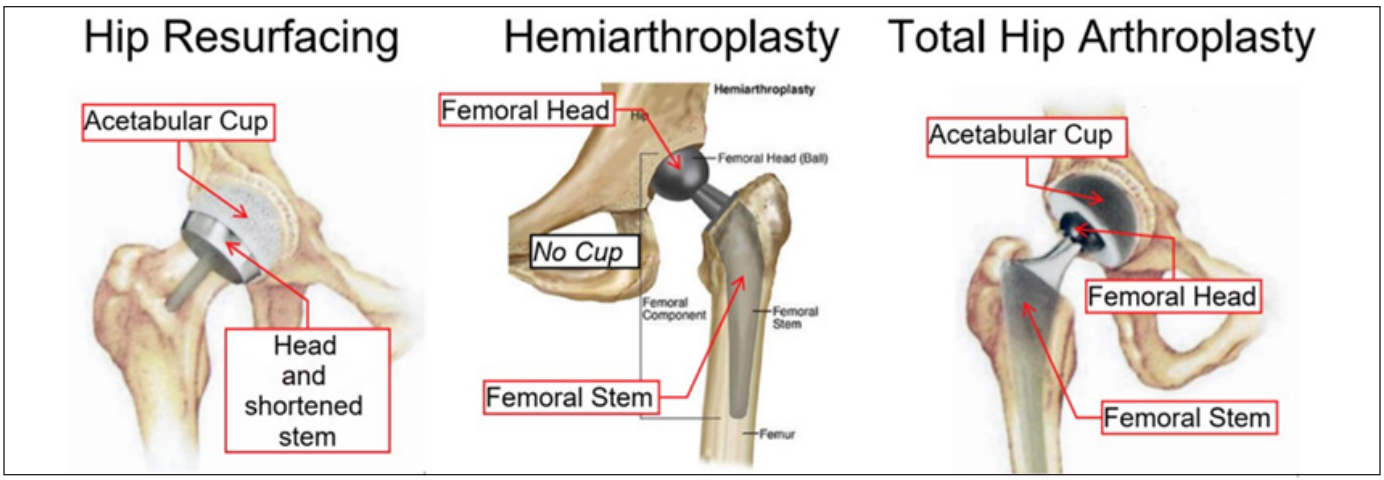

Figure 1

An illustration from discovery documents showing the components of a natural hip and the typical components utilized in total hip arthroplasty.

Olin Parker, 805 Boston Ave., Lubbock, TX 79409-9831, (832) 472-3930, Olin.Parker@ttu.edu

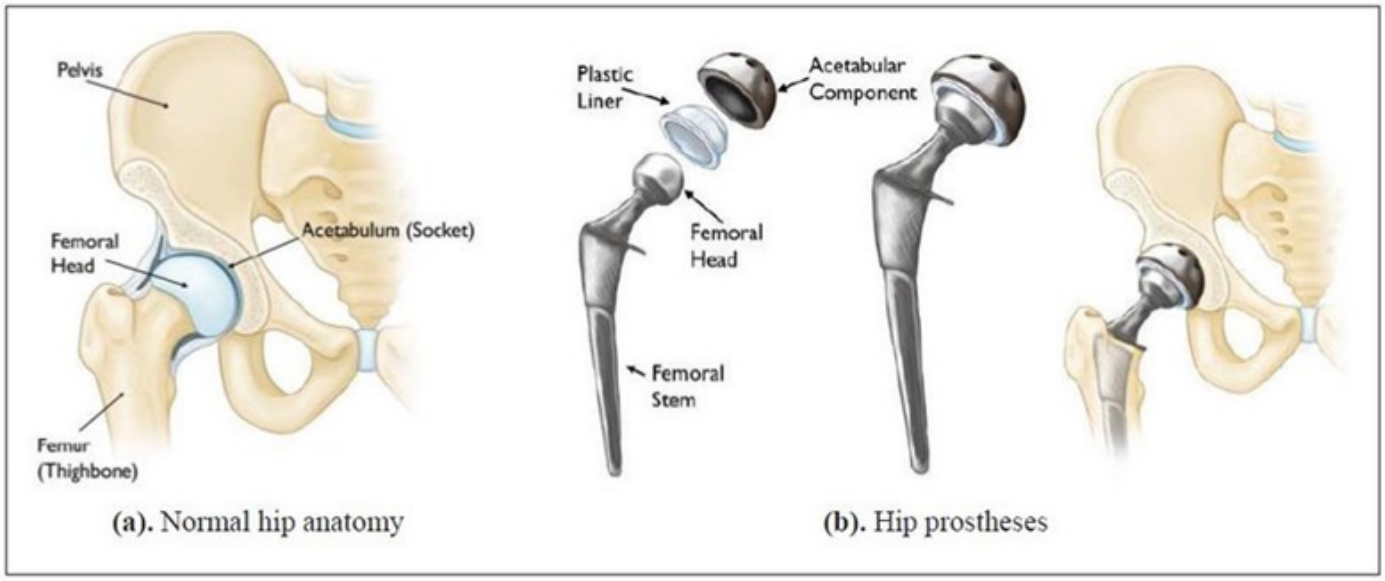

Figure 2
Illustration showing the components of a natural hip and the typical components utilized in total hip arthroplasty[2].

Of these operations, THA is the most common method for the treatment of fatigued or broken hips — with approximately 2.5 million people (or 0.83% of the U.S. population) having undergone such surgery[1]. In THA, the broken, aged, or diseased femoral head is replaced by an artificial femoral head, and a stem is implanted in the patient's femur. This artificial femoral head is then fitted into an acetabular component (cup), which has replaced the natural acetabular socket the femoral hip would fit into. **Figure 2** shows the configuration of components typically utilized in THA.

All prosthetic hips experience wear due to the forces imparted on them during use. In the pursuit of minimizing wear (and the issues wear debris can cause), a variety of different combinations of materials has been used for the head and cup interface: metal on polyethylene (MoP), ceramic on polyethylene (CoP), metal on metal (MoM), ceramic on metal (CoM), and ceramic on ceramic (CoC). Pictures of these material combinations are shown in **Figure 3**. All these material-type combinations have had varying levels of success. At the time of this report, the most commonly utilized combinations are MoP and CoP — due to the high wear resistance of crosslinked polyethylene.

Early hip implants, such as those marketed in the 1950s and '60s, primarily utilized MoM bearings. However, these early devices suffered from high wear and loosening of the implants, causing high failure rates that necessitated the surgical removal and replacement of the devices. MoP soon came to the forefront of the field due to the success of the Charnley hip prosthesis device in the '60s. As a result, MoM implants became less commonly utilized. However, as time passed, it became apparent that MoP implants were susceptible to high wear, and the wear particulate of the polyethylene liners caused the decay of nearby tissue and loosening of the implant. These problems with MoP devices lead to the development of CoC

Figure 3
Illustration showing five of the various material combinations that have been utilized in hip replacement[3].

and CoP implants in the ’70s, yet these bearings displayed high rates of fracture, both with Alumina ceramics in the 1970s and the Zirconia ceramics in the ’80s and ’90s. The growing concerns regarding MoP wear debris and the failure of these early ceramic devices led to a renewed interest in MoM devices due to their greater wear resistance and higher mechanical strength compared to ceramic alternatives. This newer generation of MoM THA implants were alleged to offer reduced wear (generating 1% to 5% of the total volumetric wear that MoP devices produce), increased stability, and increased range of motion, elevating these devices back to the forefront of the field and the market[4].

Case Background

A medical implant manufacturer developed a modular MoM hip prosthesis system (**Figure 4**) for use in THA surgery. By offering the device in a modular format, the operating surgeon can implant the femoral stem and then use a modular taper to affix an appropriately sized femoral head, providing surgeons with the intra-operation flexibility they need to select components that properly match the patient’s unique geometry, thus decreasing the number of failures that occur due to mispositioning of the device[5]. Modularity in THA devices can be provided through a variety of methods, such as, but not limited to, modular necks and adapter sleeves. The modularity provided by the manufacturer of the subject MoM THA device was in the form of an adapter sleeve. At the time of publication for this paper, modular hip components are commonly used in THA devices, yet the materials utilized for these connections have shifted toward titanium alloys instead of the CoCr utilized on the device at issue[6].

According to the 2021 data of the Australian Orthopedic Association’s National Joint Registry (AOA NJR), the reported cumulative revision (i.e., surgical removal and replacement of a failed device) rate for hip implants is 4.4% at 10 years and 6.5% at 15 years. The most common reasons for revision are aseptic loosening (23.19%), instability of the system (22.43%), and infection (22.13%)[7,8].

After the new generation of MoM THA systems went on the market around 1997[10], the reoperation and revision rates of the device rapidly climbed to unacceptable levels.

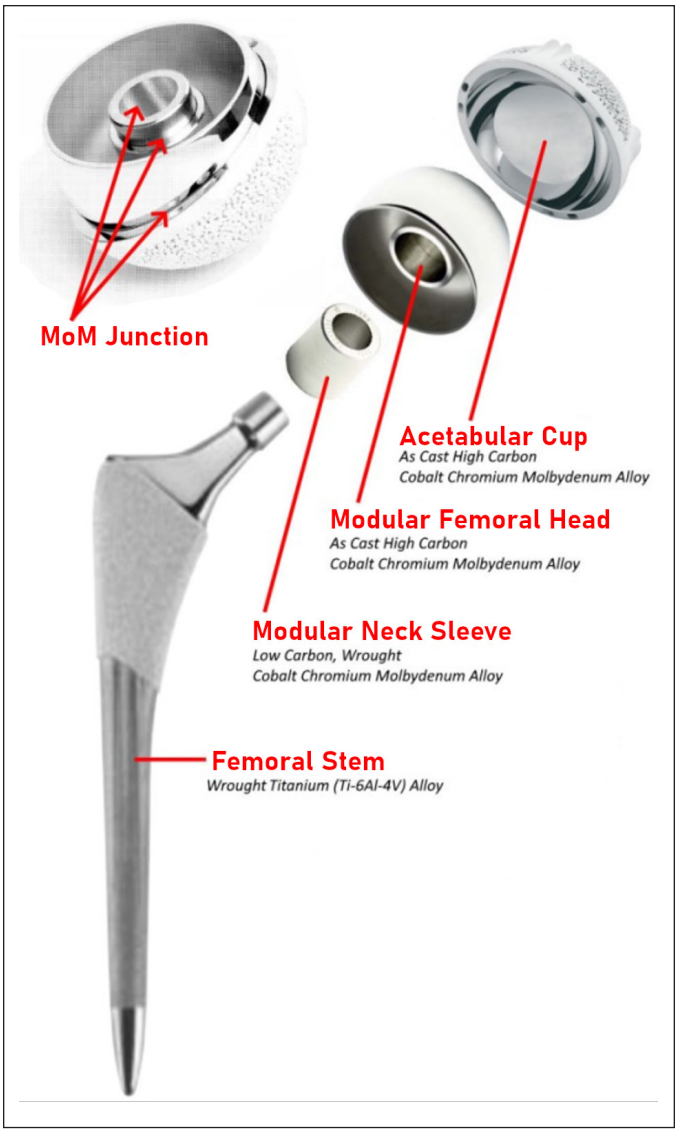

Figure 4
Exploded view of components used by the manufacturer and their relative position during a total hip arthroplasty.

The five-year revision rate of all MoM implants has been recorded to be on average 7.5% — more than twice the rate of alternative THA devices (3.15%).[9,11]. It should be noted that even back in 2011 (the latest year by which the devices the authors investigated were implanted), the 10-year revision rate of all THA system was 6.4%, relatively similar to the current 10-year revision rate[12]. As shown in **Figure 5**, the modular MoM implant at issue was found to exhibit revision rates far in excess of those recorded in

	5-Year Revision Rate	10-Year Revision Rate	15-Year Revision Rate
All THA Implants	3.7%	6.1%	9.1%
Modular MoM Implant at Issue	Data not available	14.3%	20.8%

Figure 5
Table showing the revision rates for all THA device and the modular MoM device investigated in this paper[9].

alternative THA devices. In contrast to the common failure modes seen in the other types of hip implant, the modular MoM THA system at issue was primarily noted to fail due to adverse reactions to metal ion and other metal-related pathology (44.8%), implant loosening (14.5%), and tissue lysis — cell breakdown resulting from damage to the outer membrane (9.2%)[9].

The authors were approached with 11 different incidents involving the revision of THA or resurfacing devices produced by the implant manufacturer and asked to analyze the evidence regarding these incidents. The device combinations and sizes of each component are listed in **Figure 6**.

Five of the devices were noted to utilize a combination of a cobalt-chromium-molybdenum (CoCrMo) liner affixed to a titanium alloy (Ti6Al4V) shell, which functioned as a substitute for the acetabular cup. **Figure 7** shows the difference in configuration between devices that utilize acetabular cups versus those that use a combination of liner and shell. Materials such as polyethylene or ceramic offer desirable wear characteristics for the articulating joint. However, due to lack of strength and other material property issues, they cannot be used for acetabular cups. Therefore, the liner-and-shell concept was developed to permit the incorporation of mixed materials in order to optimize performance. Occasionally, metal liners were utilized for MoM THA systems. Since a metal shell could be implanted with fixation screws, the use of a metal shell allowed for improved fixation on atypically shaped hip sockets.

Out of the 13 devices in these 11 incidents, only 11 were available for physical analysis. The remaining devices were noted to have been disposed of or destroyed by the corporate representative attending the revision surgery, violating the requirements of ASTM E11885 and the manufacturer's own corporate policies. ASTM E11885 outlines the standard practice for documenting and preserving evidence when investigating an incident that could become the subject of litigation[13]. The likelihood that the premature failure of an implanted medical device would likely become the source of litigation should have been apparent at the time the device was removed. As such, the destruction of medical devices — which more likely than not were a significant contributing cause of a user undergoing revision surgery — is intentional spoliation of evidence.

Metal Ions and Metallosis

All of the recipients of the devices in the presented cases were stated to have underwent revision surgery (i.e., removal and replacement of their implants) due to high levels of cobalt and chromium ions in their blood. According to the manufacturer as well as available literature on the subject, wear and corrosion of the implanted THA devices resulted in the release of these metal ions. The build-up of metallic debris and metal ions in soft tissues results in development of a phenomenon known as "metallosis" (shown in **Figure 8**). Metallosis has been found to result in aseptic fibrosis, neurotoxicity, local necrosis, or loosening of nearby implanted medical devices (commonly referred to as the development of "pseudotumors")[14]. These metal ions are able to spread through the body's lymphatic system to locations distant from the implanted device, such as the liver, spleen, and brain, causing metallosis and toxicity in these organs[15,16].

While essential in small amounts for the proper function of the human body, the toxic nature of the elements cobalt and chromium is well documented and has been widely known to the engineering and medical communities for the past century. Chromium toxicity was first noted by the modern scientific community in the late 19th century, when Scottish chrome pigment workers were found to be developing nasal tumors. Since then, the development of cancer and other toxicological responses in chromate workers and individuals exposed to chromium has become a well-known issue with various government bodies establishing regulations to prevent its occurrence[18].

The 20th century saw a number of incidents involving cobalt poisoning, ranging from exposure to industrial dust, medical treatment utilizing cobalt, and cobalt additives in beer. Given the widespread knowledge surrounding cobalt and chromium toxicology, a reasonably prudent manufacturer should have been aware of the fact that the release of cobalt and chromium ions from MoM implants would lead to toxicological responses.

Macroscale Analysis of Retrieved Hip Implants

All retrieved devices were cleaned in accordance with ASTM Standard F561-19. Examination of the retrieved implants showed the presence of a significant amount of corrosion particulate present on the interface of contacting components. As shown in **Figures 9** and **10**, black corrosion debris was observed on the interior and exterior surfaces of the taper sleeve in the majority of devices, appearing concentrated in parallel lines (likely due to the micro-grooved surfaces of the mated taper sleeve).

Digital microscopy of the femoral heads revealed the presence of numerous surface scratches consistent with

Patients	Components				
1	56 mm CoCrMo Acetabular Cup	50 mm CoCrMo Modular Femoral Head	+4 mm offset 12/14 CoCrMo Modular Taper Sleeve	Size 15 Ti6Al4V Femoral Stem	
2	56 mm Ti6Al4V Shell	44 mm CoCrMo Modular Femoral Head	12/14 CoCrMo Modular Taper Sleeve	Size 13 Ti6Al4v Femoral Stem	44 mm ID, 56 mm OD CoCrMo Liner
3	52 mm Ti6Al4V Shell	40 mm CoCrMo Modular Femoral Head	12/14 CoCrMo Modular Taper Sleeve	Size 13 Ti6Al4v Femoral Stem	40 mm ID, 52 mm OD CoCrMo Liner
4	66 mm Ti6Al4V Shell	54 mm CoCrMo Modular Femoral Head	12/14 CoCrMo Modular Taper Sleeve	Size 9 Ti6Al4v Femoral Stem	54 mm ID, 66 mm OD CoCrMo Liner
5	54 mm CoCrMo Acetabular Cup	46 mm CoCrMo Modular Femoral Head	-4 mm offset 12/14 CoCrMo Modular Taper Sleeve	Size 12 Ti6Al4v Femoral Stem	
6	52 mm CoCrMo Acetabular Cup	46 mm CoCrMo Modular Femoral Head	12/14 CoCrMo Modular Taper Sleeve	Size 12 Ti6Al4v Femoral Stem	
7 (Hip 1)	58 mm CoCrMo Acetabular Cup	52mm CoCrMo Modular Femoral Head	12/14 CoCrMo Modular Taper Sleeve	Size 15 Ti6Al4v Femoral Stem	
7 (Hip 2)	58mm CoCrMo Acetabular Cup	52 mm CoCrMo Modular Femoral Head	12/14 CoCrMo Modular Taper Sleeve	Size 15 Ti6Al4v Femoral Stem	
8	54 mm CoCrMo Acetabular Cup	46 mm CoCrMo Modular Femoral Head	+4 Offset 12/14 CoCrMo Modular Taper Sleeve	Size 6 Ti6Al4v Femoral Stem	
9 (Hip 1)	58 mm Ti6Al4V Shell	46 mm CoCrMo Modular Femoral Head	12/14 CoCrMo Modular Taper Sleeve	Size 13 Ti6Al4v Femoral Stem	46 mm ID, 58 mm OD CoCrMo Liner
9 (Hip 2)	56 mm Ti6Al4V Shell	44 mm CoCrMo Modular Femoral Head	12/14 CoCrMo Modular Taper Sleeve	Size 13 Ti6Al4v Femoral Stem	44 mm ID, 56 mm OD CoCrMo Liner
10	54 mm CoCrMo Acetabular Cup	46 mm CoCrMo Modular Femoral Head	CoCrMo Modular Taper Sleeve	Size 15 Ti6Al4v Femoral Stem	
11	52 mm CoCrMo Acetabular Cup	46 mm CoCrMo Modular Femoral Head	-4 mm offset CoCrMo Modular Taper Sleeve	Size 12 Ti6Al4v Femoral Stem	

Figure 6
Table listing the components utilized to form each device implanted in each of the recipients.

abrasive wear in addition to areas of corrosive degradation (**Figure 11**).

Figure 7
Illustration displaying the differences between a THA system with an acetabular cup (left) and a shell and liner combination (right)[3].

On the devices utilizing the combination of CoCrMo liners and Ti6Al4V shells, a series of square imprinted markings was present on the surface of the liners in

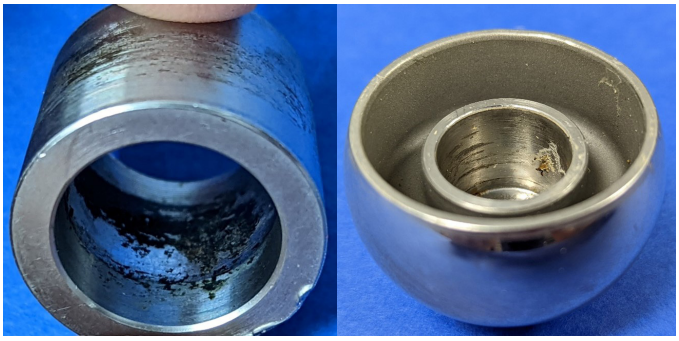

Figure 9
Images of the taper sleeve (left) and femoral head (right) from one of the retrieved devices, displaying black corrosion features and imprinted lines.

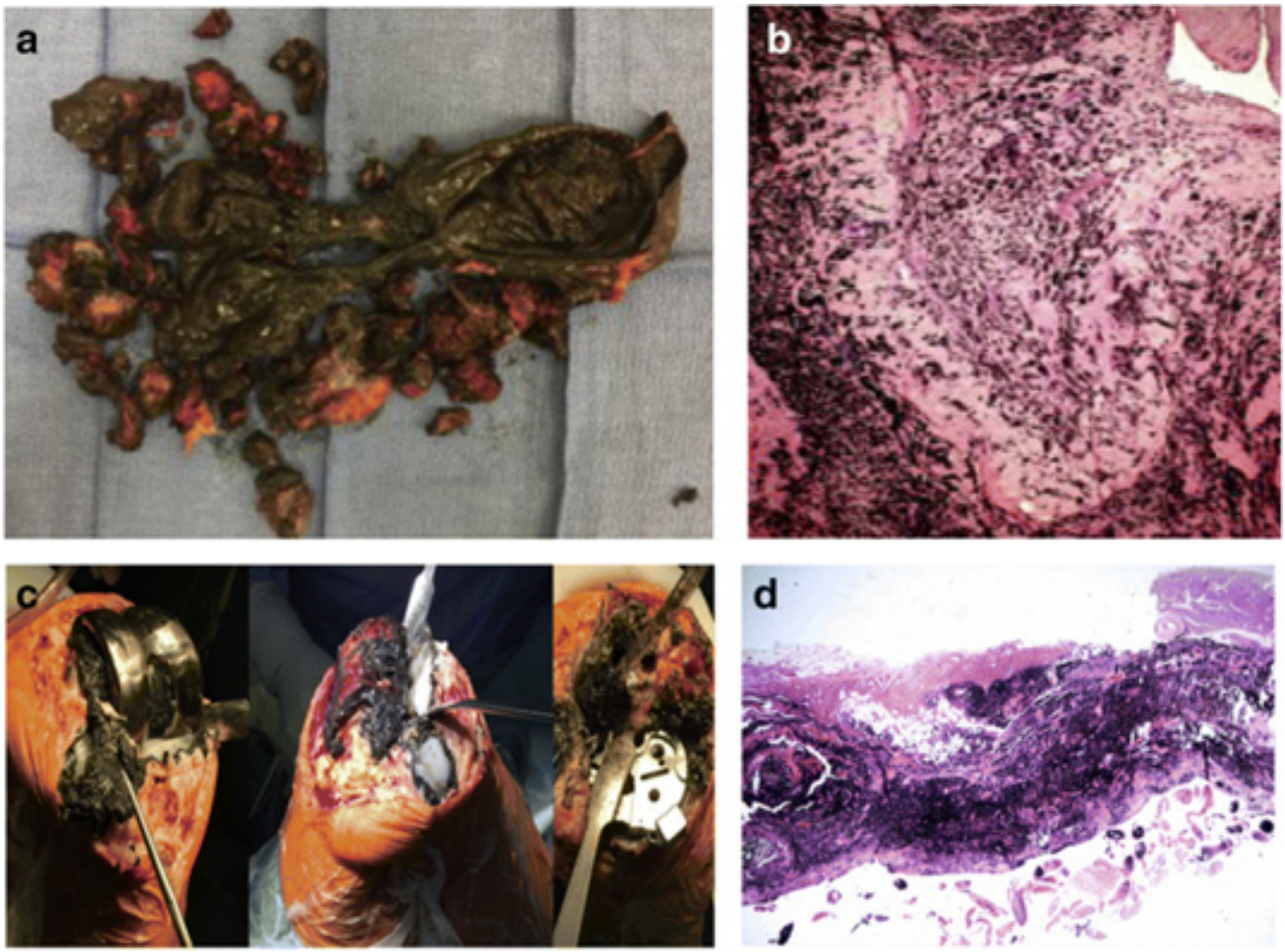

Figure 8
Explanted pseudotumor (a), microscopic view of pseudotumor tissue (b), black staining of tissue around an MoM implant (c), and microscopic photo of stained tissue (d)[17].

contact with the shell (**Figure 12**). These markings matched up with similarly sized square teeth on the shell, and the areas where direct connection existed between the liner and shell showed an increased level of corrosion and discoloration.

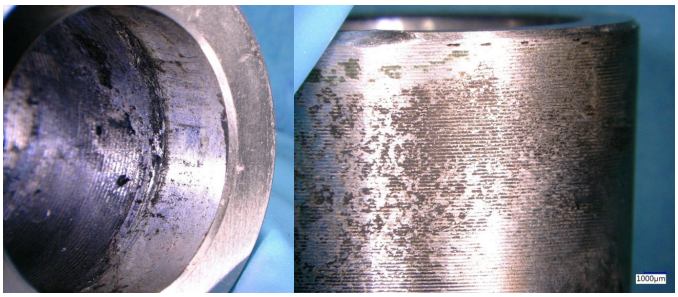

Figure 10
Images of the taper sleeve from one of the retrieved devices, displaying black corrosion features and imprinted lines.

Metal-on-Metal Wear

Devices with contacting metal surfaces in motion relative to one another are known to be susceptible to both abrasive and adhesive wear. According to Donald Askeland's "The Science and Engineering of Materials," adhesive wear:

> *"...occurs when two solid surfaces slide over one another under pressure. Surface projections, or asperities, are plastically deformed and eventually welded together by the high local pressures. As sliding continues, the bond between these welded surfaces breaks, producing cavities on one surface, projections on the second surface, and frequently tiny, abrasive particles — all of which contribute to further wear of the surfaces."*[20]

A diagram illustrating adhesive wear is shown in

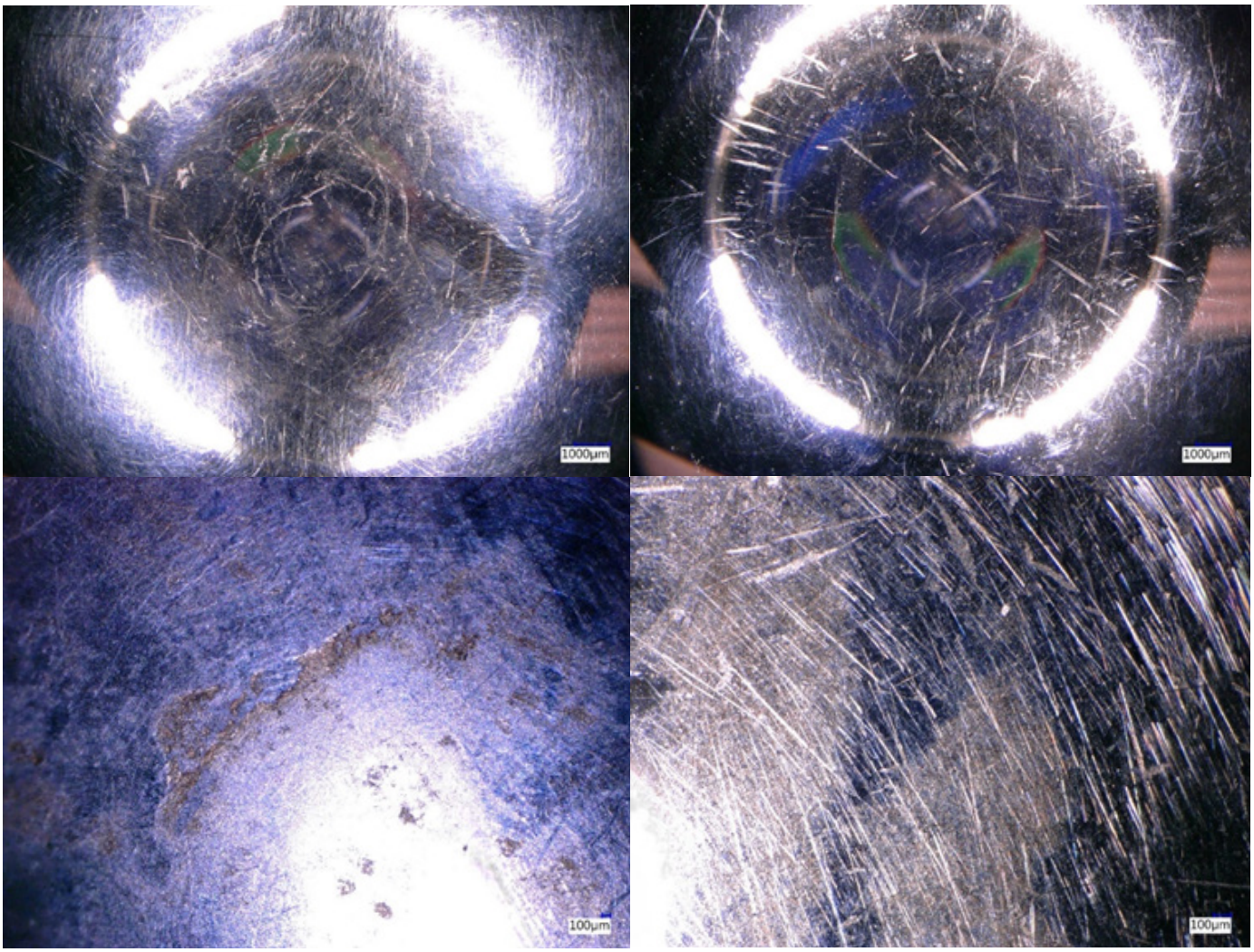

Figure 11
Image of the top of two femoral heads, showing a large number of surface scratches indicative of abrasive wear as well as corrosion.

Figure 12
Image of the imprinting marks left behind on the outer surface of the metal liner (top) and a Ti6Al4V shell similar to the one it was connected to, displaying similarly sized rectangular teeth (bottom).

Figure 13.

Abrasive wear, on the other hand, occurs when a hard material moves across a surface, removing particulate material from this surface. These hard particles can exist either as particles on a surface or as loose particles between two surfaces. According to Dieter and Schmidt's *Engineering Design*:

> *"abrasive wear is usually divided into low-stress and high-stress abrasive wear. In low-stress wear, the particles plow wear scars like shallow furrows or scratches, but they do not fracture off chips. In high-stress abrasive wear, the stress is sufficient to cause the abrasive particles to fracture or crush, producing many sharp edges that remove material by plowing the surface into deep scratches."*[21]

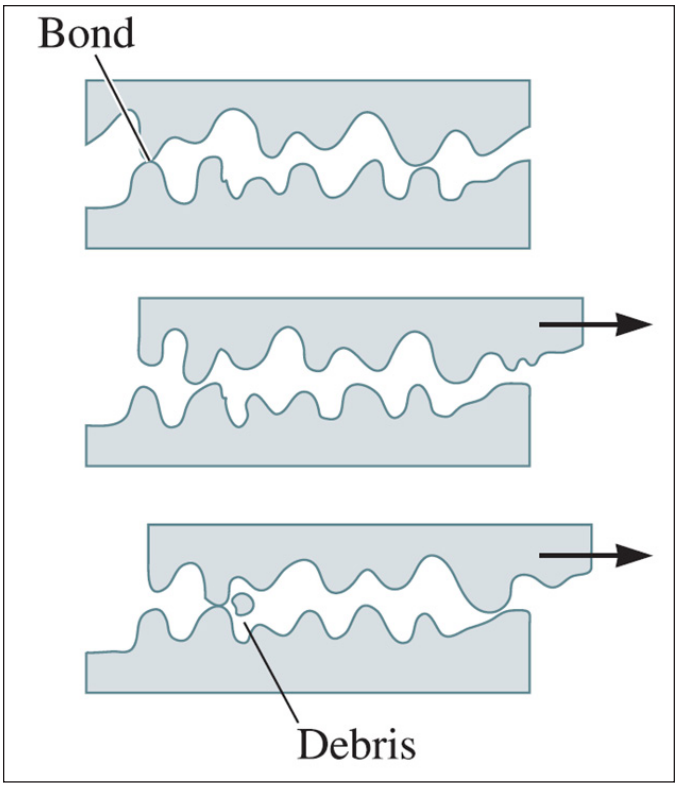

Figure 13
Diagram of adhesive wear[20].

When relative motion occurs between two contacting surfaces where debris or foreign particles are trapped at the interface of the surfaces, the debris can dig into the mating surfaces, resulting in "furrows" and additional debris (**Figure 14**), which, in turn, will result in further occurrence of abrasive wear.

To prevent adhesive and abrasive wear from occurring on articulating surfaces, a variety of factors must be considered. Low loads, smooth surfaces, and effective lubrication are effective methods of reducing wear, but material properties of the mating surfaces are equally important. Generally, if both surfaces have high hardness values, the wear rate is considerably decreased. High strength, high toughness, and general ductility that also help prevent the tearing of material from surfaces can be beneficial under certain loading environments[20].

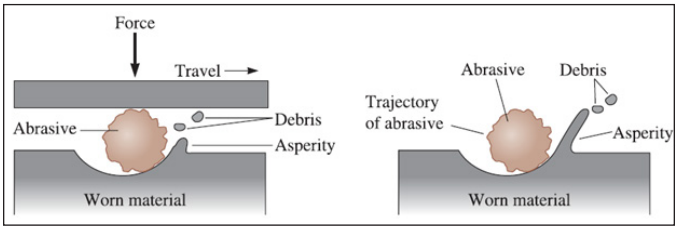

Figure 14
Diagram of abrasive wear[20].

The occurrence of abrasive and/or adhesive wear due to small, oscillatory movements is referred to as "fretting." The modular interfaces within the MoM THA at issue are known to be susceptible to micromotion, creating the conditions necessary for fretting wear to occur.

A study by the manufacturer investigated the wear rates between MoM and MoP bearings. While they found that the volumetric wear rate of the MoM bearings was lower than MoP, the number of particles generated was significantly higher (around 13 to 500 times more, according to another study[22]). In addition, these particles were an order of magnitude smaller than those generated in the MoP bearings, and due to their high specific surface area, promoted the dissolution of the metal into ions and promoted their travel (migration) into the surrounding tissues. As a result, they concluded that MoM wear debris was significantly more hazardous than MoP debris.

Micromotion and Its Causes

The combination of a person's weight and external forces acting upon one's body results in the transmission of loads approximately 3.3 times an individual's weight through the hip joint during day-to-day activities[23]. As a result of these loads, individuals with a modular hip implant are known to experience movement and rotation at the modular connections of such implants. This phenomenon, referred to as "micromotion" in the medical community, will result in fretting wear[24]. **Figure 15** diagrams the loads causing micromotion.

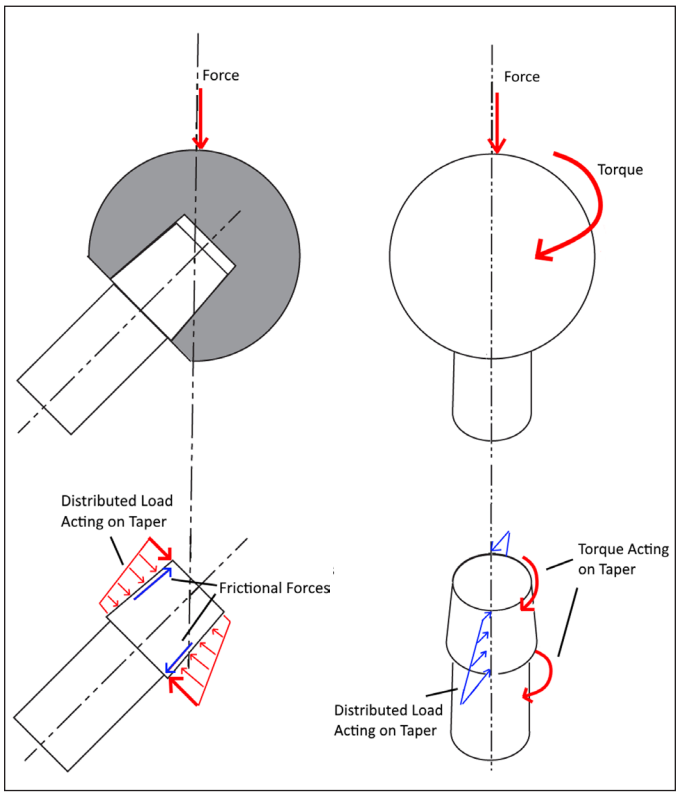

Figure 15
Forces acting at the head/taper interface of a modular hip implant due to downward load and torque applied on top of a femoral head during normal activity.

In modular MoM THAs, such as the device at issue, an angular "mismatch" exists between the interface of the taper sleeve and the head as well as the interface of the taper sleeve and the femoral stem[16]. According to the manufacturer, the purposes of these angular mismatches are to avoid higher tension on the assembly, provide less variation in the final position of the head, and allow physicians to assemble the device more easily.

In contrast to conventional hip implants, which only have a single angular mismatch between the head and stem, modular designs present angular mismatches at the interface of the taper sleeve and the head as well as the interface of the taper sleeve and the femoral stem (**Figure 16**). As the presence of angular mismatches are known to accelerate wear, the existence of an additional interface (where angular mismatch occurs) results in correspondingly increased wear-particle production by this device[16,25].

According to studies performed on hip implants, an increase in the diameter of the femoral head results in

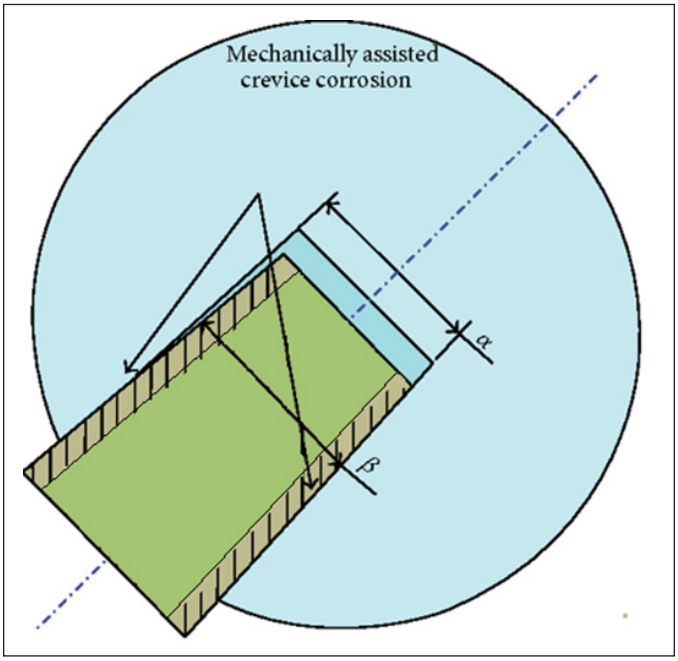

Figure 16
Angular mismatch interface between the tapered sleeve and femoral head[26].

increased micromotion because of the greater magnitude of torque (i.e., effect of a force on an object causing rotation about its axis) applied to the taper. As a result of this, large-diameter femoral heads (i.e., those greater than 36 mm in diameter) have a higher failure rate[27,28,29]. Since the femoral head on the subject devices were all greater than 36 mm in diameter, the micromotion experienced at the taper junction was greater than would have been experienced with the smaller diameter heads used in the average THA. As a result, the wear experienced by the device increased.

Mechanically Assisted Crevice Corrosion

The human body has a highly saline environment containing not only salts and corrosive ions, but also proteins that can lead to immune responses to foreign objects such as medical implants. To ensure that medical devices continue to function as intended without causing detrimental immune responses, medical devices must be designed to resist the highly corrosive environment of the human body[30].

In general, metals are oxidized through anodic reactions, (i.e., $M \rightarrow M+ + e-$), which causes ions of the metal to break off from the bulk material and migrate to the surrounding environment. As previously discussed, these metal ions can lead to the development of metallosis[14,15,16]. Due to their high electrochemical reactivity, cobalt and chromium (metals making up the bulk of the implants at issue) oxidize rapidly, forming a passive "oxide layer" that blocks and protects the metal from the nearby corrosive solution, thereby reducing the amount of corrosion that can occur. However, the protective passive oxide layer can be destroyed by macro- and/or micromotion-induced wear, exposing the bulk metal to the surrounding corrosive environment and resulting in increased levels of corrosion until the passive oxide layer builds up again (**Figure 17**)[24,31].This circular phenomenon of the combined action of wear and corrosion, which creates more material degradation than would have otherwise occurred, is referred to as tribocorrosion[16,32].

The narrow crevices between the modular connections of MoM THAs can allow penetration of bodily fluids that induces a mechanism known as crevice corrosion (or "differential-oxygen corrosion"), an accelerated form of corrosion that occurs when a metal is partially shielded from an environment. Should micromotion-induced fretting wear occur at this interface, the material becomes susceptible to a phenomenon known as mechanically assisted crevice corrosion (MACC)[34].

Documenting the manufacturer's comprehensive understanding of the issue, a report issued by the manufacturer takes their knowledge of MACC and applies it to the modular interface of hip implants. This report explains the phenomenon of crevice corrosion and MACC as follows: "Crevice corrosion occurs when the metal surfaces are partially shielded from the environment… In modular connections, narrow crevices can allow fluid penetration due to the tolerances of the connections. During loading, the passive oxide film of the metal is ruptured, leading to dissolution of metal ions in the crevice fluid. The exposed metal surface reacts with the oxygen in the fluid to form passive oxide and depletes the solution of oxygen. As the fluid is entrapped in a crevice, it has no access to fresh fluid to increase oxygen concentration… This particular model does not require that the mating surfaces be dissimilar for

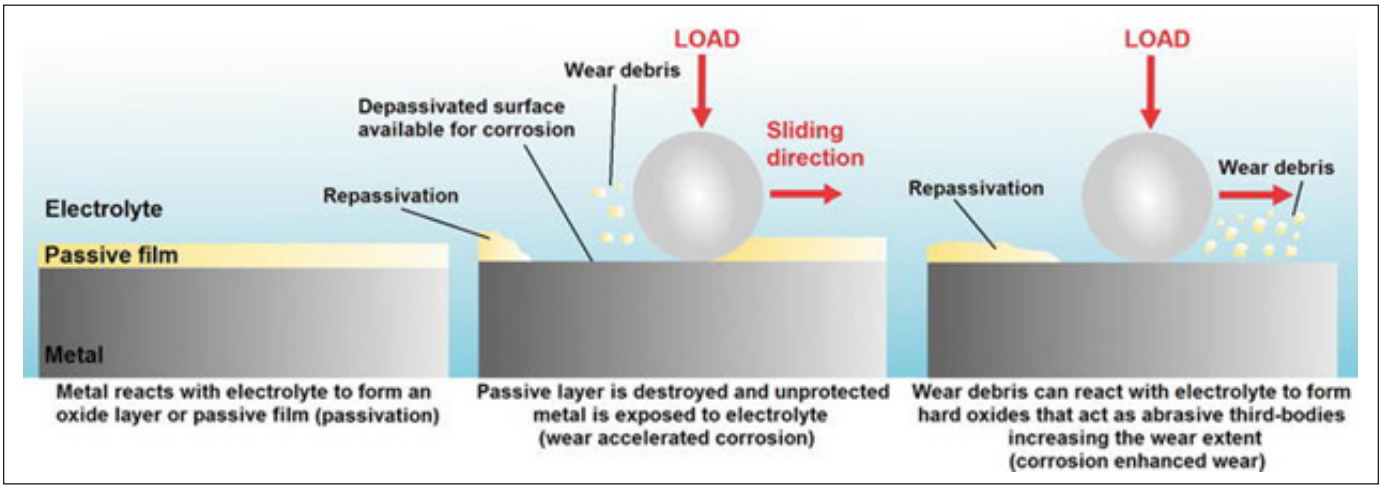

Figure 17
Process of degradation and wear of the passive oxide film layer, known as "tribocorrosion"[33].

galvanic interaction. In the mechanically assisted crevice corrosion, breakage of the surface oxide due to repeated loading/motion, restricted transport of oxygen in the crevice leads to significantly lower pH (as low as 3.5 or lower), which can lead to the active attack of the metals."

MACC can be further accelerated by "cell-assisted corrosion" as a result of the in-vivo environment. Wear particles released from micromotion wear attract inflammatory immune cells to the site. Immune responses to the foreign wear particles cause the cells to release corrosive chemicals, which further accelerate the corrosion occurring due to MACC and cause the crevice environment to become more acidic[35].

It is important to point out that MACC is not a linear phenomenon. As the femoral head or taper sleeve experiences wear, the protective oxide film inhibiting corrosion is abraded and destroyed, which allows for the freshly exposed surface to experience corrosion that would have otherwise not manifested. The process of corrosion changes the surface of the material and the local environment around it, causing increased acidity, cathodic excursions, and an altered oxide film, which, in turn, increases the amount of wear experienced. This creates a positive feedback loop where more corrosion causes more wear — and more wear causes more corrosion, causing the number of released metal ions to exponentially increase, as shown in **Figure 18**.

MACC at the Taper Junction and Liner of Modular MoM THA

Prior studies performed by the manufacturer regarding the wear and corrosion of modular MoM THA devices were conducted in simulated (i.e., in-vitro) environments that showed low rates of wear at these modular interfaces.

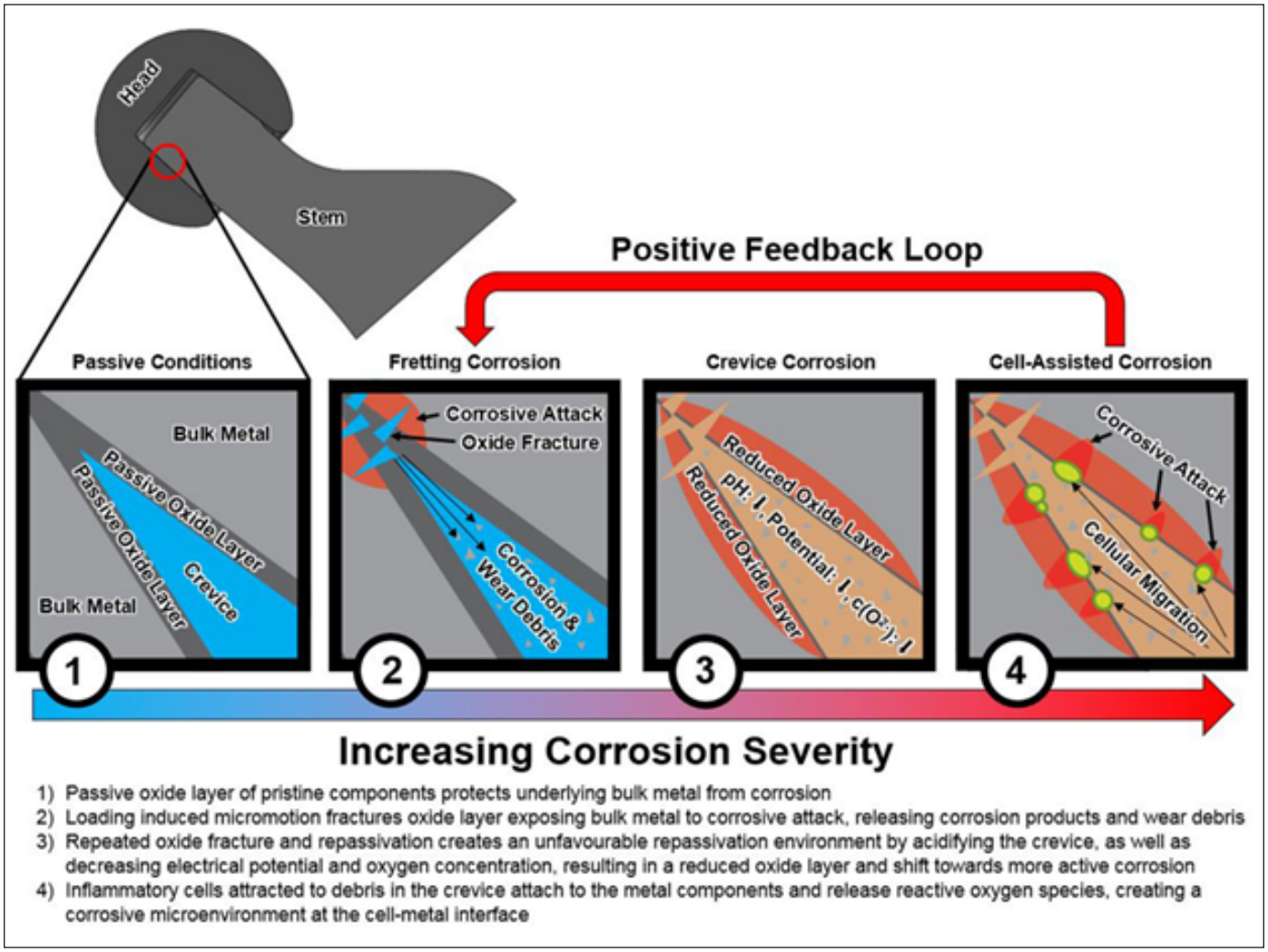

Figure 18
Stages of MACC, showing that the severity of corrosion increases over time[32].

However, once on the market, it was noted that the observed corrosion of the retrieved devices were orders of magnitude higher than their tests had predicted. As these wear and corrosion particles are capable of reducing into metal ions, metallosis and the development of so-called pseudotumors were discovered in recipients of these modular MoM THA devices, necessitating revision.

Based on review of the manufacturer's internal documents as well as publicly available research, metal ions can originate from not only the articulating surface of the femoral head, but also the modular connection at the femoral stem taper[36,37,38,39,40,41] as shown in **Figure 19**. These studies ultimately concluded that the primary cause of wear at this modular connection was due to MACC and fretting wear. Some of these papers detailing the above phenomenon date back as early as 1993. Furthermore, according to available discovery documents, the manufacturer knew about the susceptibility of CoCrMo sleeves to MACC as early as 1997. However, despite this knowledge, there is no indication that any design alterations or measures were implemented to prevent its occurrence.

Studies have revealed that modularity has been shown to give more interfaces where corrosion can occur and lead to an increased number of metal ions[29,43,44]. Both neck modularity and sleeve modularity provide such interfaces for MACC to occur and release a greater number of metal ions. A study from 2014, which reviewed registries and published literature, found that the seven-year revision rate increased from 4.2% to 8.9% when modularity was introduced. The revision rates of these modular systems were stated to further increase when paired with an MoM articulating bearing. This study also found similar revision rates for modular THAs regardless of how the modularity was provided[45].

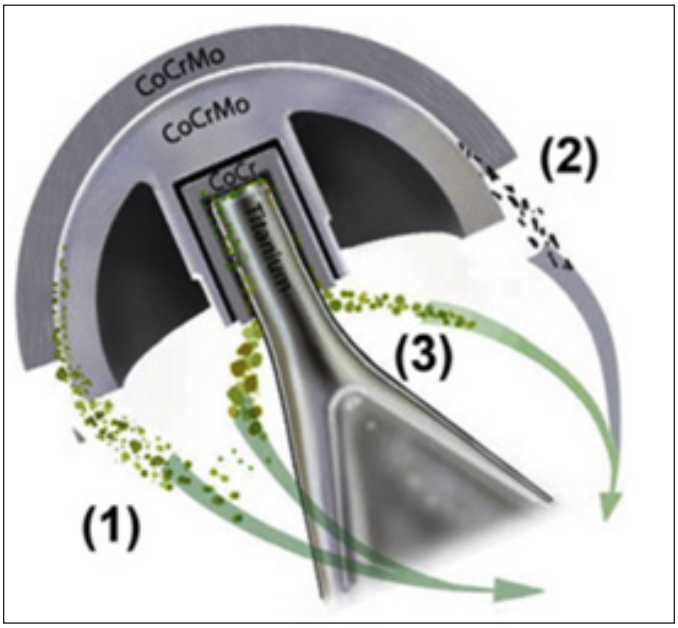

Figure 19
Diagram showing the locations of metal ion release from the modular connection of the hip implant[42].

This suggests that the use of both modular necks or taper sleeves present the same issues in regard to increased rates of revision. A more recent review by Fokter provides further evidence that the number of modular interfaces increases the revision rates of THA implants. Their study found that "dual-modular" systems had a nine-year revision rate of 7.4% as compared to "single-modular" stem, which had a nine-year revision rate of 3%[46].

In addition to the aforementioned data, the National Joint Registry has noted that the revision rates of MoM THAs are approximately 50% greater than MoM resurfacing implants, which lack the taper junction in THAs[47]. Combined with the aforementioned reasons for revisions in MoM THA, this indicates that the use of a taper junction is a significant factor in increased revision. A report by the manufacturer stated that it knew of the increased revision rate for modular devices and theorized that the taper may play a contributing factor in these outcomes.

Modular MoM THA devices that utilized metal liners presented yet another modular interface for MACC to occur. As shown by the square teeth-shaped imprinting marks, there were portions of the liners that were directly mated to the shell with the imprinting marks left behind by the areas that were not directly mated as a result of the square gaps in the shell. The micromotion that took place between the metal liner and shell further generated the release of metal ions into the recipients bodies[48]. More recently, dual mobility components consisting of a polyethylene liner, mated between a metal liner and femoral head, have been noted to suffer from elevated metal ions as a result of the coupling between the CoCrMo liner and Ti6Al4V shell. This adds further support for the conclusion that the use of metal liners significantly increased the level of metal ions in a recipient's body[49,50].

The occurrence of MACC at the taper junction of modular devices is not limited solely to THA implants. Modular devices that are utilized in hemiarthroplasty or resurfacing have also been reported to experience MACC and adverse tissue reactions as a result of metallosis[51]. Even if the devices at issue were utilized without an

acetabular cup as a hemiarthroplasty device, these devices would still have experienced micromotion and MACC at the taper junction, resulting in the accelerated released of metal ions and the development of metallosis

Scanning Electron Microscopy and Energy Dispersive X-Ray Spectroscopy Analysis

The femoral heads of the implants removed from recipients who required revision were examined using SEM and EDS in order to help determine the mechanisms behind the release of metal particles.

During SEM/EDS examination of the femoral heads, several surface imperfections were discovered, which were found to have an elemental makeup different from the bulk CoCrMo material. EDS results revealed a spike in the amounts of silicon and carbon (**Figures 20** and **21**) as well as aluminum and oxygen (**Figures 22** and **23**) present in the vast majority of these imperfections. Based on the observed geometry of these particles, it was concluded that these imperfections were SiC particles and Al_2O_3 particles — both being very hard materials often used in surface polishing applications.

The manufacturer disclosed that the 600-grit Kemet green silicon carbide powder and Kemet kemox abrasive suspension type -0-800 were used during the polishing process (**Figure 24**). To verify that the embedded surface particles were indeed SiC and Al_2O_3, which were left behind from the polishing process, samples were obtained (**Figure 25**).

SEM and EDS analysis were performed on the SiC powder to determine if it is similar to the microscopic

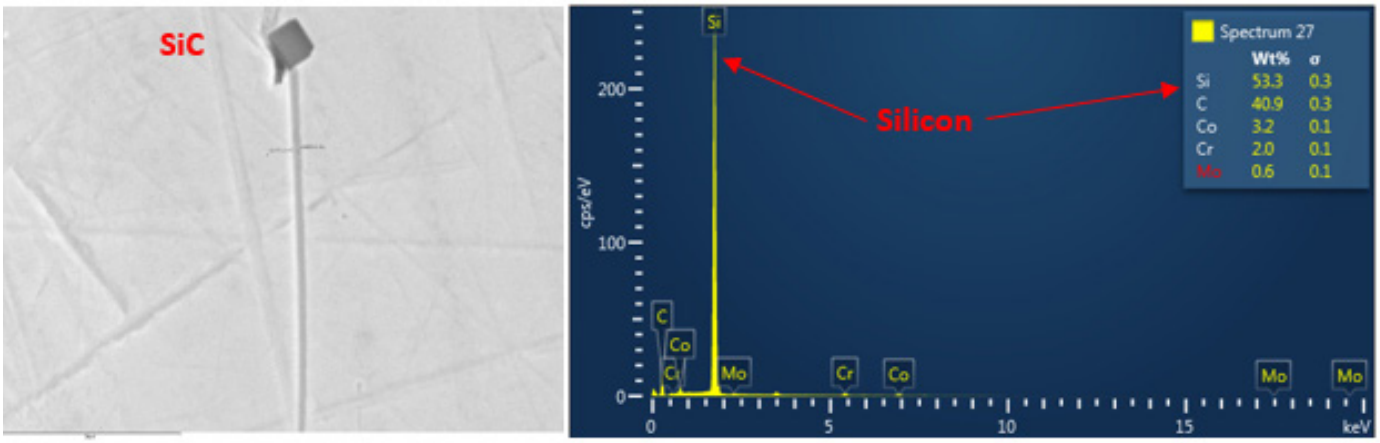

Figure 20
SEM image (left) and EDS results (right) showing a high concentration of silicon and carbon. The silicon-based imperfection was also noted to be embedded at the end of a deep surface scratch, most likely caused by said particle.

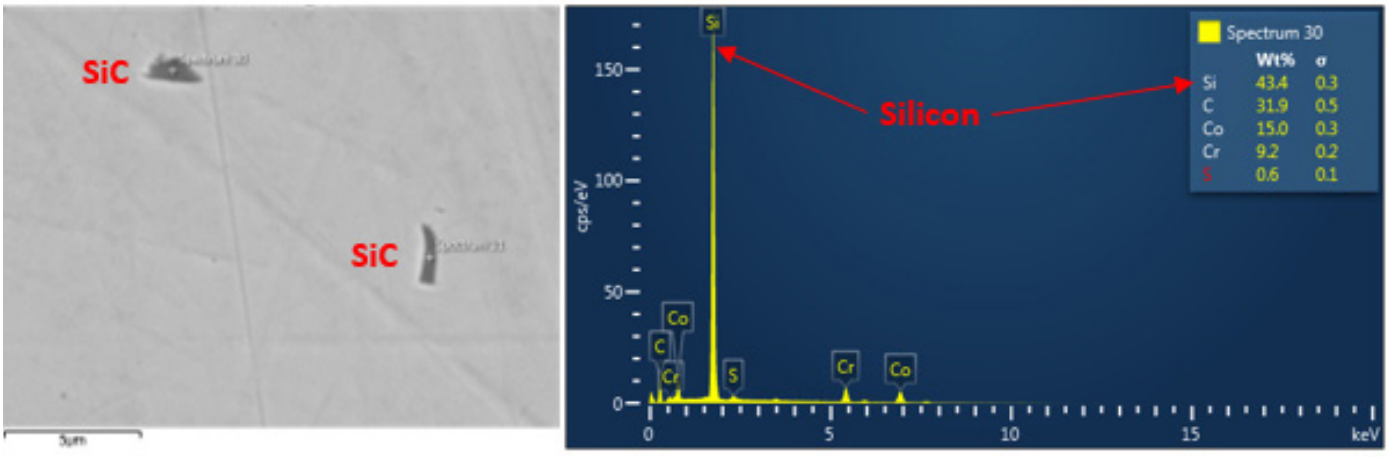

Figure 21
SEM image (left) and EDS results (right) showing embedded particles containing a high concentration of silicon and carbon.

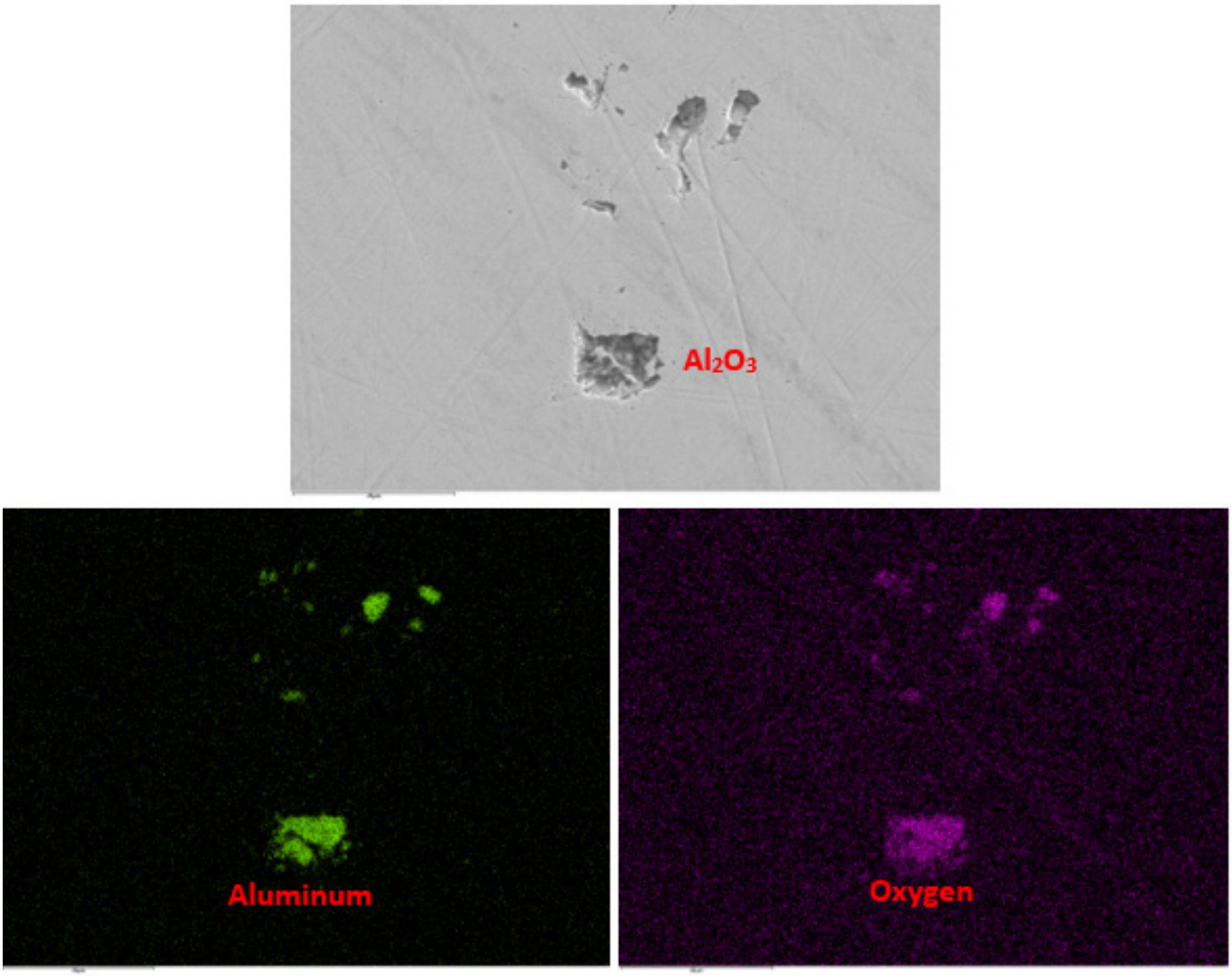

Figure 22

SEM image (top) and its associated EDS maps showing the presence of aluminum (bottom left) and oxygen (bottom right) concentrated in cracks and furrows on the hip, identifying the embedded surface particle as aluminum-oxide, which is routinely used in polishing compounds.

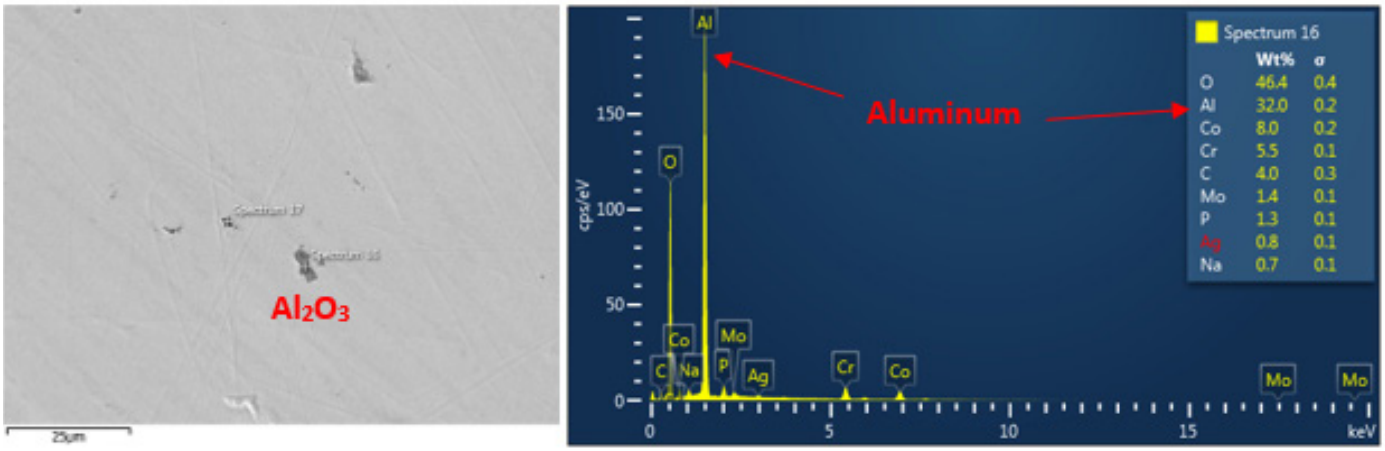

Figure 23

SEM image (left) and EDS results (right) showing high concentration of aluminum and oxygen, indicative of the presence of a micron-sized particle consisting primarily of aluminum and oxygen.

particles found on the manufacturer's modular femoral heads.

As shown in **Figures 26** and **27**, EDS of the SiC powder and Al_2O_3 cleaning slurry showed similar elemental weight percentages to the previously identified embedded silicon-rich particles and aluminum-rich particles. High amounts of carbon were detected in the Al_2O_3

- Rolol Ultragrind Carbide – Code 51719
- Kemet w3 Lubricating Fluid
- Kemet silicone carbide Green powder 600 Grit.
- Kemet 3KC 697 – Paste Diamond
- Kemet 1-05-C3 – Paste Diamond
- Kemet CO-42 Cleaning Fluid
- Hydra Clean DGL4
- Kemet Cleaning Fluid Type A
- Kemet kemox abrasive suspension type -0-800
- Kemet Liquid Type K
- Distilled water.
- *Components then Ultrasonic cleaned in items 8 & 11.*

Figure 24
Table of known contaminants as represented in the design history file with SiC and Al_2O_3 indicated by the red rectangles.

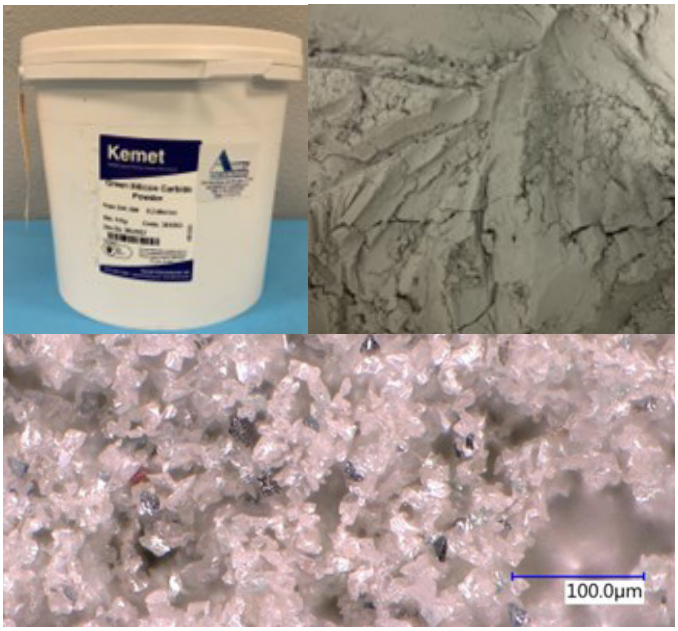

Figure 25
Photographs of the Kemet green silicon carbide powder container (top left) and the silicon carbide powder (top right) and image of silicon carbide particles taken with a digital microscope under 500x magnification (bottom).

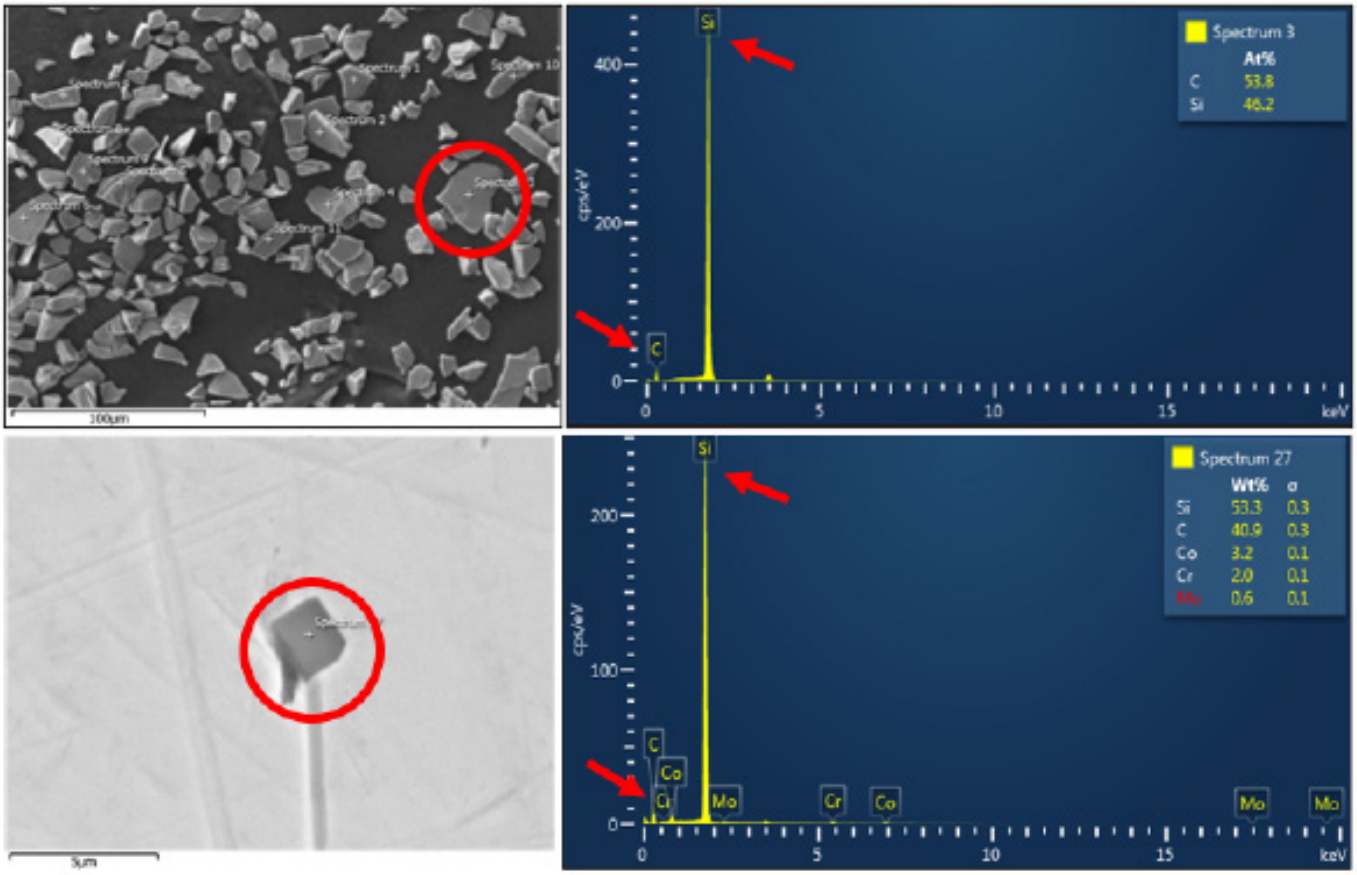

Figure 26
Comparison between exemplar SiC powder (top) and subject explant surface (bottom) with SEM images (left) and EDS results (right). Location of EDS analysis indicated by red circle. Silicon (Si) and carbon (C) EDS results are indicated by red arrows.

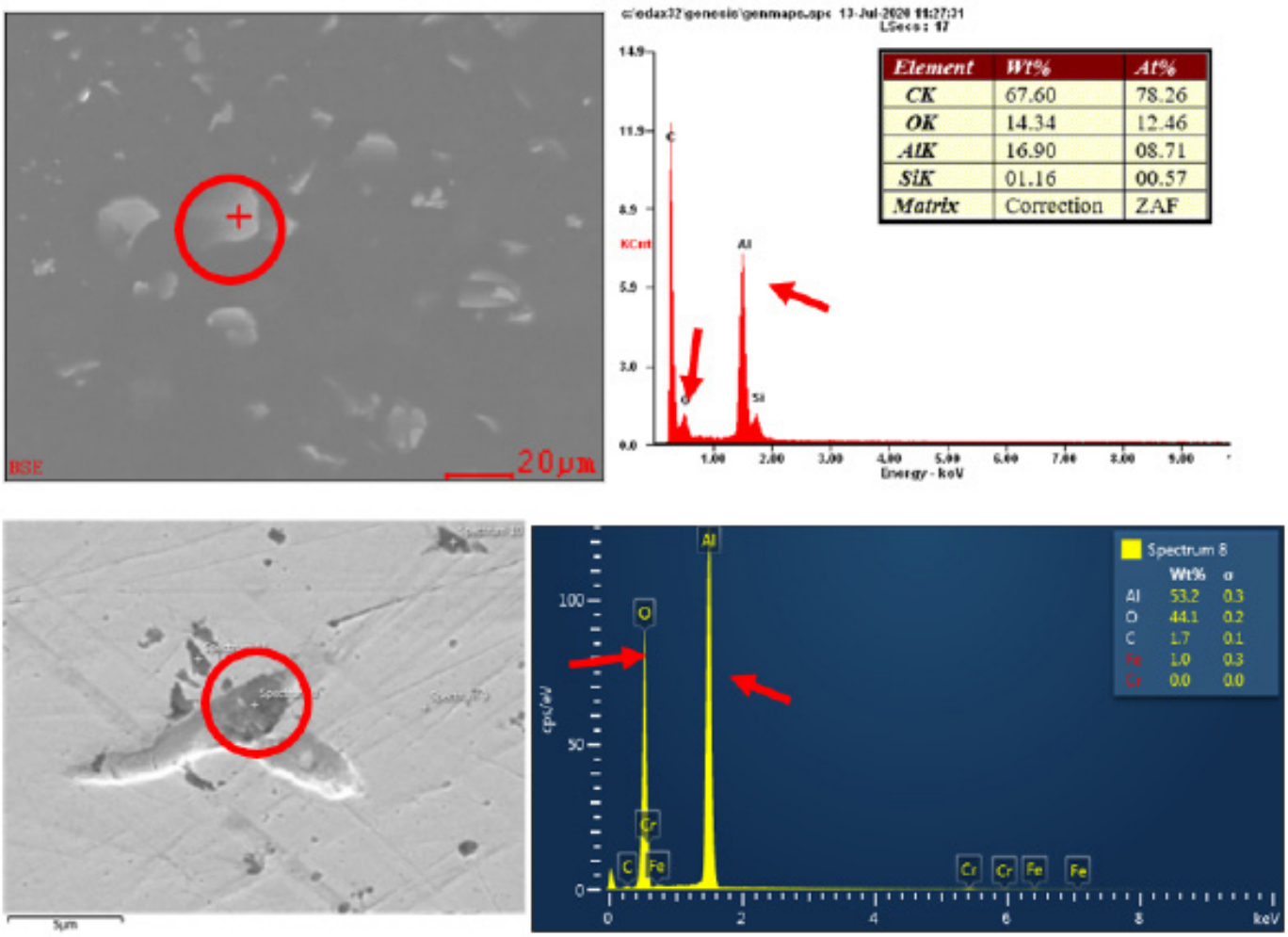

Figure 27

Comparison between exemplar Al_2O_3 slurry (top) and subject explant surface (bottom) with SEM images (left) and EDS results (right). Location of EDS analysis indicated by red circle. Aluminum (Al) and oxygen (O) EDS results are indicated by red arrows.

slurry; however, this was determined to be due to a number of factors. The smaller size of these particles resulted in the elemental readings from the carbon mounting tape to impact the overall results, making the sample appear as though it had more carbon than it actually did. In addition, Al_2O_3 was suspended in a hydrocarbon oil-based slurry that needed to be dried out in order to prevent damage to the SEM. The residue from these hydrocarbons more likely than not left behind a film of carbon on the particles and carbon tape, which further increased the carbon reading in the EDS spectra.

Additionally, the morphology of the particles on the explants were very similar to those found in the SiC powder and Al_2O_3 slurry. In the absence of alternative explanations for the presence of these imperfections, it was concluded the particles observed on the surface of the femoral heads were most likely SiC and Al_2O_3 left behind from the polishing process. Corroborating this conclusion, one of the deposed corporate representatives in these cases stated that it is foreseeable for at least 1-micron-sized SiC particle to be left behind on the surface of the devices.

As SiC and Al_2O_3 particles were from polishing slurries intended to remove material to smooth out the surface of the implant, the manufacturer's failure to completely remove these abrasive particles following polishing triggered an unnecessary and avoidable increase in wear. Due to this increased abrasive wear, small metal particles — and thus cobalt and chromium ions — would be released that can result in the local death of tissues and the formation of pseudotumors.

A 2008 journal article entitled "Characterization of the Running-in Period in Total Hip Resurfacing Arthroplasty: An in Vivo and in Vitro Metal Ion Analysis" discussed

third-body wear caused by hard polishing-agent particles remaining on a device surface during testing. "Other possible causes for the delayed running-in period are aluminum oxide and silicon oxide-filled pits and scratches originating from these pits. These compounds are used as polishing agents during manufacturing. Residua of these very hard compounds may become incorporated into the surface and could later be released during simulation, thus causing third-body wear. This would explain the abrasive scratches originating from these pits. It is, however, questionable whether these particles are released exactly after 300,000 cycles."[52]

In this study, these hard, polishing-agent particles were embedded in the surface of the device. SEM analysis of the device surface after testing showed scratches originating from pits (**Figure 28**). Based on this evidence, it is reasonable to conclude that the Al_2O_3 and SiC particles were, in fact, residua left over from polishing of the hip implants and caused the large gashes observed on the devices.

An email from the manufacturer explicitly refers to the presence of polishing compounds as being causative in increased third-body wear, and that a "…high content of aluminum oxide and silicon oxide in these pits suggested the presence of residua from the polishing agent."

Not only does this provide more evidence for the aforementioned conclusion that these silicone and carbon-rich particles were polishing compounds, but it also goes to show that the manufacturer was aware of the potential for polishing agents to be left behind on their devices — and that such particles would more likely than not increase the experienced wear.

The authors' team was unable to quantify the number of embedded particles in these femoral heads due to the lack of necessary equipment. However, this proved to be unnecessary for their work as the sheer magnitude of embedded particles was sufficient to demonstrate the sheer magnitude polishing debris left behind. Future work by retrieval analysts should attempt to quantify the amount of polishing compounds left behind on devices and determine their influence on the wear of hip replacement devices.

Further SEM/EDS analysis was conducted on the taper sleeves, acetabular cups, and metal liners. On at least eight of the 11 devices available for analysis, the taper sleeves were unable to be removed from their respective modular head. As a result, SEM/EDS of the taper's surface and interior was impossible because there was not an angle the authors could position the embedded taper that would allow for proper SEM. For these cases, the team opted to utilize the SEM/EDS results of previously inspected tapers and relate the observations from these other devices to the devices where taper analysis was impossible. As shown in **Figures 29** and **30**, biological products and chromium-rich corrosion debris were observed on the taper sleeves, distinct from the underlying CoCrMo alloy.

Analysis of the metal liners revealed similar SiC particles to those found on the heads. A coating of iron and nickel was observed on the surface of these liners, likely

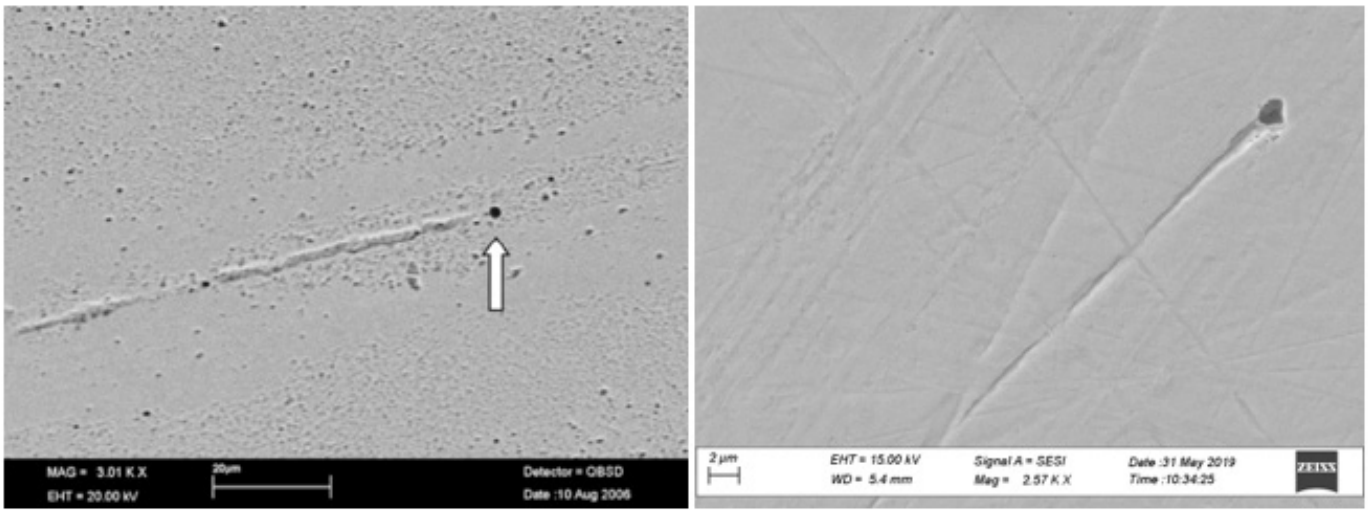

Figure 28

SEM image showing a figure from a study with "scratch originating from alumina filled pit ([white] arrow)" (left) and SEM image from the subject modular S&N femoral head with a similar scratch or furrow adjacent to the pit (right), which exhibited high levels of aluminum (Al) and oxygen (O) consistent with aluminum oxide (Al_2O_3), another polishing agent used during the polishing step of manufacturing.

left behind by biological debris (**Figure 31**).

The results of the authors' SEM and EDS analysis provide further corroboration of these observations. It is more likely than not that the presence of not only the polishing compounds' residue contributed to the increased wear and corrosion of the device, which, in turn, resulted in increased presence of metal ions and the ensuing metallosis in the recipients.

Analysis of Taper Crevice Debris

In order to provide insight into the nature of the corrosion debris observed on the head and taper of one of the explants at issue, a piece of carbon tape, typically utilized for affixing smaller samples for SEM analysis, was utilized to extract corrosion particulate from the interior surface of the taper sleeve (**Figure 32**). While there is no specific ASTM standard for debris removal methodology, the use of carbon tape for nondestructively removing corrosion products and residue for observation is a common practice in materials science applications in a wide range of industries.

SEM and EDS analysis of the recovered corrosion debris revealed the presence of chromium, molybdenum, titanium, and oxygen (**Figures 33** through **35**).

These results held some similarities to the wear debris previously observed during EDS of the taper sleeves.

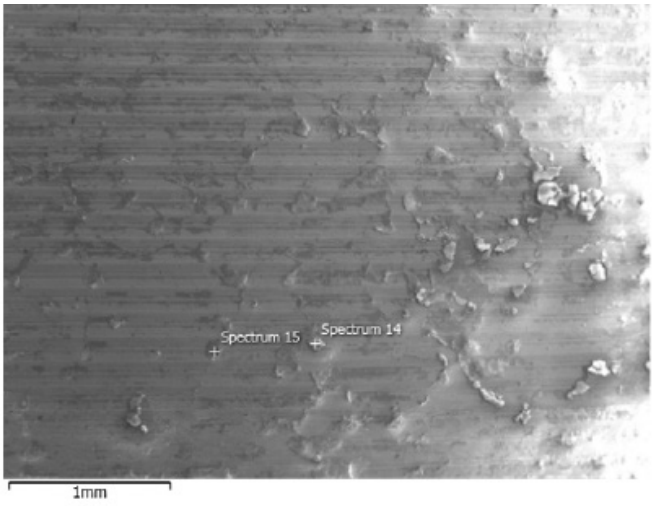

Figure 30
SEM and EDS results from one of the tapers available for such analysis. These images show macroscopically visible particles containing chromium, carbon, and oxygen.

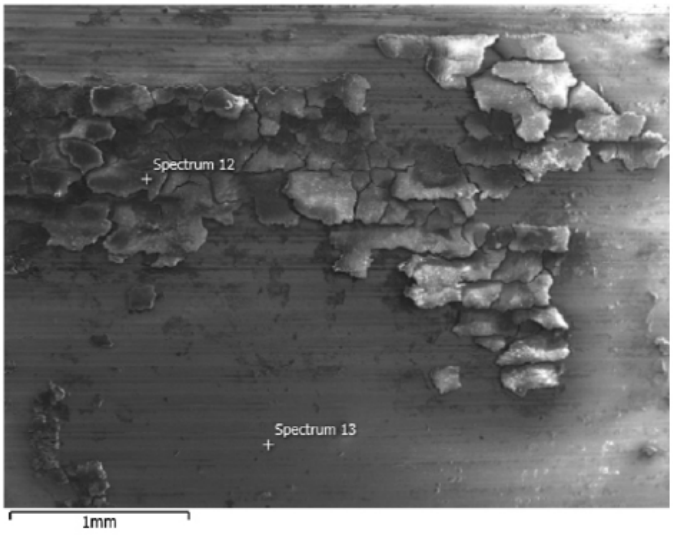

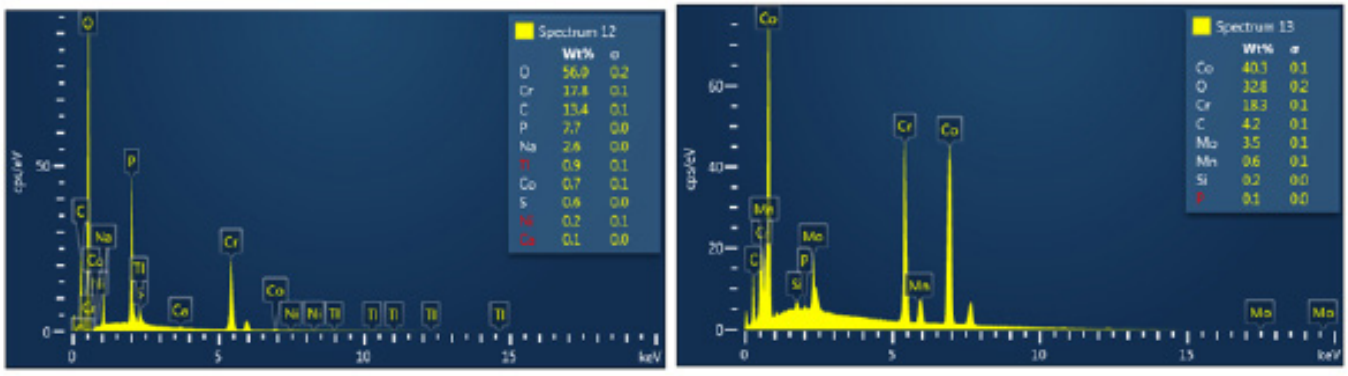

Figure 29
SEM and EDS results from one of the tapers available for such analysis. These images show the presence of chromium and oxygen-rich debris distinct from the base alloy.

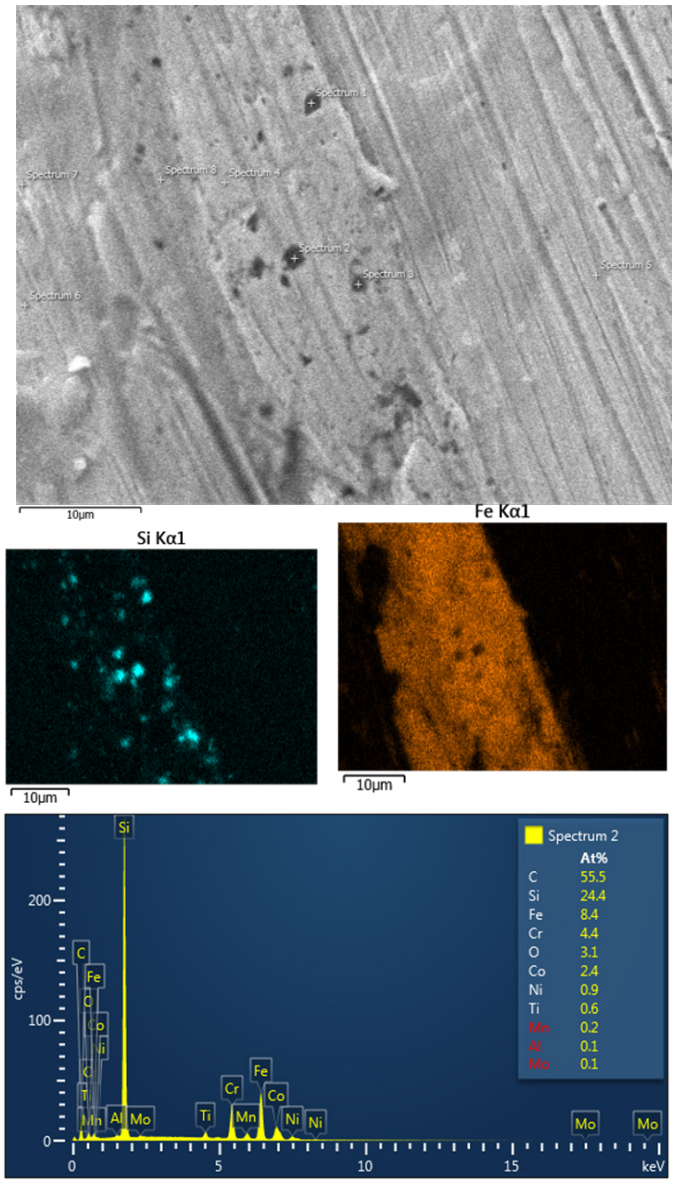

Figure 31
SEM and EDS of a metal liner, showing embedded SiC particle and biological products.

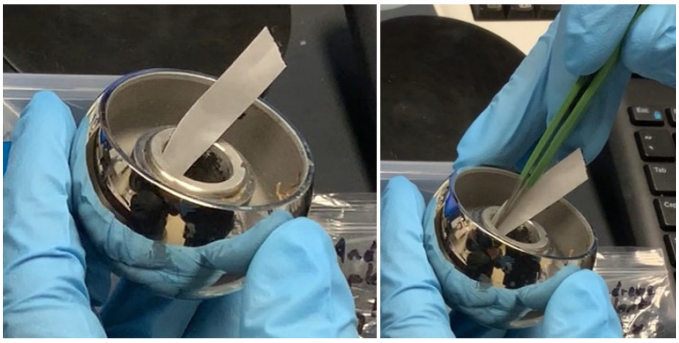

Figure 32
Images showing the process utilized to extract corrosion debris from the interior surface of the taper sleeve.

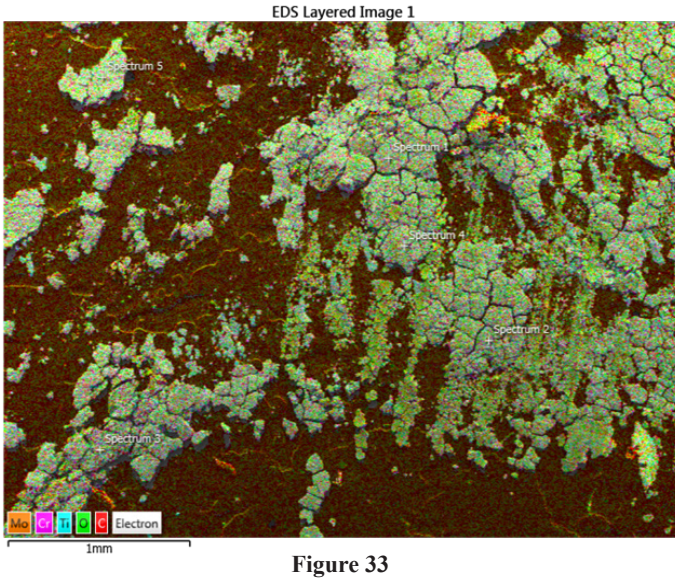

Figure 33
EDS map of the debris collected from the interior surface of the subject taper sleeve.

Based on the EDS maps and percent weight of these elements at various analysis points, it was concluded that, on a more-likely-than-not basis, the debris recovered from the interior surface of this taper sleeve primarily consisted of chromium, molybdenum, and titanium corrosion products produced as a result of MACC.

A number of research papers (as well as the manufacturer's internal testing) found that the taper junction preferentially releases cobalt ions and that chromium is left behind on the taper, producing the chromium-rich debris such as that observed on the debris in the conducted test[53,54]. A 2014 study titled "Influence of Implant Design on Blood Metal Ion Concentrations in Metal-on-Metal Total Hip Replacement Patients" postulates that the main source of metal ion debris in patients suffering from metallosis in modular THA devices is from the modular taper junction, given that the blood cobalt concentrations of these patients were nearly twice those of chromium concentration[55]. This is supported by the manufacturer's own internal testing, which concluded that high Co/Cr ion ratios indicate that "…the magnitude of wear from the bearing area is considerably less than that from the taper area."

Based upon the results of the conducted test, as well as the information presented in the aforementioned research, the chromium-rich debris along with the elevated levels of cobalt ions found in the blood of the recipients of the devices indicate that, within a reasonable degree of scientific and engineering probability, the majority of wear particulate and metal ions found in their body originated

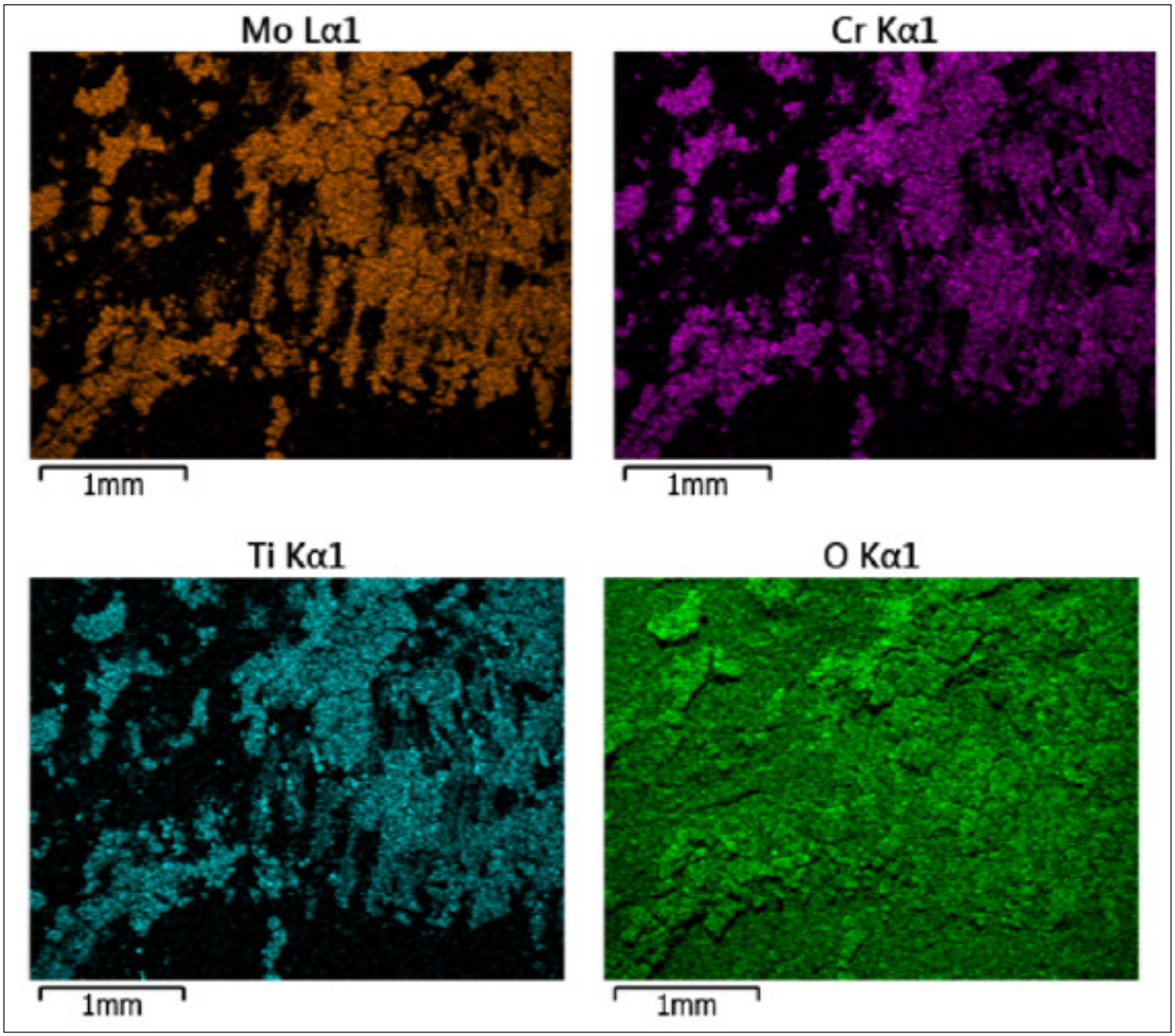

Figure 34
EDS maps of individual elements from the debris collected from the interior surface of the subject taper sleeve.

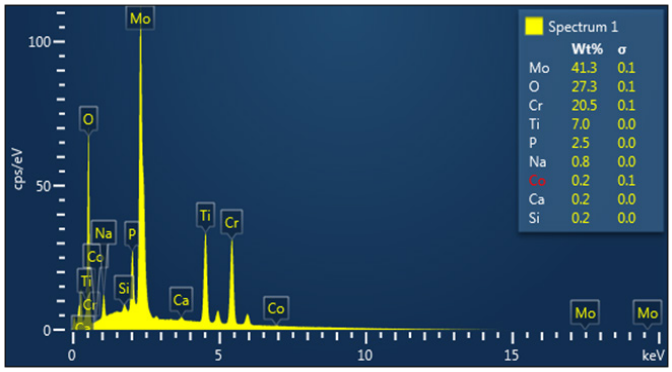

Figure 35
EDS results from the debris collected from the interior surface of the subject taper sleeve.

from the taper interfaces.

Inappropriate Material Combinations

The taper sleeve utilized in the subject device was noted to have been manufactured using low-carbon CoCr-Mo, while the femoral heads were manufactured using high-carbon, as-cast CoCrMo. The subject femoral stem was manufactured using a titanium alloy (Ti6Al4V). According to a wear study conducted by the manufacturer that explores "the wear characteristics of various cobalt-chromium (Co-Cr) alloy combinations," low-carbon Co-Cr alloys exhibited the highest rate of wear out of the alloys amongst the materials tested (**Figure 36**). Since the taper

sleeve was being manufactured from this vulnerable alloy, one can expect any tribocorrosion and fretting wear at the modular interface to be greater than it would have been had a different alloy been selected for use in the taper sleeve.

In addition, the wear rate of the low-carbon CoCrMo would be exacerbated by the differential hardness between the mated materials (low-carbon CoCrMo taper sleeve mated with the high-carbon CoCrMo femoral head and titanium femoral stem). Since micromotion occurs at both of these modular junctions, the use of low-carbon CoCrMo at this junction would result in additional wear.

Galvanic corrosion is a type of corrosion that occurs when two dissimilar metals are in contact (a couple) with each other, creating an electrochemical reaction that can accelerate the corrosion commensurate with the electropotential difference between the metals. The combination of CoCrMo and Ti at the modular interface between the taper and stem creates a "galvanic couple" resting in accelerated corrosion at this interface.

A number of research papers have shown that when the passive oxide layers for CoCrMo and Ti6Al4V are maintained, mating of these two materials results in negligible galvanic current. However, the removal of these passive oxide layers due to wear and the prevention of their reformation can cause the galvanic corrosion to become a significant issue[56,57,58.]

While the individual mechanics of the galvanic coupling among the different phases and corrosion particulate of these material are rather complex, a general understanding of the corrosion behavior can be determined using the open circuit potential (also known as equilibrium or corrosion potential) and the placement of the materials on the galvanic series. Based on these principles, it is found that for the unpassivated coupling of CoCrMo and Ti6al4v, CoCrMo will act as the "anode" in the couple and experience preferential dissolution[59,60].

Convex/Concave	Convex Wear	Concave Wear	Total Wear
As-cast/As-cast	4.1 ± 4.0	65 ± 45	69.1 ± 49.0
S.T. cast/S.T. cast	37 ± 31	114 ± 34	150 ± 51
S.T. cast/As-cast	3.1 ± 0.7	102 ± 12	105.1 ± 12.7
Low carbon/Low carbon	471 ± 51	187± 28	658 ± 77
Low carbon/S.T. cast	470 ± 54	29 ± 5	499 ± 57
High carbon/High carbon	69 ± 60	85 ± 74	154 ±134
High carbon/S.T. cast	86 ± 81	68 ± 40	154 ± 121
High carbon/As-cast	0	0.02	0.02

Figure 36
Experimental results for Co-Cr alloy average weight loss (mg) and standard deviation after 250,000 cycles with 100±50µm diametral clearance with low carbon Co-Cr alloy results highlighted by the red box.

According to the manufacturer's documentation, they knew that the passivation layer was what made the coupling of CoCrMo and Ti6al4v somewhat acceptable. The corrosion resistance provided by this passive oxide layer made the galvanic potential between the coupled metals a rather insignificant factor due to their overall low corrosion. However, as the passive oxide layers on the CoCr and Ti alloys utilized in the head/taper sleeve and taper sleeve/stem connections were abraded due to micromotion at these interfaces, the galvanic current between these two interfaces greatly increased. Despite this knowledge, the manufacturer made no attempt to alter the design of its devices.

The effect of this galvanic coupling can be seen from the revision rates in registries and literature. A recent meta-analysis of modular THA implants concluded that modular connection of CoCrMo and Ti6Al4V had an excessively high failure rate in comparison with other material connections, and, as such, CoCr necks should be abandoned in favor of purely Ti6Al4V connections[61].

ISO 21534:2007 "Non-Active Surgical Implants — Joint Replacement Implants — Particular Requirements" states in Annex B that a combination of cobalt chromium (CoCr) and titanium (Ti) is not an acceptable material combination for articulating surfaces of implants[62]. As previously mentioned, the motion associated with the articulating nature of the components results in the progressive breakdown of the oxide layer, which, in turn, results in the creation of small metal debris particles as well as exposure of fresh metal to continue this oxidation/wear cycle. Therefore, since the "motion" associated with the articulation mechanism is of concern within the spirit of ISO 21534:2007, even micromotion can result in the same phenomenon as described above, thereby creating micron and sub-micron-sized debris in the process.

The above observation regarding creation of micron and sub-micron sized metal particle debris as a result of micromotion at tapered junctions was also made by multiple employees of the manufacturer. One of these employees stated that "…all modern tapers, independent of design, have some degree of micromotion that, in my opinion, makes a taper a junction between articulating surfaces." Therefore, based on the above observations,

the micromotion between the CoCr sleeve and Ti taper would also break down the passive oxide layer between the surfaces and result in the accelerated corrosion of this junction. Therefore, the combination of CoCr and Ti at the taper junction in the devices at issue would have been unacceptable according to ISO 21534:2007.

Testing Performed by the Manufacturer

Prior to the revision of the implanted devices studied in this paper, a number of similar MoM devices produced by other manufacturers were noted to have been recalled due to high failure rates as defined by the degree of metal ion release. A number of manufacturers with similar MoM THA implants were noted to have experienced five- to seven-year failure rates ranging from 12% to 50.4%[63]. As was shown in documents provided by the manufacturer, the manufacturer of the devices at issue knew that its products were similar to these recalled implants.

Review of provided discovery documents also revealed that the manufacturer previously conducted in-vitro (simulated) testing via "hip simulators" in order to accelerate the wear experienced by the device over its useful life in an attempt to assess its long-term wear resistance. However, while such tests utilized a typical hip simulator to accelerate the wear process, the test components were immersed in a solution of simulated body fluid (pH 7). As a result, the corrosion environment to which the devices were subjected was not accelerated like the in-vivo wear was, and thus failed to provide an accurate long-term tribocorrosion environment.

As accelerated wear tests are intended to reproduce the equivalent of many years of wear in a short amount of time, by failing to combine the wear tests with a similarly accelerated corrosion environment, their testing resulted in misleading information regarding the resistance of these devices to tribocorrosion. Had the manufacturer combined accelerated corrosion and wear tests, this would have more accurately simulated the environment the THA implants would be subjected to and would have shown the manufacturer that its modular devices presented an unreasonable risk of corrosion and exposure to metal-ion to recipients of the device.

It was also revealed that the manufacturer had previously conducted accelerated corrosion tests as early as 2004 to reproduce the "imprinting" corrosion marks observed on some of its devices. The solution utilized for this test was an "acidified ringers solution" with a pH of 1. This solution properly provides an accelerated environment consistent with the manufacturer's knowledge that the in-vivo pH of this crevice environment was approximately 3.5 or lower. In addition, research by the manufacturer and by the scientific community as far back as the early 1990s found that the crevice environment of these modular devices was acidified by the creation of hydrochloric acid due to the migration of chloride ions into the crevice environment[37,59].

The "acidified ringers solution" with a pH of 1 would have been able to properly simulate not only the natural environment of the human body, but also reproduce the long-term effects the hydrochloric acid crevice environment would have on MACC in a significantly shorter time period. Although this method was able to properly reproduce said imprinting marks, the manufacturer did not utilize this accelerated corrosion test (or a modified version of it) in combination with its typical accelerated wear tests. They also made no attempt to utilize this method or combine a variation of it with their mechanical wear tests for any of their pre-clinical studies for the devices at issue.

The manufacturer knew — or should have known — that this accelerated corrosion/wear environment would allow its in-vitro tests to simulate the conditions of the human body more accurately[64]. In addition, the results of these tests were not submitted to the FDA during the manufacturer's attempts to get regulatory approval for the subject device combination, although this test would have been more in line with the "worst-case" scenario the FDA requires for these applications.

By the time lawsuits regarding metal poisoning from their THA devices began in 2013, the manufacturer used the aforementioned accelerated corrosion test on the modular femoral head and modular taper. When it did, the tests reproduced the severe imprinting they had observed for years on explant (i.e., the implants that have been removed from a recipient) retrievals. In addition, the material loss observed at the modular interfaces far exceeded the amounts observed in previous studies. Had the manufacturer performed this combined accelerated wear/corrosion testing in its pre-clinical trials, it would have seen the susceptibility of its modular devices to tribocorrosion and realized that the modular implants were not safe enough to be placed on the market.

Off-Label Use

In addition, a number of these incidents were noted to involve off-label combinations of the manufacturer's components (i.e., physicians legally utilizing them in

combinations that had not been specifically approved by the FDA).

The 510(k) applications submitted by the manufacturer to the FDA to gain clearance for the device combinations utilized in the cases at issue to be utilized in THA operations were rejected by the FDA because the manufacturer was unable to provide appropriate clinical data for the safety and effectiveness of these device combinations. Ultimately, the FDA granted clearance for the acetabular cup in the device combination at issue to be utilized in resurfacing operation and clearance for the modular head and taper to be utilized to hemiarthroplasty procedures.

Despite this, the surgeon training, device labels, as well as marketing and promotional materials presented the device combinations at issue as FDA-cleared THA systems, despite neither device being cleared for such operations. In addition, the manufacturer's sales representatives were routinely bringing the modular femoral head and sleeves into THA procedures, even when the doctor did not request those parts (as was done in a number of the cases investigated in this paper).

Summary

Modular metal-on-metal THA implants exhibit excessive failure rates, mostly associated with the release of hazardous metal ions into the recipient's body. These ions, resulting from the wear and corrosion of the implant's CoCrMo alloy, can result in damage or death of local tissue, loosening of nearby implants, development of pseudotumors, and other adverse consequences.

Modular interfaces, such as the junction between the femoral head/taper sleeve and/or the femoral stem/taper sleeve, experience "micromotion" that can destroy the metal's protective passive oxide layer at these interfaces, leading to the occurrence of MACC and fretting wear. This combined action of wear and corrosion mechanisms at the modular interfaces creates a positive feedback loop that exponentially increases material loss. The manufacturer knew of its modular MoM THAs' susceptibility to MACC but failed to properly guard against it or seek alternative designs

SEM and EDS analysis of the subject femoral head showed surface imperfections and embedded surface particles containing an inhomogeneous elemental makeup inconsistent with the nominal surface topography of the base material surface. A comparison of the elemental make-up, as well as size and geometry, of the imperfections/debris discovered on the surface of the subject explant with particles in a polishing compound utilized by the manufacturer, concluded that the discovered surface imperfections/debris were silicon carbide (SiC) and aluminum oxide (Al_2O_3) particles left behind from the polishing process. The presence of these particles accelerated the wear on bearing surface, increasing the number of metal ions released into the bodies of the recipients.

SEM/EDS of the taper sleeves as well as examination of corrosion debris extracted from the taper of one of the devices identified chromium-rich corrosion debris. The presence of these chromium-rich deposits combined with the high ratio of cobalt to chromium ions in this individual's blood, coincides with previous findings that elevated levels of cobalt are indicative that the taper junction is the main source of metal ion release in these individuals. Similar signs of chromium-rich debris along with the elevated levels of cobalt ions found the blood of all the recipients indicate that — within a reasonable degree of scientific and engineering probability — the majority of wear particulate and metal ions originated from the taper interfaces.

The taper sleeve of the subject device was manufactured from low-carbon CoCrMo, which has been shown to exhibit relatively poor wear resistance. Coupling of this low-carbon CoCrMo taper with a Ti6Al4V femoral stem results in increased wear characteristics due to the materials' differential hardness. In addition, the use of dissimilar materials created a galvanic couple that further increased the corrosion and wear at the sleeve-stem interface.

Review of provided documents revealed that the manufacturer performed pre-clinical testing on the device at issue. Such testing involved the use of a hip simulator to accelerate the wear experienced by the device in order to assess its long-term wear resistance. However, by not creating conditions that would also accelerate the experienced corrosion, the performed testing failed to properly simulate the tribocorrosion (coupled effect of corrosion and wear) environment to which the device would be subjected during the device's useful life.

By failing to perform coupled accelerated corrosion and accelerated wear testing, the manufacturer failed to properly simulate the environment of the human body and provided misleading information regarding the performance of its modular MoM THA system. The manufacturer had previously conducted accelerated corrosion tests to reproduce characteristics observed on retrieved

devices, yet failed to implement this more accurate condition into its wear tests.

Conclusion

It is the authors' hope that the information and methodology discussed in this paper can be utilized as an outline for expert witnesses in cases involving the failure of MoM and modular THA implants as the number of lawsuits for these devices continues to increase. The team's findings also raise questions related to the quality of testing performed by manufacturers and the knowledge they had regarding the dangers their devices presented. It is the opinion of the authors that disasters similar to the mass recall of MoM hips in the early 2010s are likely to occur in the future should such negligent testing and product marketing be allowed to continue without consequence.

Acknowledgements

The authors would like to thank the legal experts they worked with on this case as well as their dedicated team of forensic engineers and interns.

References

1. H. M. Kremers et al. "Prevalence of Total Hip and Knee Replacement in the United States" J Bone Joint Surg Am.; vol. 97 no. 17, Sep., pp. 1386–1397, 2015.

2. J. R. H. Foran, "Total Hip Replacement" AAOS orthino, June 2020. [Online]. Available: https://orthoinfo.aaos.org/en/treatment/total-hip-replacement/ [Accessed Dec. 10, 2022].

3. W. Kurtz "Hip Replacement Implants" nashvillejointreplacement.com. [Online]. Available: https://www.nashvillejointreplacement.com/hip-implants [Accessed Dec. 10, 2022].

4. C. Y. Hu andT. Yoon, "Recent Updates for Biomaterials Used in Total Hip Arthroplasty" Biomater. Res. vol. 22, Dec., 2018.

5. R. Grunert, et al. "Novel concept of a modular hip implant could contribute to less implant failure in THA: a hypothesis" Patient Saf Surg. vol. 12, Jan, 2018.

6. T. M. Zink and B. J. McGrory, "Mechanically Assisted Crevice Corrosion in a Metal-on-Polyethylene Total Hip Presenting With Lower Extremity Vascular Compromise" Arthroplasty Today, vol. 6, no.3, Sep., pp. 445–450, 2020.

7. D. Fabi et al. "Metal-on-metal total hip arthroplasty: Causes and high incidence of early failure," Orthopedics, vol. 35, no. 7, June, pp. e1009–16, 2012.

8. C. Kenney, S. Dick, J. Lea, J. Liu, and N. A. Ebraheim, "A systematic review of the causes of failure of Revision Total Hip Arthroplasty" J Orthop. vol. 16, no.5, Sep-Oct. pp. 393–395, 2019.

9. Australian Orthopaedic Association National Joint Replacement Registry (AOANJRR). "Hip, knee and shoulder arthroplasty: 2021 Annual Report." Adelaide, Australia, Australian Orthopaedic Association, 2021.

10. D. Cohen, "Hip implants: how safe is metal on metal?" BMJ, vol. 344, Mar. pp.18-24, 2012.

11. National Joint Registry for England and Wales "National Join Registry 18th Annual Report 2021" London, UK, National Joint Registry, 2021.

12. Australian Orthopaedic Association National Joint Replacement Registry (AOANJRR). "Hip, knee and shoulder arthroplasty: 2011 Annual Report." Adelaide, Australia, Australian Orthopaedic Association, 2011.

13. "Collection and Preservation of Information and Physical Items by a Technical Investigator" ASTM E1188-11, ASTM International, West Conshohocken, PA, USA, Mar., 2017

14. C. A. Oliveira, I. S. Candelária, P. B. Oliveira, A. Figueiredo, and F. Caseiro-Alves "Metallosis: A diagnosis not only in patients with metal-on-metal prostheses" Eur J Radiol Open. vol. 2 pp. 3-6, 2015.

15. J. Drummond, P. Tran, and C. Fary "Metal-on-Metal Hip Arthroplasty: A Review of Adverse Reactions and Patient Management" J Funct Biomater, vol. 6, no. 3, Jun, pp. 486-99, 2015.

16. M. Feyzi, K. Fallahnezhad, M. Taylor, and R. Hashemi "The mechanics of head-neck taper junctions: What do we know from finite element analysis?" J Mech Behav Biomed Mater, vol. 116, Apr., pp. 104338, 2021.

17. C. C. Ude et al. "The Mechanism of Metallosis After Total Hip Arthroplasty" Regenerative Engineering and Translational Medicine, vol. 7, no. 3, Sep., pp.247–261, 2021.

18. D. G. Barceloux, "Chromium" Journal of Toxicology: Clinical Toxicology, vol. 37, no. 2, pp. 173–194, 1999.

19. D. G. Barceloux, "Cobalt" Journal of Toxicology: Clinical Toxicology, vol. 37, no. 2, pp. 201–216, 1999.

20. D. R. Askeland, "Wear and Erosion." in The Science and Engineering of Materials 7th Edition, Cengage Learning, Boston, MA, 2016, pp. 824–827.

21. G. E. Dieter and L. C. Schmidt "Types of Wear." Engineering Design 4th Edition, McGraw-Hill Higher Education, New York, NY, USA, 2009, pp. 544–546.

22. P. F. Doorn, P. A. Campbell, J. Worrall, P. D. Benya, H. A. McKellop, and H. C. Amstutz, "Metal wear particle characterization from metal on metal total hip replacements: Transmission electron microscopy study of periprosthetic tissues and isolated particles" J Biomed Mater Res., vol. 42, no. 1, Oct., pp. 103–111, 1998.

23. J. Corona-Castuera, D. Rodriguez-Delgado, J. Henao, J. C. Castro-Sandoval, and C. A. Poblano-Salas "Design and Fabrication of a Customized Partial Hip Prosthesis Employing CT-Scan Data and Lattice Porous Structures" ACS Omega, vol. 6, no. 10, Mar., pp. 6902–6913, 2021.

24. M. Feyzi, K. Fallahnezhad, M. Taylor, and R. Hashemi, "A review on the finite element simulation of fretting wear and corrosion in the taper junction of hip replacement implants" Comput Biol Med. vol. 130, Mar., pp. 104196, 2021.

25. A. Ashkanfar, D. J. Langton, T. J. Joyce 2017, "A large taper mismatch is one of the key factors behind high wear rates and failure at the taper junction of total hip replacements: A finite element wear analysis" J Mech Behav Biomed Mater, vol. 69, May, pp. 257-266, 2017.

26. S. Hussenbocus, D. Kosuge, L. B. Solomon, D. W. Howie, and R. H. Oskouei "Head-Neck Taper Corrosion in Hip Arthroplasty" Biomed Res Int, Apr., 2015

27. R. M. R Dyrkacz, J. Brandt, O. A. Ojo, T. R. Turgeon, and U. P. Wyss, "The influence of head size on corrosion and fretting behaviour at the head-neck interface of artificial hip joints" J Arthroplasty, vol. 28, Jun., pp. 1036-1040, 2013.

28. D. Langton et al. "Investigation of Taper Failure in a Contemporary Metal-on-Metal Hip Arthroplasty System Through Examination of Unused and Explanted Prostheses" J Bone Joint Surg Am. vol. 99, no.5, Mar., pp. 427-436, 2017.

29. A. M. Kop and E. Swarts, "Corrosion of a hip stem with a modular neck taper junction." J Arthoplasty, vol. 24, no. 7, Oct., pp. 1019-1023, 2009.

30. D. C. Hansen "Metal Corrosion in the human body: the ultimate bio-corrosion scenario" The Electrochemical Society Interface, vol. 17 no. 2, pp. 31-34, 2008.

31. Y. Liao, E. Hoffman, M. Wimmer, A. Fischer, J. Jacobs, and L. Marks, "CoCrMo Metal-on-Metal Hip Replacements" Phys Chem Chem Phys, vol. 15, no. 3, Jan., 2013.

32. C. M. Wight and E. H. Schemitsch, "In vitro testing for hip head-neck taper tribocorrosion: A review of experimental methods" Proc Inst Mech Eng H, vol. 236, no. 4, Apr., pp. 469-482, 2022.

33. E. Fuentes, S. Alves, A. López-Ortega, L. Mendizabal, and V. Sáenz de Viteri, "Advanced Surface Treatments on Titanium and Titanium Alloys Focused on Electrochemical and Physical Technologies for Biomedical Applications", Biomaterial-supported Tissue Reconstruction or Regeneration. IntechOpen, May 22, 2019.

34. R. M. R. Dyrkacz et al. “Finite element analysis of the head–neck taper interface of modular hip prostheses” Tribology Int., vol 91, Nov., pp. 206-213, 2015.

35. D. R. Bijukumar et al. “In Vitro Evidence for Cell-Accelerated Corrosion within Modular Junctions of Total Hip Replacements” J Orthop Res. vol. 38, no. 2, Feb., pp. 393–404, 2020.

36. J. R. Goldberg, J. L. Gilbert, J. J. Jacobs, T. W. Bauer, W. Paprosky, and S. Leurgans, “A multicenter retrieval study of the taper interfaces of modular hip prostheses” Clin Orthop Relat Res, vol. 401, Aug., pp. 149–161, 2002.

37. J. L. Gilbert , C. A. Buckley, and J. J. Jacobs, “In vivo corrosion of modular hip prosthesis components in mixed and similar metal combinations. The effect of crevice, stress, motion, and alloy coupling” J. Biomed. Mater. Res., vol. 27, no. 12, Dec., pp. 1533-44, 1993.

38. E. B. Mathiesen, J. U. Lindgr en, G. G. A Blomgren, and F. P. Reinholt, “Corrosion of Modular Hip Prostheses” J. Bone and Joint Surg., vol. 73-B, July, pp. 569-575, 1991.

39. S. A. Brown et al. “Fretting Corrosion Accelerates Crevice Corrosion of Modular Hip Tapers” J Appl Biomater, vol. 6, no. 1, pp. 19-26, 1995.

40. V. Swaminathan and J. L. Gilbert, “Fretting corrosion of CoCrMo and Ti6Al4V interfaces” Biomaterials, vol. 33, no. 22, Aug., pp. 5487-503, 2012.

41. J. L. Gilbert and J. J. Jacobs, “The Mechanical and Electrochemical Processes Associated with Taper Fretting Crevice Corrosion: A Review” ASTM special technical publications, 1997.

42. Z. Xia et al. “Nano-analyses of wear particles from metal-on-metal and non-metal-on-metal dual modular neck hip arthroplasty” Nanomedicine, vol. 13, no. 3, Apr., pp. 1205-1217, 2017.

43. H. J. Cooper et al. “Adverse local tissue reaction arising from corrosion at the femoral neck-body junction in a dual-taper stem with a cobalt-chromium modular neck.” J Bone Joint Surg Am, vol. 95, no. 10, May, pp. 865-872, 2013.

44. G. Higgs et al. “Retrieval analysis of metal-on-metal hip prostheses: Characterizing fretting and corrosion at modular interfaces.” Bone Joint J, vol. 95-B, No. SUPP_15, Mar., pp. 108, 2013.

45. W. M. Mihalko, M. A. Wimmer, C. A. Pacione, M. P. Laurent, R. F. Murphy, and C. Rider, “How have alternative bearings and modularity affected revision rates in total hip arthroplasty?” Clin Orthop Relat Res., vol. 472, no. 12, Dec., pp. 3747-3758, 2014.

46. S. K. Fokter, N. Noč, V. Levašič, M. Hanc, and J. Zajc, “Dual-Modular Versus Single-Modular Stems for Primary Total Hip Arthroplasty: A Long-Term Survival Analysis” 2023.

47. National Joint Registry for England and Wales “National Join Registry 10th Annual Report 2013” London, UK, National Joint Registry, 2013.

48. K. C. Ilo, E. J. Derby, R. K. Whittaker, G. W. Blunn, J. A. Skinner, and A. J. Hart, “Fretting and Corrosion between a metal shell and metal liner may explain the high rate of failure of R3 modular metal on metal hips” J Arthroplasty, vol. 32, no.5, May, pp. 1679-1683, 2017.

49. R. Civinini, A. C. Lepri, C. Carulli, F. Matassi, M. Villano, and M. Innocenti, “Patients Following Revision Total Hip Arthroplasty With Modular Dual Mobility Components and Cobalt-Chromium Inner Metal Head are at Risk of Increased Serum Metal Ion Levels” J Arthroplasty, vol. 35, no. 6S, Jun, pp. S294-S298, 2020.

50. N. Patil, P. Deshmane, A. Deshmukh, and C. Mow, “Dual Mobility in Total Hip Arthroplasty: Biomechanics, Indications and Complications–Current Concepts” Indian J Orthop, vol. 55, no.5, Oct., pp. 1202-1207, 2021.

51. B. F. Moore, and P. F. Lachiewicz, “Corrosion and adverse tissue reaction after modular unipolar hip hemiarthroplasty” Arthroplasty Today. vol. 3, no. 4, Dec., pp. 207–210, 2017.

52. C. Heisel, N. Streich, M. Krachler, E. Jakubowitz, and J. P. Kretzer, "Characterization of the Running-in Period in Total Hip Resurfacing Arthroplasty: An in Vivo and in Vitro Metal Ion Analysis" Journal of Bone & Joint Surgery, vol. 90, no. 3, Aug., pp. 125-133, 2008.

53. M. Lavigne, E. L. Belzile, A. Roy, F. Morin, T. Amzica, and P. A. Vendittoli, "Comparison of Whole-Blood Metal Ion Levels in Four Types of Metal-on-Metal Large-Diameter Femoral Head Total Hip Arthroplasty: The Potential Influence of the Adapter Sleeve" J Bone Joint Surg Am, vol. 93 Suppl 2, May, pp. 128-36, 2011.

54. Griffin et al "Are Metal Ion Levels a Useful Trigger for Surgical Intervention?" The Journal of Arthroplasty vol. 27, no. 8 Supplement, Sep., pp. 32-36, 2012.

55. G. S. Matharu, F. Berryman, L. Brash, P. B. Pynsent, R. B. Treacy, and D. J. Dunlop, "Influence of implant design on blood metal ion concentrations in metal-on-metal total hip replacement patients" Int Orthop. vol. 39, no. 9, Sep, pp. 1803-11, 2015.

56. T. Manaka et al. "Galvanic Corrosion among Ti 6Al 4V ELI Alloy, Co Cr Mo Alloy, 316L-Type Stainless Steel, and Zr 1Mo Alloy for Orthopedic Implants" Materials Transactions, vol. 64, no. 1, pp. 131-137, 2023.

57. N. Eliaz, "Corrosion of Metallic Biomaterials: A Review" Materials (Basel). vol. 12, no. 3, 2019.

58. S. Virtanen, I. Milosev, E. Gomez-Barrena, R. Trebse, J. Salo, and Y. T. Konttinen "Special modes of corrosion under physiological and simulated physiological conditions" Acta Biomater., vol. 3, no. 3, Dec., pp 469-76, 2008.

59. J. P. Collier, V. A. Surprenant, R. E. Jensen, M. B. Mayor, and H. P. Surprenant, "Corrosion Between the Components of Modular Femoral Hip Prostheses" J Bone Joint Surg Br., vol. 74, no. 4, Jul., pp. 511-517, 1992.

60. G. Hao, D. Zhang, K. Chen, and Q. Wang, "Galvanic corrosion behavior between Ti6Al4V and CoCrMo alloys in saline solution" Materials Express, vol. 4, no. 3, Jun., pp. 213-220, 2014.

61. G. Solarino, G. Vicenti, M. Carrozzo, G. Ottaviani, B. Moretti, L. Zagra, "Modular neck stems in total hip arthroplasty: current concepts" EFORT Open Rev., vol. 6, no. 9, Sep., pp. 751-758, 2021.

62. "Non-Active Surgical Implants – Joint Replacement Implants – Particular Requirements" ISO 21534, Annex B.2, International Organization for Standardization, 2007.

63. Langton et al. "Accelerating failure rate of the ASR total hip replacement" J Bone Joint Surg Br, Aug; vol. 93, no. 8, Aug., pp. 1011-6, 2021.

64. E. Hornus et al. "A new experimental method to simulate dynamic crevice corrosion in modular hip arthroplasty" Corrosion Science, vol .190, Sep, 2021.

FE Investigation of Maintenance and Operational Factors Contributing to the Collapse of a Crane Boom

By Olin Parker, Jahan Rasty, PhD, PE, DFE (NAFE 768S), and Matthew Mills, PE, DFE (NAFE 1199A)

Abstract

During the coating of a natural gas pipeline, all 14 bolts securing the pedestal of a crane boom to a truck bed failed, causing the boom to fall and strike a worker in the head. The bolts exhibited excessive corrosion indicative of exposure to a harsh corrosive environment prior to the failure. Review of provided documents revealed that the crane was kept in an uncovered yard for two years. Afterward, it was rented to petrochemical companies for use in heavy oil and gas industrial environments. The fracture surfaces of the bolts revealed signs of excessive fatigue, which were determined to be caused by loadings that the previous renters of the crane had subjected it to. Bolt fatigue drastically reduced their strength, allowing them to fail under loads well below the recommended load capacity of the crane. Maintenance records indicated that the lessor failed to perform adequate inspection of the crane, allowing bolt corrosion and fatigue to go unnoticed. Had proper inspections and maintenance instructions been provided and performed, the incident would not have occurred.

Keywords

Fatigue, heat treatment for fasteners, hydrogen embrittlement, crane boom, periodic inspections, forensic engineering

Case Background

A pipeline maintenance company was in the process of re-coating an excavated natural gas pipeline. Discovery documents describe their recoating procedure as follows: A heating ring is lowered onto the pipe via a crane and latched in place. The ring heats the pipe and is then relocated farther down the pipeline. A coating ring is then attached to the hot pipe segment and applies a spray coating to the area. A crew is typically able to repeat this procedure between 45 to 65 times per day.

At the time of the incident, the crew had lowered a heating ring onto the pipeline and heated the pipeline to the required temperature. One of the workers then walked over to the heating ring to detach it so it could then be taken off of the pipe. After unlatching the heating ring from the pipeline, the worker moved away and signaled the crane boom operator to lift the unlatched ring. Suddenly and unexpectedly, all 14 bolts securing the subject boom to the truck body failed, causing the crane boom to collapse, striking the worker on the head/back, and resulting in a traumatic brain injury. As a result of this incident, litigation was filed against the equipment lessor, the crane manufacturer, and the bolt manufacturer. The authors were retained in order to investigate the mode of failure/design of the crane and assess the quality of the preventive maintenance performed by the lessor.

Subject Crane Boom

The subject crane boom was sold to an oil and gas equipment lessor on December 30, 2014. It was a hydraulic crane rated to have a maximum lifting capacity of 12,000 pounds. According to company documents, it was reportedly initially mounted to a truck body in 2016; however, the exact date of installation was not recorded. For all of 2015 and part of 2016 (between purchase date and installation date), the subject crane and the 14 provided attachment bolts were stored in an outdoor, unprotected storage yard. After installation, the crane was moved to another outdoor yard where it was stored for an undisclosed amount of time before it was first leased out.

After it was mounted to the truck body, the crane was reportedly used for more than two years and logged a total of 1,412 hours by the time the pipeline maintenance company acquired it. Provided records indicated that the

Olin Parker, 805 Boston Ave., Lubbock, TX 79409-9831, (832) 472-3930, Olin.Parker@ttu.edu

crane was previously rented out five times for projects in several oil and gas work sites, including, but not limited to, Brownsville, Texas; Ellenboro, West Virginia; Midland, Texas; Yukon, Oklahoma; and Hollidaysburg, Pennsylvania.

These locations are known areas of heavy shale oil activity, where equipment is regularly exposed to corrosive liquids and pushed to their limit. It is unknown if the crane boom was subjected to misuse and/or abuse prior to its acquisition by the final lessee. Inspection documentation from the lessor was noted to be inadequate and based on cursory visual inspections. As a result, any damage that would have occurred to the bolts due to misuse was not noted. Other than the lessor testifying to the fact that they had no idea how the equipment was used (or if it was misused), there were no additional discovery documents available to ascertain previous excessive loading or loading frequency.

The crane was last recorded to have undergone full service on August 15, 2019 by the equipment lessor. The maintenance company acquired the crane on or around November 14, 2019, and used it at the job site between 45 to 60 days prior to the incident. No records of any other inspection or maintenance between the last full service and the date of incident were available. A 24-inch induction heating ring was used with the subject crane at the time of the incident for pre-heating of the finished pipe joint to prepare for the epoxy coating process (**Figure 1**).

Inspection of the crane revealed that, at the time of the incident, the crane was at a 35° angle and was extended approximately 18.27 feet (219.25 inches). According to the crane's load chart, the crane boom's max load capacity at this angle was over 3,600 pounds (**Figure 2**). Testimony

Figure 1
The collapsed crane boom at the site of the incident.

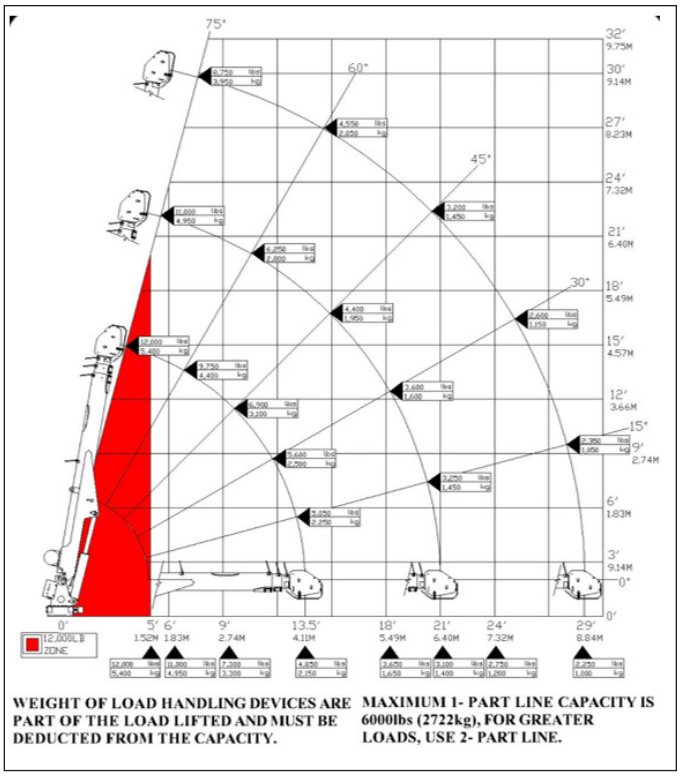

Figure 2
Chart showing the load capacity of the crane boom at different extension lengths and orientations.

from the crane operator and workers on site at the time of the incident stated that the crane failed as soon as the heating ring began to be lifted. The crane operator also testified that he was lifting the heating ring at a slow speed and that it was no longer connected to the pipe.

The separation at the connection between the rotation base and the pedestal is shown in **Figure 3**. A total of 14 bolts were utilized to affix the crane pedestal to the truck body. All 14 of the pedestal bolts were recovered and labeled in accordance with the identification numbers in the crane's owner's manual (**Figure 4**). According to the owner's manual, these bolts were $^{5}/_{8}$ inch-11 × 3-$^{1}/_{2}$ inch SAE J429 Grade 8 Hex cap fasteners with a 5µm thick yellow zinc coating (i.e., a coating consisting of chromate applied over a zinc coating). This coating was applied via an electroplating process. These fasteners were noted to have a minimum proof strength of 120,000 lbs/in^2 (psi) and an ultimate tensile strength of 150,000 psi.

At the time of the forensic examination, 12 of the failed bolts were still inside the pedestal while the remaining two bolts were found lying on the truck body.

All of the examined bolts exhibited a lack of yellow

Figure 3
Overall and close-up views of the bolt circle where the failed bolts were attached.

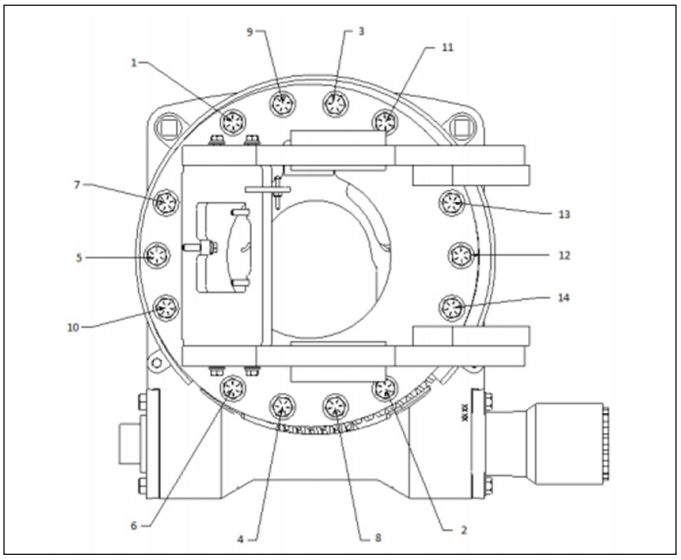

Figure 4
Diagram of the crane pedestal with each of the 14 bolts labeled with numbers 1 through 14. Note that bolts 7, 5, and 10 are located on the far side (rear) of the pedestal.

zinc on their heads, and a number of the bolts displayed significant depletion of this coating on the bolt shank and threads (**Figure 5**). It is likely that the yellow zinc coating was depleted from the bolt heads over a long period of exposure to water or other corrosive mediums while these same corrosive mediums stagnated in the notches and bolt holes, allowing for the coating on the body of the bolt to

Figure 5
Heavily oxidized (rusted) surface of bolt #9, displaying iron oxide and traces of the chromate and zinc galvanic coating (highlighted by the white arrows).

be removed and result in the corrosion of the bolt shank and threads. While a small amount of corrosion was noted on the fracture surfaces of some of the bolts (**Figures 6** and **7**), comparison with extensive corrosion noted on the exterior surface of the bolts (**Figure 5**) indicates that this corrosion likely occurred following the failure as the fracture surface was exposed to four days of snowfall before the bolts were retrieved during the authors' inspection.

A common fracture pattern noticed amongst the failed bolts was the presence of area (A), having features consistent with fatigue, followed by an intermediate region (B) with rough, parallel crack arrest marks (indicative of particularly low cycle fatigue), and finally a region (C) indicative of fast fracture through an inclined fracture plane (shear lip), as shown in **Figure 8**.

Figure 6
One of the failed bolts, showing a metallic yellow coating characteristic of yellow zinc.

Figure 7
Bolts 7, 5, and 10 — still in their bores at the time of inspection. Note the severity of corrosion.

According to the owner's manual, the bolts are required to be torqued at 220 pounds-foot when dry and 170 pounds-foot when oiled. If bolts are overloaded in an amount exceeding the load stated in the load chart, then the bolts may become damaged and decrease the overall strength of the bolt. Examination of the bolt threads showed no signs of deformation consistent with overtorquing. In addition, red threadlocker (an adhesive applied to bolt threads to prevent loosening) was found in most of the bolt holes and around the bores. In the absence of any documentation that would indicate the bolts were torqued beyond their recommended level, in addition to the absence of any physical witness marks in the form of thread-stripping, the overtorquing of the bolts as a potential mechanism for their failure was overruled.

Other than the failed pedestal bolts, the only observed signs of damage were on top of the heating ring, the traveling block (a device consisting of the crane's hook and sheave pulley), the spreader bar (a beam that is attached to the crane's hook and distributes the load between two or more points), and minor damage to the rigging. This damage was concluded to have occurred as a result of the crane boom falling and striking the pipeline following the failure of the pedestal bolts.

Hypotheses for Failure

Bolts are known to fail in a variety of modes, yet the

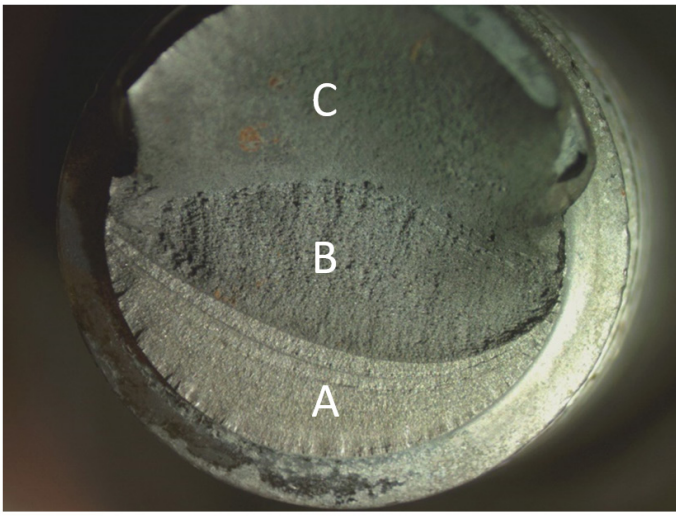

Figure 8
Fracture regions observed in a typical failed bolt fracture surface: A (fatigue beach marks), B (low-cycle crack arrest marks), and C (final sudden fracture).

most documented failure modes are overload and fatigue[1]. Overload failure is the ductile or brittle failure of a material that occurs when the stress exceeds the material's strength. While all material failures could be argued to occur in this manner, the term "overload" generally refers to instances where the applied stress exceeds the nominal strength of the material as considered in the design stage — either through misuse of the equipment, improper design, or improper material selection. In threaded fasteners, overload typically occurs when tension, shear, bending, and/or tortional forces exceed the nominal strength of the overall material cross section.

Fatigue is a failure mode that is characterized by the initiation and propagation of cracks within a material over time under the action of cyclical loading[1,2]. As the load cycles continue, the fatigue cracks progress further through the material's cross section, increasing the stress placed upon the remaining cross section. Eventually, the applied stress exceeds the material's nominal strength, and the remaining cross section of material suffers from an overload failure. The two stages of fatigue failure prior to the final fracture are shown in **Figure 9**.

Fatigue failures are typically characterized by markings such as beach marks, striation marks, and ratchet marks. Beach marks are elliptical or semi-circular macroscopic markings that are indicative of crack progression followed by periods of serve interruption and are seen as one of the primary indicators of fatigue. Beach marks typically radiate out from crack initiation sites. Striation marks are similar to beach marks yet represent each individual cycle of loading. As such, they are very small and cannot be observed macroscopically[1]. Ratchet marks are small step-like features caused by the overlap of multiple separately initiated fatigue cracking regions[3].

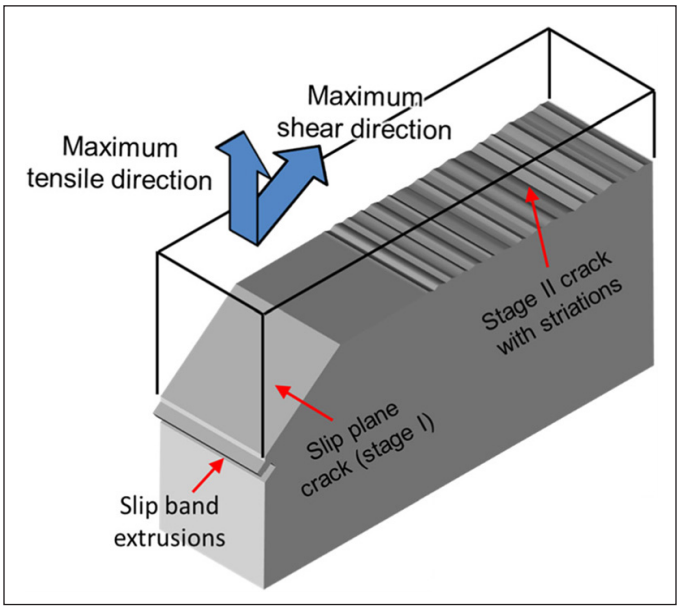

Figure 9
Schematic showing crack initiation (Stage I) and crack propagation (Stage II) of an advancing fatigue crack[5].

These separate fatigue initiation sites can be caused by stress concentration factors such as inclusions or corrosion pitting[1]. The manner in which fatigue occurs depends upon the rate and intensity of the cyclic loading. High cycle fatigue involves low-amplitude cyclic loads applied over an extended period of service. Elastic deformation of the material occurs under such conditions, resulting in the slow expansion of existing cracks or the creation of new ones. As such, high cycle fatigue exhibits very fine striations and beach marks. Conversely, low cycle fatigue involves high-amplitude loads applied over a short period of service. The higher stress amplitude experienced by the material results in local plastic deformation ahead of the crack front, which results in more extensive cracking. This can be seen by the larger, sharper striations and further displaced beach marks[4]. It is also important to note that fatigue is considered to be one of the most common mechanisms of failure in threaded fasteners, such as the bolts at issue[6].

Based on the above concepts, two competing hypotheses for failure of the bolts were developed. One hypothesis postulated that the heating ring may have not been properly detached, the crane could have been pulling on the heating ring while it was still attached to the 20-inch diameter pipeline, causing the bolts to experience an overload failure. Another hypothesis postulated that failure of the bolts occurred due to progressive fatigue fracture of the bolts as a result of combined environmentally induced embrittlement of the bolts and the cyclical loading experienced during the day-to-day operation of the crane.

The heat ring being lifted by the crane boom was reported to have weighed between 400 and 500 pounds, significantly below (12% to 14%) the maximum load capacity of the crane as specified by the crane's load chart for the specific crane boom length and orientation at the time of failure. These heating rings are designed to drop down over a pipe and close around the pipe via a light clamp at the bottom of the pipe, as shown in **Figure 10**.

According to a report by the crane manufacturer as well as the manufacturer of the heating ring, this clamp was not designed to carry any loads. The clamp on the

Figure 10

Images of the heating ring, displaying no apparent signs of damage to the ring itself or the securement clamp (circled in white).

heating ring would have failed, or, at a minimum, displayed clear signs of damage if the heating ring had been used to raise any section of the pipe. Visual examination of the heating ring showed no signs of damage to either the clamp joint or the bottom portion of the heating ring itself, indicating that the crane boom was not overloaded through improper detachment of the heating ring. This conclusion was further corroborated by the failure analysis reports of the crane boom manufacturer and bolt manufacturer, both of which came to the conclusion that the heating ring was undamaged, and an overload failure did not occur.

The first hypothesis for failure can thus be ruled out based on the aforementioned information, which shows that the pedestal bolts did not fail purely as a result of the imposed loading.

Failed Bolts Fractography

Optical microscopy and scanning electron microscopy (SEM) were performed on the 14 failed pedestal bolts to examine their fracture surfaces. As previously mentioned, examination of the bolts revealed that at least half displayed fracture surfaces with three distinct regions. Beginning from the exterior surface of the bolts (at the bottom of the fracture surfaces shown in **Figure 11**) is a region displaying distinct beach marks (B), with a number of bolts possessing ratchet marks (R), signifying multiple fatigue crack origins. There is a marked transition to the intermediate region, displaying rough, parallel, crack arrest marks (C), indicative of very low-cycle fatigue. Finally, there is a steep transition to a "fast fracture" region where final failure occurred through an inclined shear fracture plane (S). Macroscopic and SEM images of a number of the bolts'

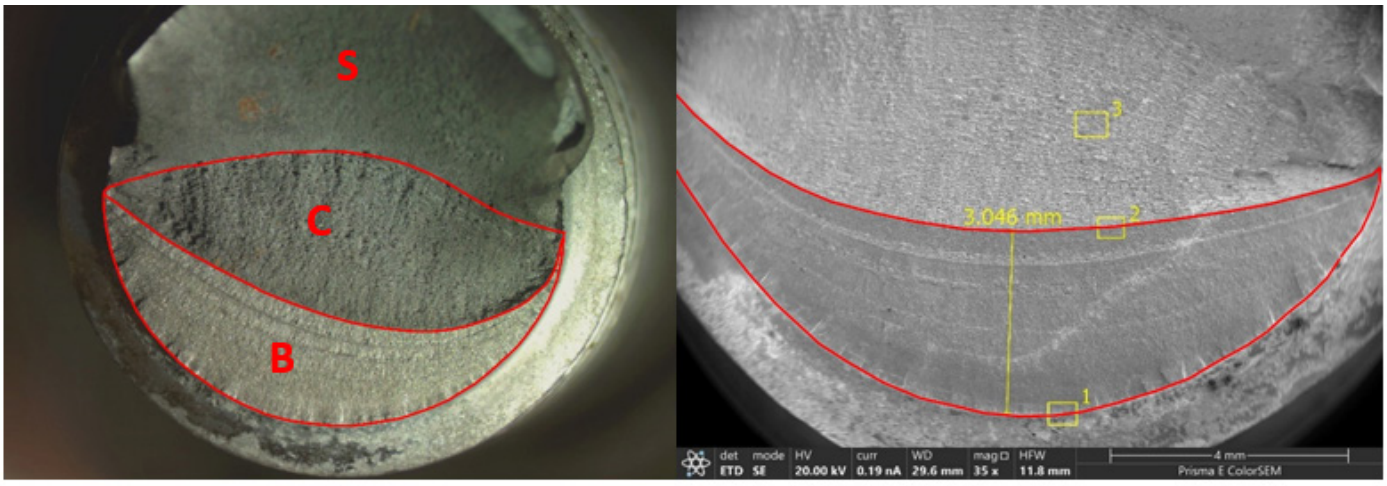

Figure 11

Fracture surface of Bolt #6, displaying three distinct regions. The presence of beach marks (B), parallel crack arrest marks (C), and a shear lip (S), are noted on the figure (left). A closer view of the beach marks and the parallel crack arrest marks are shown in the image to the right.

cross sections are shown in **Figures 11** through **15**. Features indicative of fatigue, such as beach marks (B), crack arrest marks (C), and ratchet marks (R), are marked on the first two sets of images. The remaining bolts were noted to exhibit large regions of parallel crack arrest marks and a lack of beach marks or patterns indicative of pure cleavage (**Figures 16** and **17**). These pronounced marks are due to the quicker fatigue fracture progression as a result of higher stresses experienced.

Figures 11 through **17** show that many of the bolts experienced regions of fatigue failure as evidenced by classical witness marks such as beach marks and ratchet marks. Some of these bolts also displayed the presence of long-term fatigue failure, evidenced by the presence of beach marks having highly differentiable corrosion texture (**Figures 14** and **15**). The combined presence of classical beach marks with highly differentiable corrosion bands suggest stress corrosion cracking as a mechanism that contributed to the failure of the subject bolts. The fracture surfaces observed on the 14 bolts also proved to be similar in nature to those that have been reported in literature[7,8] (**Figure 18**). Based upon this evidence, fatigue failure was identified as the primary mode of failure of the subject bolts.

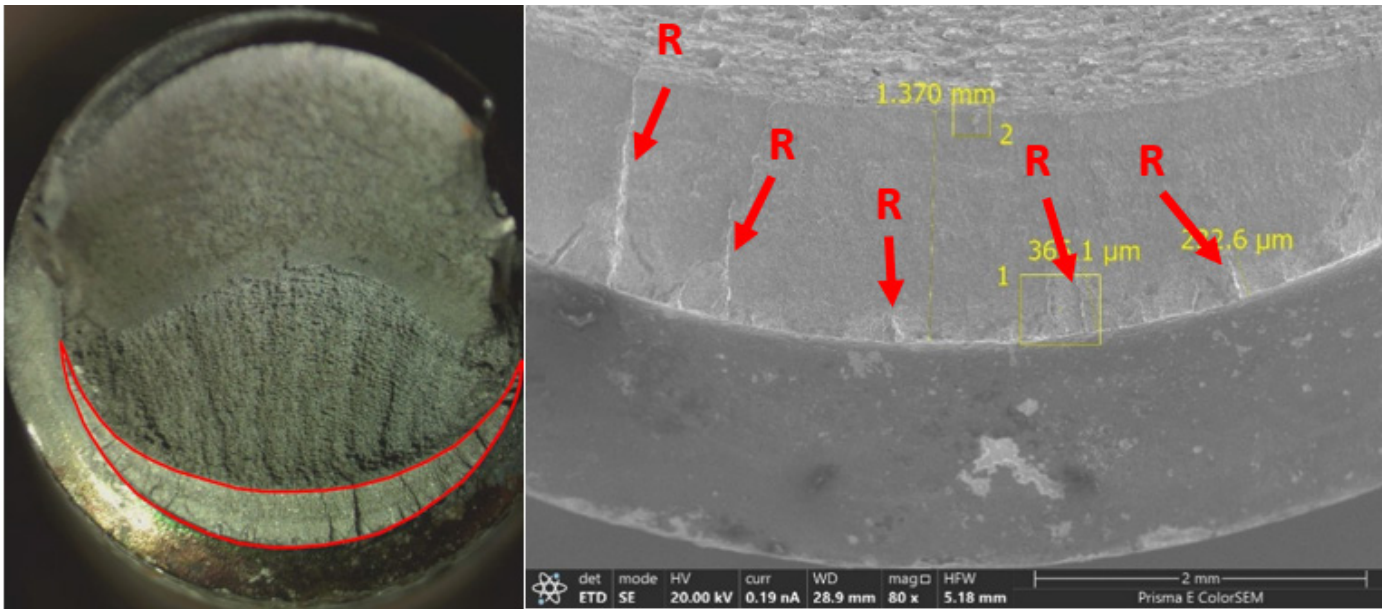

Figure 12
Fracture surface of Bolt #1, displaying crack arrest marks reaching up to the middle of the cross section. A smooth, outer zone with beach marks can be seen, signifying fatigue (left image). The fatigue region of this bolt also displays a number of ratchet marks, highlighted by the red arrows (right image).

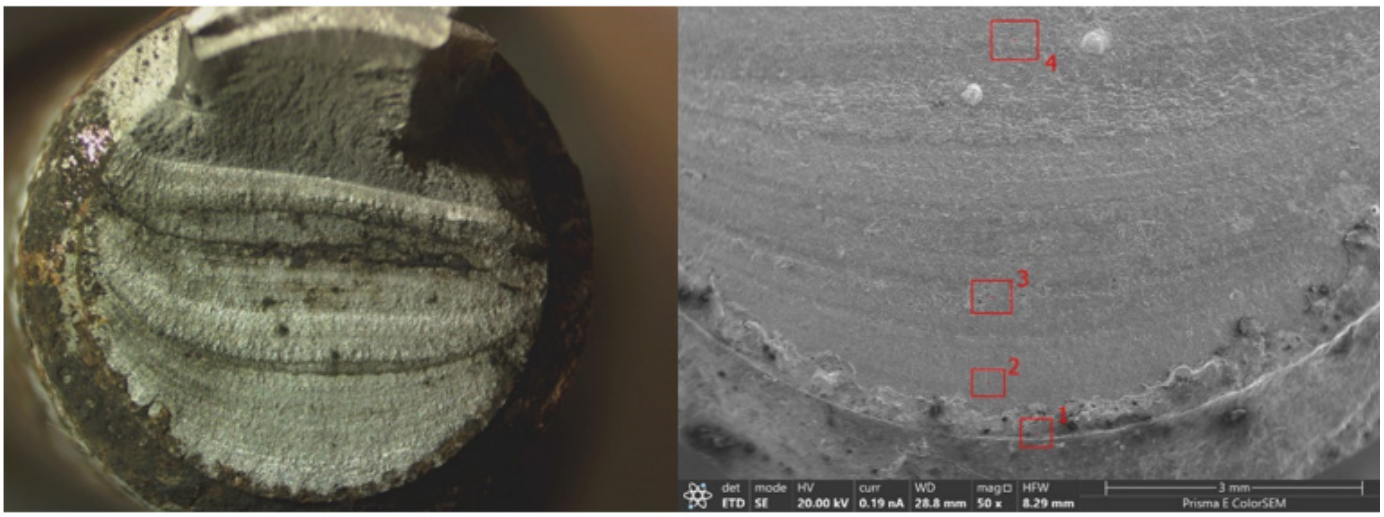

Figure 13
Fracture surface of Bolt #10, displaying a significantly large region of beach marks that extend through a majority of the bolt cross section.

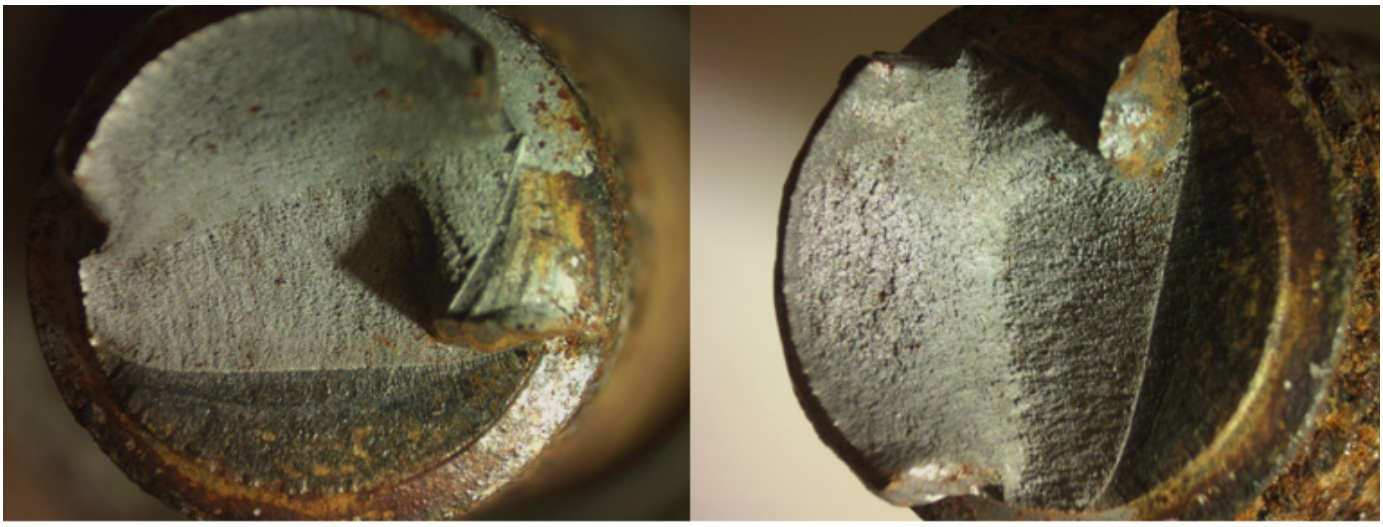

Figure 14
Fracture surface of Bolt #5, displaying a corroded beach marks region, indicative of the exposure of these bolts to a highly corrosive environment after the initial propagation of this fatigue region.

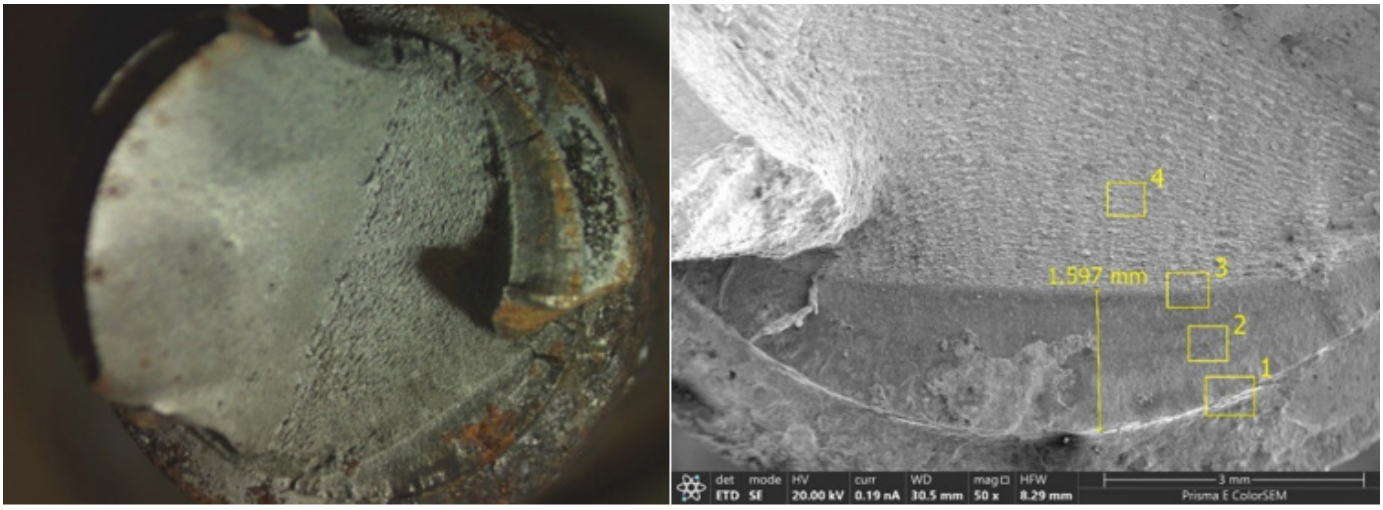

Figure 15
Fracture surface of Bolt #7, displaying a small finely fatigued region covered in corrosion products.

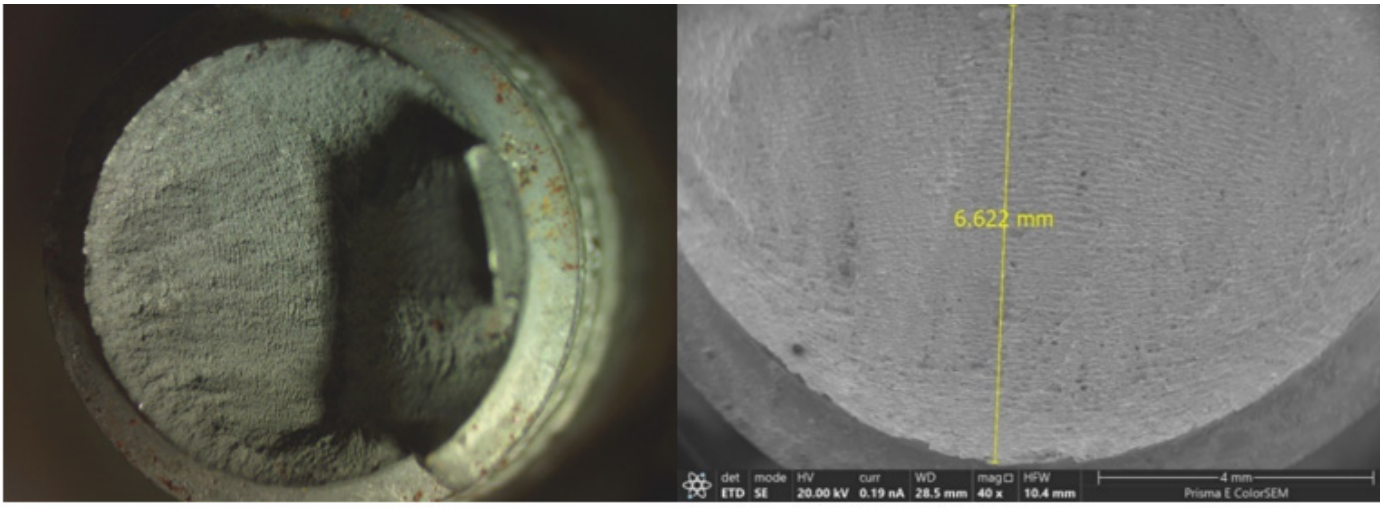

Figure 16
Parallel crack arrest marks observable on Bolt #3, covering more than half of the bolt's surface.

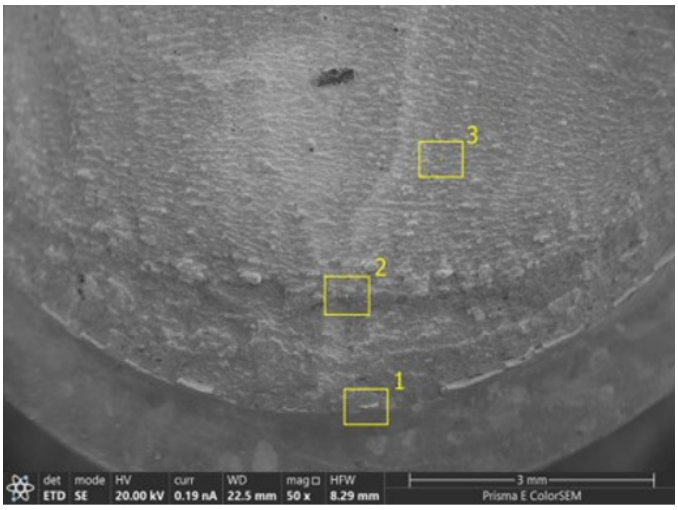

Figure 17
Fracture surface of Bolt #14, showing a region of crack arrest marks.

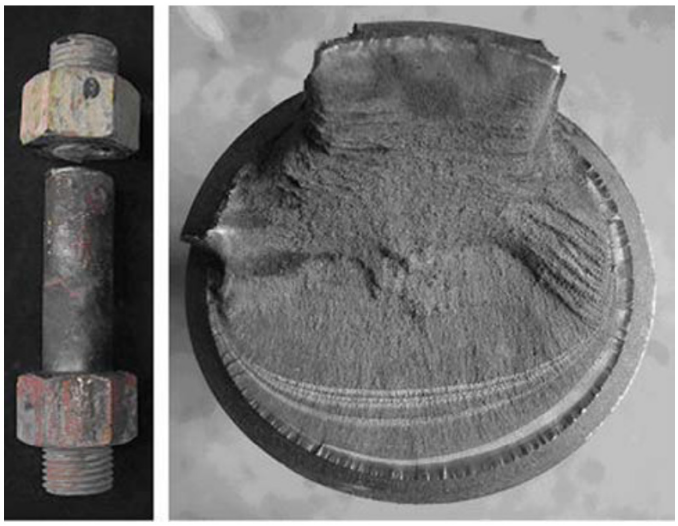

Figure 18
An example of a similar bolt fracture surface as reported in the literature[7].

Based on the operational history of the crane and the fatigue markings noted earlier, it was concluded that failure of the bolts initiated well before the last commission of the crane, but went undetected due to improper maintenance and inspection by the equipment owner (lessor), as will be discussed in later sections.

While it is believed that fatigue failure of the bolts initiated during earlier commissions of the crane, the number of load cycles during early commissions was not sufficient to induce failure. Later commissions of the crane subjected the already partially fatigued bolts to additional cyclical loading as well as operation within a corrosive environment that drove the fatigue cracks further into the bolts' cross section. As the fatigue cracks drove further into the bolts' cross section with each new commission of the crane, the remaining cross section of material experienced high-stress-low-cycle fatigue as evidenced by the pronounced crack arrest marks (**Figures 11** through **17**). By the time the pipeline maintenance company acquired the crane, the bolts were significantly fatigued and close to failure.

To summarize, the bolts at issue were suffering from metal fatigue and stress corrosion cracking before the crane was rented by the maintenance company. The cyclic stresses the bolts had previously been subjected to propagated cracks throughout the material and greatly decreased the nominal level of stress the material could take. The corrosion present on the bolts further exacerbated the decrease in their fracture toughness.

Given the fact that the maintenance company did not expose the crane to loads in excess of the weight of the heating ring, which weighed 500 pounds at most, the possibility of an overload failure can be ruled out. The fact that fatigue fracture occurred at such a low level of loading indicates that fatigue had progressed over an extended period of time to a critical level, and the failure was inevitable, given the history of the crane.

Inspection and Maintenance

The crane's owner's manual requires that, as part of daily maintenance, the crane be inspected for "evidence of broken structural components such as welds and loose fasteners." The manual also states that quarterly inspections are to be done to identify loose bolts on the crane body and the pedestal. In addition, the lubrication and maintenance schedule calls for the owner and operator to check and tighten the pedestal bolts as well as all other bolts on the crane on a weekly basis.

The lessor's inspection logs showed that they failed to perform nearly all the inspections required by the owner's manual. If these inspections were performed, they were not documented. The lessor insisted that, though they did not have a daily, weekly, monthly, or quarterly maintenance schedule as the owner's manual required, there was no need for them to do so — as this requirement only applies to the operators. However, the owner's manual does not contain any section limiting maintenance to the operator. Furthermore, OSHA Regulation 1910.180 "Materials Handling and Storage: Crawler Locomotive and Truck Cranes" requires frequent and periodic inspections to be performed and does not limit inspection to only be performed by one entity in the supply chain[9]. OSHA 1910.180

contains requirements for performing enhanced inspections on cranes left idle for periods between one and six months — and even more extensive inspection for cranes left idle for periods more than six months[9].

The lessor testified that the few inspections they did perform were purely visual inspections and claimed that this was sufficient — and in accordance with the requirements of the manual. While the owner's manual does not state the method by which one should conduct the inspections, this does not limit bolt inspection to being purely visual. Visual inspection of the head of a bolt does not reveal anything about the condition of the bolt below its head.

The inspector should have pulled out the bolts and inspected the interior surface and threads to determine the state of the bolts on at least a quarterly basis. Even if the inspector was justified with visually inspecting only the exterior head of the bolts, the loss of the bolt head's chromium coating should have alerted the inspector that the bolts had been subjected to a degrading environment that was likely to be worse in confined areas such as the bolt holes. Even if the lessor's sole reliance on visual inspection was sufficient, the lessor only performed this inspection immediately after repairs (and before it handed the equipment over to renters), which were documented by the lessor to have been performed on 7/26/2017, 3/3/2018, 11/21/2018, 7/15/2019, 8/15/2019, and 9/20/2019. This frequency of inspection falls well below the requirements stated in the owner's manual.

In addition, the manner in which these inspections were conducted was found to be insufficient. According to their own testimony, the lessor neglected to check for signs of overload after their cranes were returned, ignoring the potential for misuse by previous renters. The lessor knew, or should have known, that their equipment could be subjected to misuse and/or overuse with the potential to exceed its design limits, even if no signs of gross misuse were present on the crane boom.

If they had taken preventive measures to inspect and repair areas of the crane that would likely be harmed by such misuse, they would have identified the progressive fatigue cracking in the bolts and promptly replaced them. The lessor did not lubricate the rotation bolts on the crane. The lubrication acts not only to keep parts running smoothly, but also to provide an additional protective layer against corrosion. Had the lessor lubricated the bolts, they would have likely not corroded as much — and would have likely been able to withstand the operating loads on the day of the incident.

According to testimony, when the bolts were first tightened, they were marked with a painted line. If this line falls out of alignment or the paint cracks, then it is a sign to the inspector that the bolt is no longer fully tightened and must be torqued. The bolts had not been torqued or checked to see if they needed to be re-torqued for the five years the lessor had the crane. The service manager for the lessor stated that it would have been reasonable for them to perform quarterly torque testing of the pedestal bolts.

The lessor's inspection protocol for rotational bolts is to perform torque tests on them, but this was never performed on the bolts. The lessor admitted that they never inspected the bolts for failure, corrosion, or degradation because they believed they only needed to verify the paint on the bolts was not broken or out of alignment. The inspector for the lessor who had inspected the cranes after each rental period was not licensed or certified. This is in clear violation of the requirement in the owner's manual that "only authorized and trained service personnel are to perform maintenance on the crane."

The lessor's documentation shows that their inspections failed to consider the bolts as something that needed to be checked. The maintenance company's crane boom operator performed daily inspections in accordance with the owner's manual. They claimed to have checked for leaks, looked over decals, made sure safety covers and guards were in place, switches functioning, controls in working condition, temperature/oil pressure, hydraulic system, leaks, machine performance, fire extinguisher charged, seat belt, brakes, transmission, tires, etc. These inspections revealed no damage or bends in the crane boom.

The maintenance company was not reasonably expected, nor in the best position, to properly inspect for rusting or cracking of the support bolts. It would be unreasonable for the lessor to expect the maintenance company to perform the necessary inspection given the short period of time the maintenance company was in possession of the crane and the light-load environment they were using the crane for. Therefore, as the next entity in the supply chain, it was the lessor's duty to regularly inspect the bolts and to replace them when necessary.

It was reasonable for the maintenance company to expect that the crane was free of any latent defects. Furthermore, it was reasonable for the maintenance company to

rely on the lessor for regular inspections and timely maintenance of any components in need of repair or replacement. Based on provided testimony, the lessor stated that it would be reasonable for the maintenance company to depend upon the inspection performed by the lessor. The lessor additionally stated that they would not hold the maintenance company negligent for not inspecting the bolts. The lessor knew (or should have known) that equipment would wear down if it was not properly maintained and that maintaining their equipment was an important aspect of their business.

The lessor testified that, given the condition of the bolts, they posed an unsafe condition to the user. Despite claiming that the owner's manual did not specify any inspection procedures for them to follow — and repeatedly stating that they followed the manual — the fact remains that the lessor did not perform the inspections required of them in the indicated time spans. Had the lessor performed these routine inspections and any preventive maintenance required by the manual, the failure of the bolts would have likely been prevented.

Though the owner's manual required inspections on the pedestal bolts, it failed to specify what exactly the inspection should entail and what these inspections should identify as deficiencies or hazards. The manual should have mentioned that the bolts could rust or fatigue and the detrimental effects this can have. The owner's manual should have also required owners and operators to remove/inspect the pedestal bolts on a quarterly basis. If such a requirement were clearly stated, the reasons behind bolt inspections would have been made apparent to the operator. This position is justified because a manufacturer/designer of industrial equipment is in the best position to know the weaknesses and hazards associated with their equipment, thereby creating a duty to inform the users of its equipment of known hazards and the most effective means for identifying and guarding against such hazards.

Furthermore, the lessor claimed that if the crane manufacturer had given clear instructions on how to perform the bolt inspections and the danger rust and fatigue posted, they would have followed these instructions. As such, it can be argued that the crane manufacturer holds partial liability in the incident for contributing to the lessor's negligence.

Hydrogen Embrittlement and Inappropriate Bolt Material

The Grade 8 bolts provided by the crane manufacturer were yellow zinc-plated as per ASTM F1941. As previously mentioned, this coating was applied via a process known as electroplating. However, it has been well documented that acid attack from the electroplating process can produce pitting in the bolt as well as inducing hydrogen embrittlement (HE), a complex phenomenon in which atomic hydrogen is absorbed into the metal, reducing the material's strength, toughness, and ductility. HE is known to occur due to a variety of different mechanisms, such as hydride formation, hydrogen-enhanced decohesion mechanism (HEDE), hydrogen-enhanced local plasticity (HELP), and adsorption-induced dislocation emission (AIDE)[10]. While these mechanisms differ dramatically from each other, ultimately, they all manifest cracking in steels through either strain-controlled plastic flow or stress-controlled decohesion.

The strain-controlled mechanism combined with concentrated plastic flow typically results in trans-granular cracking while stress-controlled decohesion results in intergranular cracking[11]. An increase of hardness allows for higher stresses to be sustained by the steel and for more hydrogen to collect at these regions of elevated stress, thereby increasing decohesion-based HE[12].

According to the literature as well as manufacturing standards such as DIN EN ISO 4042, it is well known in the industry that hardness values above 32 HRC will make the material more susceptible to HE[13,14]. While hardness values approaching 40 HRC are considered highly susceptible to HE, materials with hardness values between 32 and 40 HRC can still have considerable susceptibility to HE. A report by one bolt manufacturer states that bolts with hardness values above 35 HRC have the potential to experience hydrogen embrittlement, though failure in bolts with hardness values below this are still known to occur. They also note that this is particularly prevalent in cases where the bolt is acting as a cathode in a galvanic couple or is operating in a caustic or sour environment, as was the case with the subject crane boom[15].

As the subject bolts were found to have hardness values of 39 HRC and were electroplated, hydrogen embrittlement was investigated as a potential factor contributing to the fatigue failure at issue. SEM of the failed bolts identified signs of stair-step cracking and intergranular fracture characteristics with pitting of exposed grains, a telltale sign of hydrogen embrittlement and stress corrosion cracking (**Figures 19** and **20**).

In addition to the stated susceptibility of electroplated bolts to premature failure, the crane manufacturer had

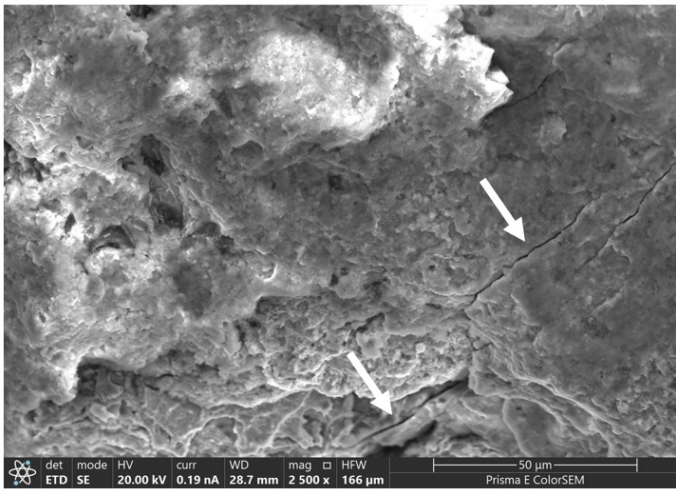

Figure 19
An SEM image of Bolt 10, showing fracture occurring along the grains of the material as well as the presence of stair step cracking along the grains of the material (white arrows).

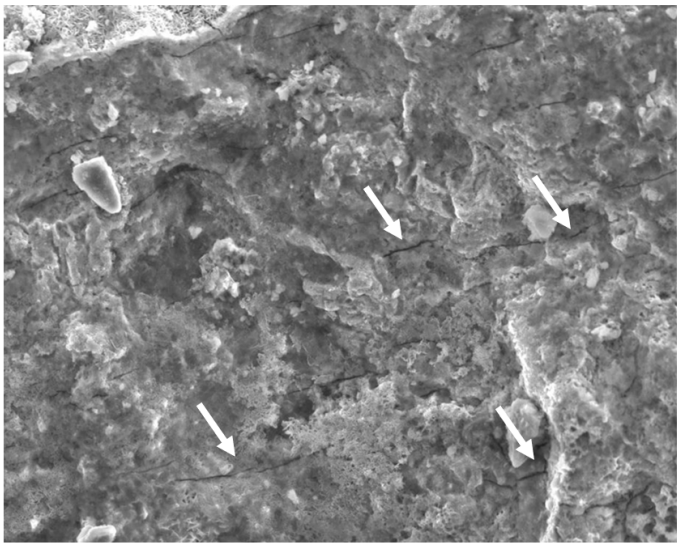

Figure 20
An SEM image of Bolt 5, displaying quasi-cleavage indicative of mixed inter and transgranular fracture.

previously experienced two different crane failures of a similar nature to the subject incident. Around the beginning of 2015, one of the crane manufacturer's cranes fell off the base of the truck body after around three years of operation. The conducted failure analysis investigation revealed corrosion of all the failed bolts as well as corrosion pitting on the threads adjacent to the fracture surfaces. In addition, it was found that the bolts had 39 HRC, above the minimum value where HE and hydrogen induced cracking is noted to be an issue. The investigation concluded that the fatigue fracture was potentially initiated due to corrosion pitting and HE.

Another one of the cranes produced by the crane manufacturer was noted to have experienced failure in March of 2018, around a year after it was first assembled. As was the case with the previously mentioned incident, all of the 14 bolts on this crane were the same Grade 8 steel fasteners utilized in the subject crane. SEM analysis revealed extensive intergranular and quasi-cleavage fracture morphology typical in bolts subjected to hydrogen embrittlement (**Figure 21**).

The failure analysis team concluded that hydrogen embrittlement was likely to have occurred during the manufacturing of these bolts and that the in-service corrosion of the bolt coating while in service provided another source of hydrogen exposure, allowing for additional embrittlement to occur. The team recommended that the manufacturer change the bolts that were utilized on these cranes, utilize lubricant, and inspect the bolts regularly/replace them if they showed signs of corrosion.

All incidents happened at least a year after the cranes were put into service. All cases showed corrosion on the fasteners, indicating the coating was insufficient to prevent hydrogen from impregnating the fasteners.

After the 2018 incident, the crane manufacturer contacted the bolt manufacturer and discussed switching the bolts used for the crane. Afterward, a technical bulletin was issued by the crane manufacturer, calling for the stock Grade 8 fasteners to be replaced with zinc/aluminum flake coated Grade 8 fasteners and providing a detailed guide on how to perform this replacement. The zinc/aluminum flake coating on these bolts provided a large decrease in the risk of HE and is shown to provide far greater corrosion resistance than yellow zinc.

This technical bulletin was issued to everyone who purchased the crane attached to its recommended truck body. However, this bulletin was not sent to those who purchased the crane individually, as was the case for the lessor in the subject incident. Had the crane manufacturer sent out this notice to all parties, including the lessor, it is likely that the lessor would have replaced the bolts, and the incident at issue would not have occurred.

According to a report by the bolt manufacturer, the susceptibility of the Grade 8 fasteners utilized in the crane at the time of the incident was well known. This report came out the same year the crane manufacturer began purchasing bolts from the bolt manufacturer. In addition, a report by the crane manufacturer acknowledged the fact

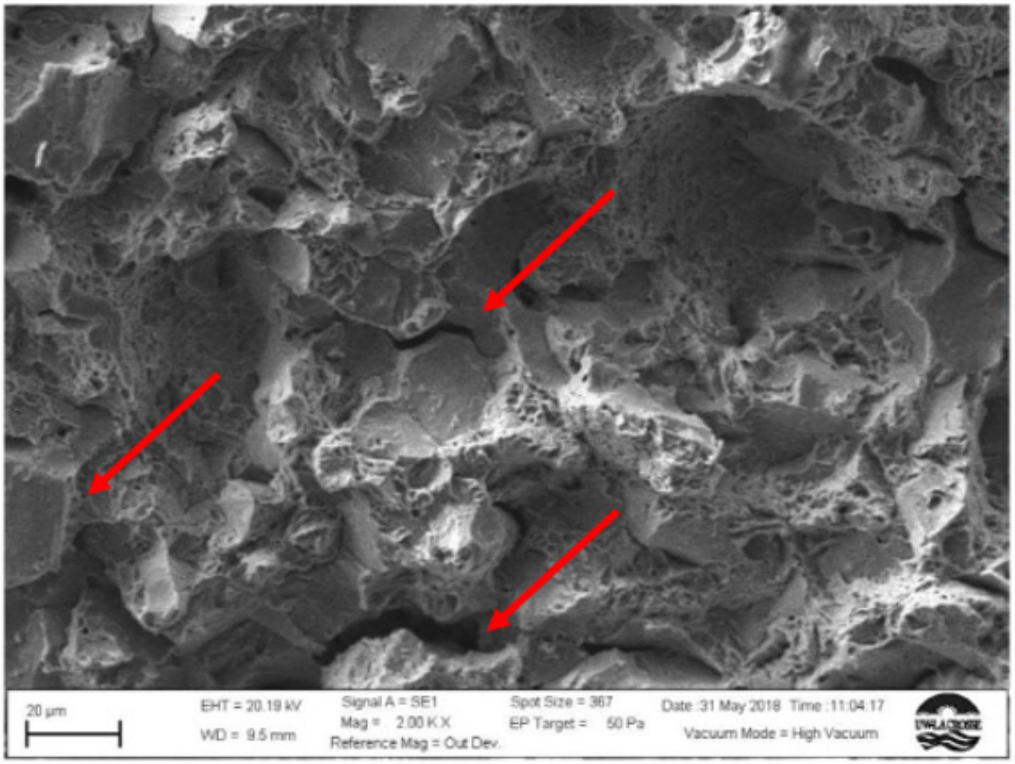

Figure 21
Intergranular fracture features on the failed bolts from the 2018 incident, indicating embrittlement took place.

that these bolts were subjected to HE from manufacturing.

Since these zinc/aluminum flake bolts have been available since 2011, the crane manufacturer knew, or should have known, about their existence — and the fact that these bolts were more practical for use in their crane. Given these previous failures, as well as documents owned by the crane manufacturer, the susceptibility of their chosen bolts to HE was well known prior to the sale of the subject crane, yet they failed to provide proper bolts for consumers.

Another contributing factor to the use of inadequate bolts was the failure of the bolt manufacturer to inform potential users regarding inappropriate applications that can make the bolts susceptible to this type of failure. Had this occurred, the crane manufacturer would have been more likely to consider purchasing bolts that would have been able to properly withstand their expected environment.

Summary

Evaluation of the failed bolts revealed extensive corrosion and the de-alloying of the zinc chromium exterior surface coatings while the fracture surfaces of the bolts showed comparatively little iron corrosion. This implies that the bolts had been subjected to a harsh corrosive environment for an extended period of time prior to the incident, possibly the lessor's outdoor yard or the heavy industrial environments where previous renters utilized the crane.

Microscopic imaging and analysis of the bolts' fracture surfaces revealed classical characteristics of progressive and partial fracturing of a significant portion of the bolts' cross section over an extended period of time (fatigue failure), prior to the final fast fracture of the bolts' remaining cross section when under relatively low-level load on the day of incident.

Given the short period of time that the crane was in use by the maintenance company, the pre-existing partial fatigue fracture of its bolts initiated prior to the maintenance company's use and continued over an extended period of time while the crane boom was subjected to cyclical loading throughout its lifetime rental history. The bolts were found in a state of severe corrosion that occurred over an extended period of time and prior to their final fracture on the day of incident. The observed corrosion of the bolts resulted in progressive degradation of the bolt material's inherent strength that made them susceptible to fatigue failure over time.

The lessor failed to perform the maintenance outlined in the owner's manual, despite knowing the bolts were potentially exposed to high load-levels as well as highly corrosive environments. The failure to perform routine inspection and maintenance of the support bolts created a latent hazard that was not discoverable by the user of crane (maintenance company). There is no evidence that the maintenance company's activities contributed to the failure at issue. Additionally, since fatigue failure and corrosion of the bolts occurred along the bolts' shaft and below the visible bolt heads, the maintenance company was not in a position to have discovered the deteriorating condition of the bolts, which led to their eventual failure on the day of incident.

Although the owner's manual required inspections on the pedestal bolts, it failed to specify what exactly the inspections should entail and what such inspections should identify as deficiencies or hazards, such as corrosion or fatigue cracks. The owner's manual should have also required owners and operators to remove and inspect the pedestal bolts on a quarterly basis. This requirement is reasonably justified as a manufacturer is in the best position to know about proper frequency of needed inspections and what such inspections should entail. As testified by the lessor's employees, had the owner's manual provided clear instructions for performing routine inspections, maintenance, and replacement of the bolts, when necessary, they would have followed such instructions.

Conclusion

This case highlights the duty of manufacturers to properly consider the function and suitability of the components they source for their products as well as the need for manufacturers to inform consumers regarding the suitability of their products and warn against use in environments known to cause premature failure. It also provides an example of fatigue failure at low levels of applied loading, displaying classical fatigue failure markings. Such an example can be utilized for future failure analysis investigations or educational purposes.

Acknowledgements

The authors would like to thank the legal experts they worked with on this case as well as their dedicated team of forensic engineers and interns.

References

1. W. T. Becker and R. J. Shipley, ASM Handbook Vol. 11: Failure Analysis and Prevention, Materials Park, OH: ASM International, 2002.
2. W. Hui-li and Q. Si-feng, "High-Strength Bolt Corrosion Fatigue Life Model and Application," Scientific World Journal, vol. 2014, 2014.
3. G.A. Pantazopoulos "A Short Review on Fracture Mechanisms of Mechanical Components Operated under Industrial Process Conditions: Fractographic Analysis and Selected Prevention Strategies," Metals, vol. 9, no. 2, pp. 148-168, 2019.
4. D. P. DeLuca, "Understanding Fatiuge," [Online]. Available: https://files.asme.org/igti/knowledge/articles/13048.pdf. [Accessed 10 December 2022].
5. P. Chowdhury and H. Sehitoglu, "Mechanisms of fatigue crack growth - a critical digest of theoretical developments." Fatigue & Fracture of Engineering Materials & Structures, vol. 39 no. 6, pp. 652–674, 2016.
6. D.J. Benac, "Technical Brief: Avoiding Bolt Failures" Failure Analysis and Prevention vol. 7, pp. 79–80, 2007.
7. M. J. O'Brien and R. G. Metcalfe "High Strength Engineering Fasteners: Design for Fatigue Resistance," Failure Analysis and Prevention, vol. 9, pp. 171-181, 2009.
8. I. P. Sari and W. Fatra, "Failure Analysis of Hydraulic Cylinder Bolt on Turntable Vibrating Compactor in Aluminum Processing Plant," Journal of Ocean, Mechanical and Aerospace, vol. 64, no. 2, pp. 63-67, 2020.
9. Crawler locomotive and truck cranes, OSHA 1910.180, 1996
10. S. K. Dwivedi and M. Vishwakarma, "Hydrogen embrittlement in different materials: A review" International Journal of Hydrogen Energy, vol. 43, no. 46, pp. 21603-21616, 2018.
11. C. J. McMahon Jr. "Hydrogen-induced intergranular fracture of steels" Engineering Fracture Mechanics, vol. 68, no. 6, pp. 773-788, 2001.

12. D. Hardie, E. A. Charles, and A. H. Lopez, “Hydrogen embrittlement of high strength pipeline steels” Corrosion Science, vol. 48, no. 12, pp. 4378-4385, 2006.

13. H.V. Umrji, L. S. Patil, N. V. Kalasapur, and V. K. Sattur, “Failure of Fasteners” International Journal of Advance Research and Innovative Ideas in Education, vol. 4, no.1, pp. 523-537, 2018.

14. Fasteners: Electroplated coating systems, DIN EN ISO 4042, 2018

15. Fastenal, "Embrittlement," [Online]. Available: https://crafter.fastenal.com/static-assets/pdfs/Embrittlement_rev_2017-02-21.pdf. [Accessed 10 December 2022].